The Pennsylvania State University

The Graduate School

Eberly College of Science

COPOLYMERIZATION OF POLAR/NON-POLAR MONOMERS: FREE RADICAL POLYMERIZATION AND PALLADIUM CATALYZED POLYMERIZATION

A Dissertation in

Chemistry

by

Ying Chen

Submitted in Partial Fulfillment
of the Requirements
for the Degree of

Doctor of Philosophy

May 2010

The dissertation of Ying Chen was reviewed and approved* by the following:

Ayusman Sen
Distinguished Professor of Chemistry
Thesis Advisor
Chair of Committee

Harry R. Allcock
Evan Pugh Professor of Chemistry

John Badding
Professor of Chemistry

T. C. Mike Chung
Professor of Materials Science and Engineering

Barbara J. Garrison
Head of the Chemistry Department
Shapiro Professor of Chemistry

*Signatures are on file in the Graduate School.

ABSTRACT

The primary theme of this thesis is the copolymerization of polar and non-polar monomers. On the one hand, chapter 2 and chapter 3 focus on the copolymerization via a free radical polymerization route. In chapter 2, I compare the effects of various Lewis and Brønsted acids on the 2,2'-azobis(isobutyronitrile) (AIBN) initiated (meth)acrylates/olefin copolymerization, and find a simple way to assess an acid's efficacy in promoting (meth)acrylate (co)polymerizations. In chapter 3, I continue to explore the potential of Lewis acid catalysts for the (meth)acrylates/olefin copolymerization by calculating the monomer reactivity ratios. Chapter 4, on the other hand, deals with late transition metal catalyzed (co)polymerizations. The synthesis of two asymmetric palladium complexes and their activities for polymerization are presented. On a different note, chapter 5 investigates a simple nickel system that oligomerizes ethylene and has high butene productivity. The final chapter, chapter 6, describes the chain transfer effects of adding olefin into the nickel(II) acetylacetonate/methylaluminoxane ($Ni(acac)_2$/MAO) catalyzed methyl methacrylate (MMA) polymerizations.

TABLE OF CONTENTS

LIST OF FIGURES

LIST OF TABLES

ACKNOWLEDGEMENTS

There are so many people that offered me so much kindly help throughout the time in my graduate school. First and foremost, I owe my deepest gratitude to my graduate advisor Dr. Ayusman Sen. This thesis would not have been possible without his support, his help and his believing in me. His encouragement makes my research more exciting and interesting. I am extremely grateful of my awesome committee members: Dr. Harry R. Allcock, Dr. John Badding and Dr. T. C. Mike Chung. I would like to thank them for their help all along and for being there for me. I get to grow and become more mature because of so many great Penn State professors.

It has been a wonderful experience working in Sen Group. I have enjoyed working with everyone in this group. I would specially like to thank Dr. Sachin Borkar, Dr. Rong Luo, Dr. Sukhendu Mandal, Dr. David Newsham and Weiran Yang for their advice and assistance.

Last but not least, I would like to thank my mother and father, Yanfei Yi and Zhiguang Chen for their support. And my boyfriend Zhi (Zack) Yang, my life in state college would be boring without him. I really appreciate his interesting questions in chemistry and his patience in helping me understand mathematical equations.

CHAPTER 1. INTRODUCTION

Polyolefins and polyacrylates are two groups of polymers that have distinct properties. Polyolefins, such as polyethylene, have good water and chemical resistance, which is good for packaging, construction and consumer goods. On the other hand, polyacrylates have excellent adhesion and wetability, and that make them good adhesive and coating materials[1,2]. By copolymerizing olefin and acrylates, there is a potential that we can combine the desirable properties of these two groups of polymers. The resulting copolymers could possess great chemical resistance and barrier, and have certain functionalities that enable them to be adhesive to substrates or to be further modified.

Generally, such acrylate/olefin copolymers can be synthesized either by free radical polymerization or by late transition metal mediated insertion polymerization. There are extensive published literatures on the synthesis of acrylates/olefin copolymers[3-9]. However, to produce acrylates/olefin copolymer with controlled composition and molecular weight is still a challenge. By means of free radical polymerization, the copolymer product is usually acrylate rich (acrylate incorporation > 50 mol%), because the acrylate monomers are more reactive than olefin monomers. Besides, it is hard to reach high molecular weight by free radical polymerization. Via insertion polymerization, olefin (mostly ethylene) rich copolymers with less than 25 mol% acrylate incorporation are obtained and the activity of the metal catalyst is generically reduced upon the addition of acrylate monomers. The rationale is an acrylate monomer inserted into the polymer chain can coordinate to the metal center via the carbonyl group, hence further chain growth requires opening of this chelate. This

rationale has been demonstrated for Brookhart's diimine complexes[8] and is also suggested for Drent's phosphino-sulfonate complexes[9].

Our polymer group has been working on the copolymerization of polar monomers with non-polar olefin, and that, of course, is the focus of my research. In our previous publications, we have reported that in 2,2'-azobis(isobutyronitrile) (AIBN) initiated free radical copolymerization of (meth)acrylates and non-polar olefin, the presence of Lewis acid could significantly increase olefin incorporation and polymerization rate[10-12]. Chapter 2 examines the interaction between various Lewis acids (or Brønsted acids) and methyl acrylate (MA) monomer by ^{13}C NMR, and finds that this interaction is related to an acid's ability to promote MA (co)polymerizations. The stronger interaction between an acid and MA monomer, the faster MA (co)polymerization would be. This correlation provides us with a simple way to determine an acid's efficacy even before running polymerization experiments. These study results were published together with Dr. Rong Luo's work on Brønsted acid promoted polymerizations[13]. For the integrity of the thesis only my work is included in chapter 2.

Chapter 3 continues to explore the effects of Lewis acids on (meth)acrylate/olefin copolymerizations, focusing on the monomer reactivity ratios. The monomer reactivity ratios r_1 and r_2 were calculated with both the Kelen-Tudos method and the non-linear least square (NLLS) method. The calculation of the latter was realized by a computer program. Both calculation results revealed that Lewis acids substantially decrease the reactivity ratio of (meth)acrylates (r_1), while the reactivity ratio of olefin (r_2) remained close to zero despite the existence of a Lewis acid. I also conducted kinetic experiments of methyl methacrylate (MMA) homo- and copolymerizations, which showed that the enhancement of the rate

constant of MMA copolymerization was much more significant than that of MMA homopolymerization. Therefore, considering the definition of r_1 and r_2, this study proved that the way Lewis acids could increase olefin incorporation was to promote (meth)acrylate cross-propagation.

Both chapters 2 and 3 deal with AIBN-initiated free radical polymerization. Chapter 4 takes another approach and presents a late transition metal catalyzed polymerization system. Two 2-formyl-1,8-naphthalenediol-based asymmetric palladium catalysts were synthesized, and their activities for polymerizations were studied. These palladium catalysts were tolerant toward functional norbornenes, and had high activity for norbornene/ethylene copolymerizations. Consecutive norbornene insertion was less likely to happen due the bulkiness of the palladium center. Utilizing the carbon monoxide isotope (^{13}CO), I was able to monitor the step by step alternating insertion of ^{13}CO and norbornene to the palladium center by ^{13}C NMR spectra at room temperature.

Chapter 5 describes a simple nickel chloride ($NiCl_2$)/aluminum trichloride ($AlCl_3$) based ethylene oligomerization system. It was first discovered by Dr. Gregory Long in our group[14]. Herein I further investigated the effect of cocatalyst and the product composition. It turned out that, in this system, $AlCl_3$ was a better cocatalyst than ethylaluminum dichloride ($AlEtCl_2$) or methylaluminoxane (MAO), and the product was mostly trans-2-butene. Replacing $NiCl_2$ with other nickel complexes did not make a large difference in its productivity. I also attempted to determine the actual reactive species. However, it could not be identified by NMR and was not suitable for X-ray crystallography analysis.

The final chapter, chapter 6, is a study of adding olefins as chain transfer agents to nickel(II) acetylacetonate ($Ni(acac)_2$)/MAO catalyzed MMA polymerization. I was trying to

find a late transition metal to copolymerize an olefin with MMA. As it turned out, in $Ni(acac)_2$/MAO catalyzed MMA polymerization, the olefin would not be copolymerized but acted as a chain transfer agent. Increasing olefin feed to this system reduced the PMMA molecular weight. There are some literatures that discussed the $Ni(acac)_2$/MAO system and suggested that it went through an insertion mechanism. However, no substantial evidence was presented. Therefore, I compared the nickel system with an AIBN initiated free radical polymerization: the products from these two systems had a dramatic difference in tacticity and composition. This ruled out the possibility that the nickel system might be a radical polymerization, and confirmed its insertion mechanism.

REFERENCES

1. Brandrup, J.; Immergut, E. H.; Grulke, E. A. *Polymer Handbook*; 4 ed.; Wiley-Interscience, 1999.
2. Chum, P. S.; Swogger, K. W. *Prog. Polym. Sci*. **2008**, *33*, 797-819.
3. Boffa, L. S; Novak, B. M. *Chem. Rev*. **2000**, *100*, 1479-1493.
4. Ittel, S. D.; Johnson, L. K.; Brookhart, M. *Chem. Rev*. **2000**, *100*, 1169-1204.
5. Liu, S.; Sen, A. *J. Polym. Sci., Part A: Polym. Chem*. **2004**, *42*, 6175-6192.
6. Domski, G. J.; Rose, J. M.; Coates, G. W.; Bolig, A. D.; Brookhart, M. *Prog. Polym. Sci*. **2007,** *32*, 30-92.
7. Berkefeld, A.; Mecking, S. *Angew. Chem. Int. Ed*. **2008**, *47*, 2538-2542.
8. Mecking, S.; Johnson, L. K.; Wang, L.; Brookhart, M. *J. Am. Chem. Soc*. **1998**, *120*, 888-889.
9. Drent. E. ; van Dijk, R.; van Ginkel, R.; van Oort, B.; Pugh, R. I. *Chem. Commun*. **2002**, 744-745.
10. Nagel, M.; Poli, D.; Sen, A. *Macromolecules* **2005**, *38*, 3029-3032.
11. Luo, R.; Sen, A. *Macromolecules* **2007**, *40*, 154-156.
12. Luo, R.; Sen, A. *Macromolecules* **2006**, *39*, 7798-7800.
13. Luo, R.; Chen, Y.; Sen, A. *J. Polym. Sci., Part A: Polym. Chem*. **2008**, *46*, 5499-5505.
14. Long, G. Ph.D. thesis, The Pennsylvania State University: University Park, PA, 2002.

CHAPTER 2. NMR STUDY OF ACRYLATE MONOMER-ACID (LEWIS AND BRØNSTED) INTERACTION: EFFECT OF ACID COMPLEXATION STRENGTH ON POLYMERIZATION RATE

2.1 INTRODUCTION

The copolymers of polar acrylate monomers with simple olefins, especially ethylene, have attracted great interest in academia and in industry due to the desirable properties the copolymers possess[1-12]. Currently, the commercial process for the copolymerization of the two is via a free radical route, and it requires high pressure and high temperature, thus limiting the range of materials available. Our group has been working on the copolymerization of polar/non-polar monomers and we found that, by adding certain Lewis or Brønsted acids to the free radical copolymerization of (meth)acrylate with simple olefin, the copolymerization rate and olefin incorporation can be significantly increased, so the pressure and temperature requirements are much lower[3,9,13,14]. The rationale is that Lewis and Brønsted acids can coordinate with the carbonyl group of the (meth)acrylate monomer and reduce the electron density of the conjugated double bond, thereby increasing the reactivity of the acrylate radical and making the radical more susceptible to attack by the relatively electron rich olefin[15-20].

Various acids have been tested as the catalyst for (meth)acrylate polymerizations, including Lewis acid, i.e., alumina, scandium triflate ($Sc(OTf)_3$) and aluminum trichloride ($AlCl_3$), and Brønsted acids, i.e., pyridinium triflate (PyH)), crosslinked poly(4-vinylpyridinium p-toluenesulfonate) (PPyH) and Nafion. However, identifying an effective acid for (meth)acrylate polymerization is not necessarily obvious and there is no easy way to

compare the efficacy of two acids before running a polymerization reaction. It would be useful to find a simple way to compare the efficacy of different Lewis and Brønsted acids.

In the work described in this chapter, I first conducted a NMR study of acrylate monomer-acid interaction, which can be used as a measure of acid complexation strength. Then I examined the relationship between the complexing ability of the Lewis and Brønsted acids vis-à-vis the acrylate carbonyl group and their ability to promote acrylate homo- and copolymerizations. I found a direct correlation between the two. Likewise, for soluble Lewis acids, there is a direct correlation between the charge/size ratio at the metal center and its ability to promote acrylate copolymerizations. Thus, this study provides a semi-quantitative way of estimating the efficacy of a given Lewis or Brønsted acid in promoting acrylate polymerizations.

2.2 RESULTS AND DISCUSSION

2.2.1 NMR STUDY OF ACRYLATE MONOMER-ACID INTERACTION

As our group reported previously, the addition of Lewis or Brønsted acids to (meth)acrylate/olefin copolymerization can significantly increase the monomer conversion and olefin incorporation. The rate and olefin incorporation enhancement for each acid can be found in our earlier papers[3, 9, 13, 14]. In fact, stronger Lewis acids, such as $Sc(OTf)_3$ and $AlCl_3$, are more effective than weaker Lewis acids, like alumina. This suggested a possible correlation between the interaction strength of the acid with an acrylate monomer and the promotional effect of the former in polymerizations.

One way to probe the complexation of the acid with the acrylate ester functionality is to monitor the ^{13}C NMR chemical shift of the carbonyl group, which is the most likely binding site. Indeed, this carbon showed the largest downfield shift upon the addition of an acid (Brønsted or Lewis) to the acrylate monomer. An example of the methyl acrylate (MA) chemical shift change in the presence of $Sc(OTf)_3$ is given in table 2.1. The chemical shift changes of the MA carbonyl carbon in the presence of different acids are summarized in table 2.2. The NMR signal is an average of all free and coordinated MA monomers. Because the free MA monomers exchange very fast with the coordinated ones, only one chemical shift was detected in the ^{13}C NMR. For insoluble acids, there is still a small amount of coordinated MA monomers, so the chemical shift change still exists. As postulated, this interaction of the acid with the ester carbonyl group will reduce the electron density of the conjugated double bond, thereby increasing the reactivity of the acrylate radical and making the radical more susceptible to attack by a relatively electron rich olefin.

Table 2.1 Methyl acrylate (MA) ^{13}C NMR in the presence and absence of $Sc(OTf)_3$[a]

Carbon	MA only (ppm)	MA with $Sc(OTf)_3$ (ppm)	Δδ (ppm)
1	129.86	131.29	1.43
2	128.25	127.87	0.38
3	165.66	167.16	1.50
4	51.17	51.89	0.72

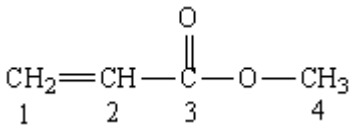

[a]Conditions: $Sc(OTf)_3$/MA = 1/10 molar ratio; NMR was conducted in $CDCl_3$ at 25 ^oC; $Sc(OTf)_3$, scandium(III) trifluoromethanesulfonate.

Table 2.2 Methyl acrylate (MA) carbonyl carbon ^{13}C NMR chemical shift change in the presence and absence of different acids[a]

Entry	Acids	C3 on methyl acrylate (ppm)	Δδ (ppm)
1	Only MA	165.66	0
2	PPyH	166.01	0.35
3	PyH	166.08	0.42
4	$La(OTf)_3$	166.13	0.47
5	Al_2O_3	166.16	0.50
6	$Y(OTf)_3$	166.24	0.58
7	$AlCl_3$	166.97	1.31
8	$Sc(OTf)_3$	167.16	1.50

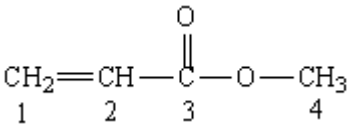

[a]Conditions: Acid/MA = 1/10 molar ratio; NMR was conducted in $CDCl_3$ at 25 ^oC; PPyH, poly(4-vinylpyridinium p-toluenesulfonate); PyH, pyridinium trifluoromethanesulfonate; $La(OTf)_3$, lanthanum(III) trifluoromethanesulfonate; $Yb(OTf)_3$, ytterbium(III) trifluoromethanesulfonate; $Sc(OTf)_3$, scandium(III) trifluoromethanesulfonate.

2.2.2 EFFECT OF ACID COMPLEXATION STRENGTH ON POLYMERIZATION RATE

The apparent polymerization rates for both MA homopolymerization and MA/1-hexene copolymerization are first-order with respect to MA concentration. A correlation of apparent MA homopolymerization rates (figure 2.1 (a)) and MA/1-hexene copolymerization rate (figure 2.1 (b)) vs. shift in the ^{13}C NMR resonance of the MA carbonyl group is shown for both Brønsted and Lewis acids. The ^{13}C chemical shift is summarized in table 2.2. All these acids showed the ability to increase the polymerization rate. Basically, the bigger NMR shift change indicates a more effective acid. In the presence of $Sc(OTf)_3$, the change of MA ^{13}C chemical shift is the largest: accordingly its polymerization rate is the highest.

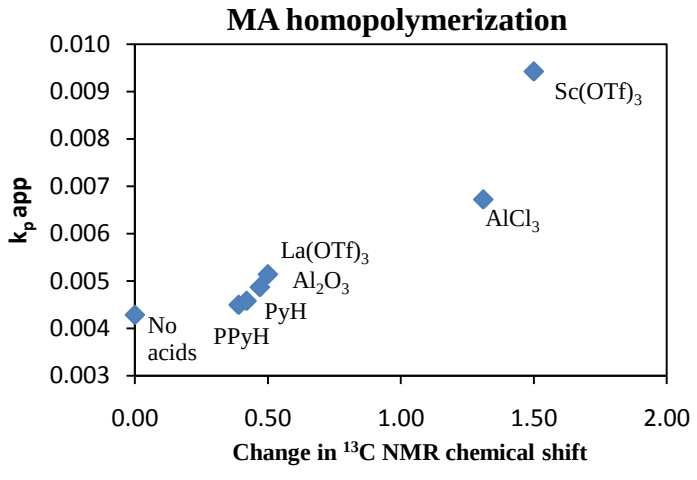

(a)

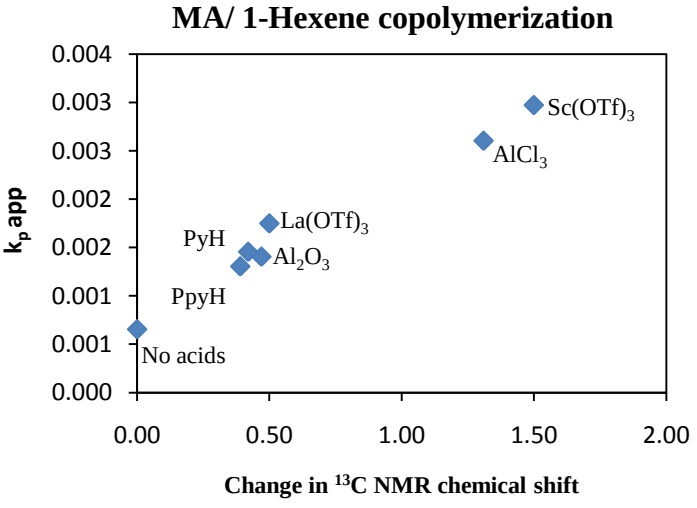

(b)

Figure 2.1 (a) Methyl acrylate (MA) homopolymerization rate vs. change in ^{13}C NMR chemical shift of the monomer carbonyl carbon. (b) MA/1-hexene copolymerization rate vs. change in ^{13}C NMR chemical shift of the monomer carbonyl carbon. Conditions (a): MA, 0.6 g; AIBN, 5 mg; toluene, 5 mL; acids, 1:10 (molar ratio) to MA; 60 ^{o}C; 2 h. (b): MA, 0.3 g; 1-hexene, 1 g; AIBN, 5 mg; toluene, 5 mL; acids, 1:10 (molar ratio) to MA; 60 ^{o}C; 4 h.

The effect of the catalyst amount on polymerization rate was also examined (figure 2.2). Herein, a soluble Lewis acid, $Sc(OTf)_3$, was firstly employed to study this relationship. Keeping methyl acrylate feed and other conditions constant, an increase of the $Sc(OTf)_3$ amount accelerated the polymerization reaction. Both homo- and copolymerization rates doubled in the presence of 1/10 $Sc(OTf)_3$ to acrylate (molar ratio). ^{13}C NMR data were obtained as well. The larger the MA chemical shift change, the faster the reaction became. The same method was used to study the heterogeneous Al_2O_3 catalyst. When the Al_2O_3 feed was increased, acrylate ^{13}C NMR shift change increased as well as the polymerization rate, although the rate change was less significant than that of soluble catalyst $Sc(OTf)_3$.

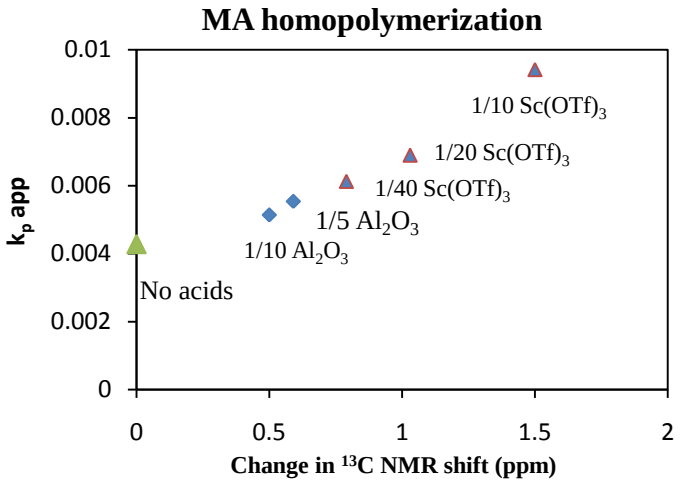

(a)

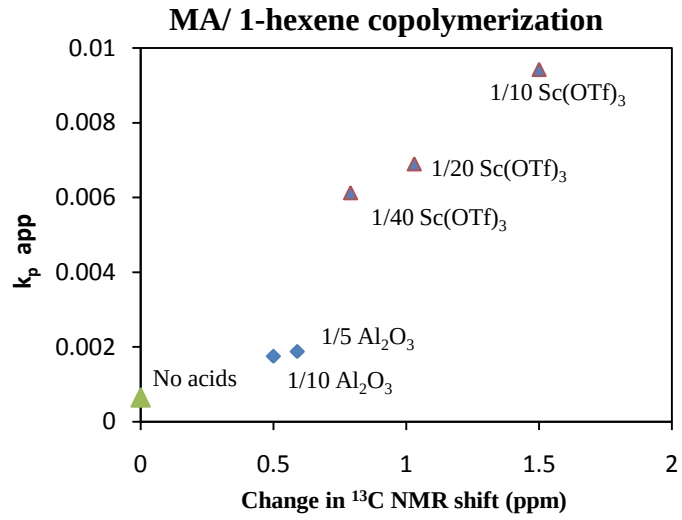

(b)

Figure 2.2 (a) Methyl acrylate (MA) homopolymerization rate vs. change in ^{13}C NMR chemical shift of the monomer carbonyl group for different catalyst/monomer molar ratios. (b) MA/1-hexene copolymerization rate vs. change in ^{13}C NMR chemical shift of the monomer carbonyl carbon for different catalyst/monomer molar ratios. Conditions (a): MA, 0.6 g; AIBN, 5 mg; toluene, 5 mL; 60 ^{o}C; 2 h. (b): MA, 0.3 g; 1-hexene, 1 g; AIBN, 5 mg; toluene, 5 mL; 60 ^{o}C; 4 h.

For Lewis acids, the charge/size ratio at the metal center is another measure of their strength and again there is a strong direct correlation between the magnitude of this number and the ability of the Lewis acid to promote copolymerizations (figure 2.3). All the three figures (figure 2.1-2.3) clearly indicate a strong correlation between the strength of the interaction of the acid (Brønsted or Lewis) with the acrylate carbonyl group and the acid's ability to promote acrylate homo- and copolymerizations. These correlations serve as useful tools to evaluate the effectiveness of a given acid in promoting acrylate homo- and copolymerizations.

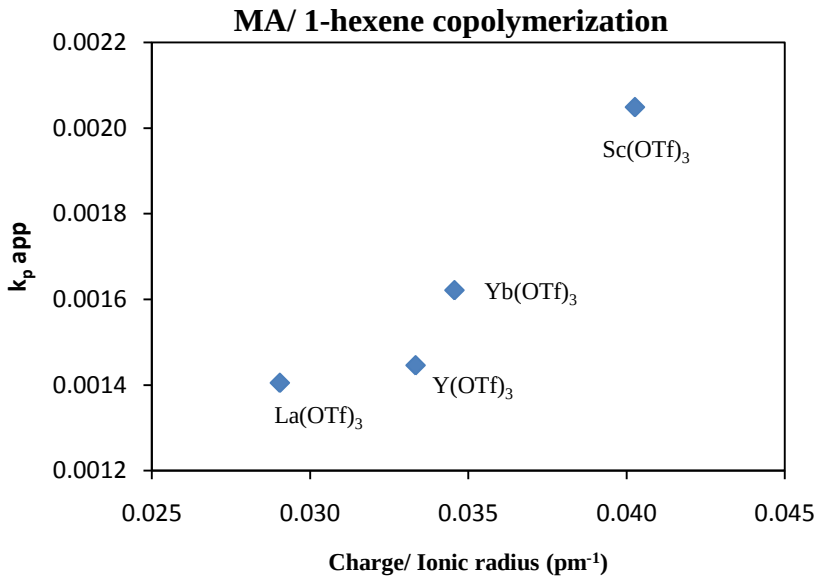

Figure 2.3 MA/1-hexene copolymerization rate vs. charge/ionic radius ratio of the metal. Conditions: MA, 0.3 g; 1-hexene, 1 g; AIBN, 5 mg; toluene, 5 mL; M(OTf)$_3$/MA, 1:10 (molar ratio); 60 ^{o}C; 4 h.

2.3 CONCLUSIONS

The addition of either soluble or insoluble Lewis and Brønsted acids to the AIBN-initiated copolymerization of acrylate with a non-polar olefin resulted in increased polymerization rates. Studies indicate a strong correlation between the strength of the interaction of the acid (Brønsted or Lewis) with the acrylate carbonyl group and the acid's ability to promote acrylate homo- and copolymerizations. This correlation can be used as a tool to determine an acid's ability to promote acrylate polymerizations.

2.4 EXPERIMENTAL SECTION

2.4.1 MATERIALS

All chemicals and reagents were obtained from Aldrich unless otherwise stated. Methyl acrylate (MA, 99%), methyl methacrylate (MMA, 99%) and 1-hexene (97%) were passed through basic alumina column to remove the inhibitor and impurities, degassed and stored under N_2. 2,2'-Azobis(isobutyronitrile) (AIBN, 98%), poly(4-vinylpyridinium p-toluenesulfonate) (PPyH, 2% crosslinked), pyridinium trifluoromethanesulfonate (PyH, 97%), lanthanum(III) trifluoromethanesulfonate ($La(OTf)_3$, 97%, Strem Chemicals), aluminum oxide (activated, acidic, Brockmann I, standard grade, ~ 150 mesh, pH = 4.5±0.5 in aqueous solution), aluminum chloride ($AlCl_3$, anhydrous, 99.99%), yttrium(III) trifluoromethanesulfonate ($Y(OTf)_3$, 98%), ytterbium(III) trifluoromethanesulfonate ($Yb(OTf)_3$, 97%) and scandium(III) trifluoromethanesulfonate ($Sc(OTf)_3$, Alfa Aesar, 98%) were used as received.

2.4.2 INSTRUMENTATION

NMR spectra were recorded using a Bruker 300-DPX spectrometer at ambient temperature (^{1}H-NMR, 300MHz; ^{13}C-NMR, 75 MHz). Chemical shifts are referenced to $CDCl_3$. Gas chromatography analysis was performed on an Agilent 5890 Series II GC. The samples were heated from 40 ^{o}C to 100 ^{o}C at a ramp rate of 4 ^{o}C/min.

2.4.3 KINETIC STUDY OF METHYL ACRYLATE HOMOPOLYMERIZATION IN THE PRESENCE OF DIFFERENT ACIDS

In a N_2-filled glovebox, MA (0.6 g), AIBN (0.005 g), acidic Al_2O_3 (0.071 g), toluene (5 mL) and tetrachloroethane (0.05 g) as an internal standard were added into a reaction

vessel equipped with a magnetic stirring bar. The reaction was stirred in 60 ^{o}C oil bath for 2 hours. GC samples were taken at different reaction times to determine MA conversion. With a constant acid to monomer molar ratio of 1/10, the same procedure was used for other Lewis and Brønsted acids.

2.4.4 KINETIC STUDY OF METHYL ACRYLATE/1-HEXENE COPOLYMERIZATION IN THE PRESENCE OF DIFFERENT ACIDS

In a N_2-filled glovebox, a reaction vessel equipped with a stirring bar was charged with MA (0.3 g), 1-hexene (1.0 g), AIBN (0.005g), acidic Al_2O_3 (0.036 g), toluene (5 mL) and tetrachloroethane (0.05 g). The reaction vessel was sealed and stirred in 60 ^{o}C oil bath for 4 hours. GC samples were taken at different reaction times to determine MA and hexene conversions. With a constant acid to MA monomer molar ratio of 1/10, the same procedure was used for other Lewis and Brønsted acids.

2.5 REFERENCES

1. Boffa, L. S.; Novak, B. M. *Chem. Rev.* **2000**, *100*, 1479-1493.
2. Ittel, S. D.; Johnson, L. K.; Brookhart, M. *Chem. Rev.* **2000**, *100*, 1169-1204.
3. Liu, S.; Sen, A . *J. Polym. Sci., Part A: Polym. Chem.* **2004**, *42*, 6175-6192.
4. Liu, S.; Elyashiv, S.; Sen, A. *J. Am. Chem. Soc.* **2001**, *123*, 12738-12739.
5. Elia, C.; Elyashiv, S.; Sen. A.; Lopez-Fernandez, R; Albeniz, A. C.; Espinet, P. *Organometallics* **2002**, *21*, 4249-4256.
6. Gu, B.; Liu, S.; Leber, D.; Sen, A. *Macromolecules* **2004**, *37*, 5142-5144.
7. Liu, S.; Gu, B.; Rowlands, H. A.; Sen, A. *Macromolecules* **2004**, *37*, 7924-7929.
8. Borkar, A.; Sen, A. *Macromolecules* **2005**, *38*, 3029-3032.
9. Nagel, M.; Poli, D.; Sen, A. *Macromolecules* **2005**, *38*, 7262-7265.
10. Tian, G. L.; Boone, H. W.; Novak, B. M. *Macromolecules* **2001**, *34*, 7656- 7663.
11. Venkatesh, R.; Klumperman, B. *Macromolecules* **2004**, *37*, 1226-1233.
12. Venkatesh, R.; Harrison, S.; Haddleton, D. M.; Klumperman, B. *Macromolecules* **2004**, *37*, 4406-4416.
13. Luo, R.; Sen, A. *Macromolecules* **2006**, *39*, 7798-7800.
14. Luo, R.; Sen, A. *Macromolecules*, **2007**, *40*, 154-156.
15. Lutz, J. F.; Kirci, B.; Matyjaszewski, K. *Macromolecules* **2003**, *36*, 3136-3145.
16. Isobe, Y.; Nakano, T.; Okamoto, Y. *J. Polym. Sci., Part A: Polym. Chem.* **2001**, *39*, 1463-1471.
17. Lutz, J. F.; Jakubowski, W.; Matyjaszewski, K. *Macromol. Rapid Comm.* **2004**, *25*, 486-492.

18. Ray, B.; Isobe, Y.; Matsumoto, K.; Habaue, S.; Okamato, Y. Kamigaito, M.; Sawamoto, M. *Macromolecules* **2004**, *37*, 1702-1710.

19. Logothetis, A. L.; McKenna J. M. *J. Polym. Sci., Polym. Chem. Ed.* **1977**, *15*, 1431-1439.

20. Logothetis, A. L.; McKenna J. M. *J. Polym. Sci., Polym. Chem. Ed.* **1978**, *16*, 2797-2802.

CHAPTER 3. EFFECT OF LEWIS ACIDS ON REACTIVITY RATIOS FOR (METH)ACRYLATE/NON-POLAR OLEFIN COPOLYMERIZATIONS

3.1 INTRODUCTION

The copolymers of polar vinyl monomers, such as methacrylates and acrylates, with simple olefin with predictable composition and architectures are of great interest because the combination of these two classes of monomers can greatly enhance the currently attainable polymer properties. However, because of the wide disparity between the respective reactivity ratios, random (meth)acrylate-rich copolymers in relatively low yields are typically obtained by free radical copolymerization of the two. Nevertheless, as we have recently reported,[1-4] the free radical copolymerization of acrylates with simple olefin in the presence of either Lewis or Brønsted acids can lead to both a significant increase in the polymerization rate and non-polar olefin incorporation. The qualitative explanation is that Lewis acids can coordinate with the carbonyl group of the acrylate monomer and reduce the electron density of the conjugated double bond, thereby (a) increasing the reactivity of the acrylate radical and (b) making the radical more susceptible to attack by the relatively electron rich non-polar olefin.

For radical copolymerizations, the copolymer composition is governed by the reactivity ratios of the two monomers. The monomer reactivity ratios, r_1 and r_2, are the ratios of the rate constants for the different propagation reactions:

$$\sim M_1^{\bullet} + M_1 \longrightarrow \sim M_1M_1^{\bullet} \qquad k_{11}$$

$$\sim M_1^{\bullet} + M_2 \longrightarrow \sim M_1M_2^{\bullet} \qquad k_{12} \qquad r_1 = k_{11}/k_{12},$$

$$\sim M_2^{\bullet} + M_2 \longrightarrow \sim M_2M_2^{\bullet} \qquad k_{22} \qquad r_2 = k_{22}/k_{21}$$

$$\sim M_2^{\bullet} + M_1 \longrightarrow \sim M_2M_1^{\bullet} \qquad k_{21}$$

Since the copolymer composition is different depending on the absence and presence of Lewis acids, it is clear that the latter have a significant influence on the reactivity ratios. To date, many Lewis acids have been used in radical copolymerizations;[1-10] however, quantitative data on their effect on monomer reactivity ratios is lacking. Herein, we describe the influence of Lewis acids on the monomer reactivity ratios for (meth)acrylates/non-polar olefin copolymerizations. The r_1 and r_2 values have been calculated in accordance with Kelen-Tudos[11] equation and non-linear least squares[12] (NLLS) method. We have also examined the kinetics of the copolymerization reactions. The results indicate that Lewis acids significantly increase the cross-propagation rate compared to self-propagation, resulting in a large decrease in the reactivity ratio (r_1) for (meth)acrylates.

In order to understand why only a catalytic amount of Lewis acid is sufficient to strongly influence the copolymerization reactions, we also closely examined the interaction of Lewis acids with both the methacrylate monomer and the polymer and found that the Lewis acid interaction with the carbonyl group of the monomer is significantly stronger than that with the polymer. Furthermore, there is a fast exchange of the Lewis acid between the carbonyl groups of the polymer and that in the monomer.

3.2 RESULTS AND DISCUSSION

3.2.1 THE EFFECT OF LEWIS ACID ON MONOMER REACTIVITY RATIOS IN METHYL METHACRYLATE/NON-POLAR OLEFIN COPOLYMERIZATION

The effect of adding increasing amounts of the Lewis acid, $AlCl_3$, on methyl methacrylate (MMA)/1-hexene copolymerization for different monomer feed ratios is graphically illustrated in Fig. 3.1. There is a clear trend towards increasing incorporation of 1-hexene with increasing amount of Lewis acid present, especially at low MMA/1-hexene feed ratios. For example, without $AlCl_3$, when the MMA mol fraction in the feed is 0.1, 1-hexene incorporation in copolymer is less than 15%. Simply by adding 0.1 equiv. of $AlCl_3$ relative to MMA, 1-hexene incorporation increased to over 30%. Some of the data is also summarized in table 3.1. To maintain the monomer feed ratio over the course of the polymerization, all the reactions were terminated before MMA conversion reached 8%.

The polymers obtained were random copolymers. There are MMA-MMA dyads and MMA-hexene dyads in the polymer chain, but no hexene-hexene dyads. The absence of the latter is evident from ^{13}C-NMR and ^{13}C DEPT135-NMR spectra (figure 3.2). The resonance at 33.5 ppm, ascribable to the CH group of sequential hexene units,[13] was absent. There was complete overlap of the gel permeation chromatographic (GPC) traces using the refractive index (RI) and ultraviolet (UV, 254 nm) detectors thereby establishing that the materials obtained were true copolymers rather than a mixtures of homopolymers. Note that the UV detector is more sensitive to the carbonyl groups present in a polymer.

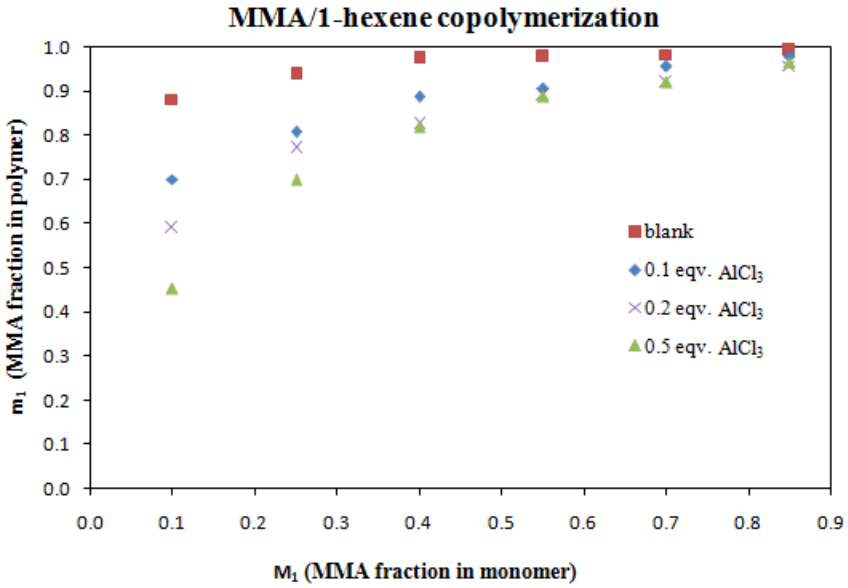

Figure 3.1 Copolymer composition versus monomer feed ratio in MMA/1-hexene copolymerization**.** Conditions: MMA, 0.3 g; AIBN, 0.005 g; toluene, 5 mL; $AlCl_3$, 0.04 g (0.1 equiv. to MMA), 0.08 g (0.2 equiv. to MMA), 0.2 g (0.5 equiv. to MMA), 60 ^{o}C.

Table 3.1 Selected data of MMA/1-hexene copolymerization[a]

Entry	$AlCl_3$/MMA molar ratio	M_1 (MMA mol fraction in monomer)	m_1 (MMA mol fraction in polymer)	MMA (% conv.)	M_n[b] ($\times 10^{-4}$)	PDI[b] (M_w/M_n)
1	0.1	0.10	0.70	1.99	2.97	1.23
2	0.1	0.25	0.81	3.39	4.14	1.29
3	0.1	0.40	0.89	6.32	4.59	1.38
4	0.1	0.55	0.90	3.43	4.36	1.35
5	0.1	0.70	0.96	2.50	4.24	1.32
6	0.1	0.85	0.98	1.41	3.92	1.28
7	0.2	0.10	0.59	5.85	3.23	1.36
8	0.2	0.25	0.77	4.72	4.88	1.35
9	0.2	0.40	0.83	2.75	4.52	1.32
10	0.2	0.55	0.89	3.84	5.19	1.37
11	0.2	0.70	0.92	1.34	4.59	1.32
12	0.2	0.85	0.96	1.67	4.33	1.34

[a]Conditions: MMA, 0.3 g; AIBN, 0.005 g; toluene, 5 mL; $AlCl_3$, 0.04 g (0.1 equiv. to MMA), 0.08 g (0.2 equiv. to MMA), 0.2 g (0.5 equiv. to MMA), 60 ^oC. [b]By GPC relative to polystyrene standards.

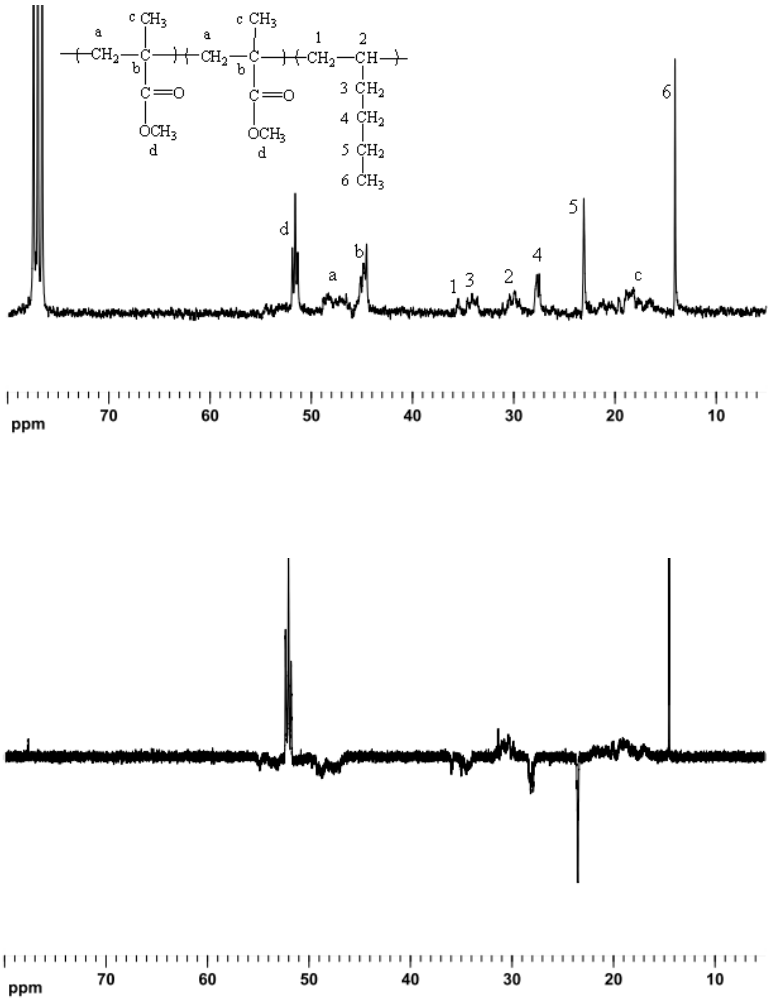

Figure 3.2 NMR of MMA/1-hexene copolymer (25 ^{o}C, $CDCl_3$, MMA molar fraction 70 %). (a) ^{13}C NMR, (b) ^{13}C DEPT135 NMR.

Using the data from Fig. 3.1, the monomer reactivity ratios for MMA and 1-hexene were calculated by Kelen-Tudos equation and NLLS method and shown in table 3.2. The r_1 value clearly decreases with increasing amount of added Lewis acid. Since both k_{11} and k_{12} are enhanced in the presence of $AlCl_3$, the increase in k_{12} must be significantly larger than in k_{11}, i.e. the Lewis acid is more effective in promoting cross-propagations (see section 3.2.2). The calculated r_2 values are negative using the Kelen-Tudos equation. These values do not have a physical meaning, only suggesting that the real value of r_2 is near zero. This is consistent with the observed absence of sequential alkene units in the copolymer backbone.

Table 3.2 Reactivity ratios for MMA/1-hexene copolymerization with or without $AlCl_3$[a]

Entry	$AlCl_3$/MMA molar ratio	Kelen-Tudos		NLLS	
		r_1 (MMA)	r_2 (1-hexene)	r_1 (MMA)	r_2 (1-hexene)
1	0	88.5	-0.11	54.0	0
2	0.1	11.2	-0.19	10.4	0
3	0.2	2.96	-0.25	6.41	0.019

[a]Conditions: MMA, 0.3 g; AIBN, 0.005 g; toluene, 5 mL; $AlCl_3$, 0.04 g (0.1 equiv. to MMA), 0.08 g (0.2 equiv. to MMA), 0.2 g (0.5 equiv. to MMA), 60 ^{o}C.

Fig. 3.3 presents the data on free radical copolymerization of MMA with norbornene at different comonomer and Lewis acid feed ratios. Again, the copolymerizations were stopped before MMA conversion reaches 8%. The trend observed is very similar to that for MMA/1-hexene copolymerizations. The corresponding reactivity ratios are given in table 3.3 and are again consistent with that observed for MMA/1-hexene copolymerizations.

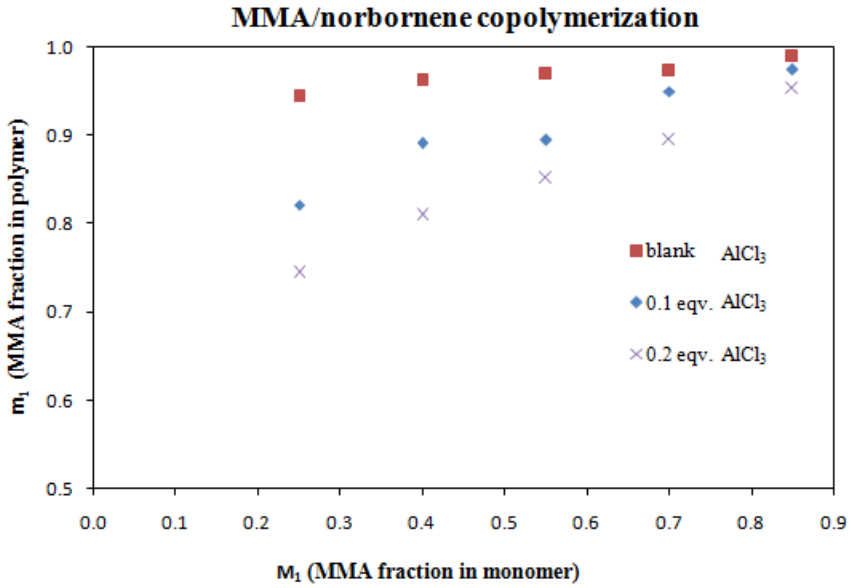

Figure 3.3 Copolymer composition versus monomer feed ratio in MMA/norbornene copolymerization**.** Conditions: MMA, 0.3 g; AIBN, 0.005 g; toluene, 5 mL; $AlCl_3$, 0.04 g (0.1 equiv. to MMA), 0.08 g (0.2 equiv. to MMA); 60 ^{o}C.

Table 3.3 Reactivity ratios of MMA/norbornene copolymerization with or without $AlCl_3$[a]

Entry	$AlCl_3$/MMA molar ratio	Kelen-Tudos		NLLS	
		r_1 (MMA)	r_2 (norbornene)	r_1 (MMA)	r_2 (norborrnene)
1	0	35.1	-0.13	39.8	0
2	0.1	5.40	-0.31	9.72	0
3	0.2	2.00	-0.37	4.77	0

[a]Conditions: MMA, 0.3 g; AIBN, 0.005 g; toluene, 5 mL; $AlCl_3$, 0.04 g (0.1 equiv. to MMA), 0.08 g (0.2 equiv. to MMA); 60 ^oC.

3.2.2 METHYL METHACRYLATE HOMOPOLYMERIZATION AND MMA/OLEFIN COPOLYMERIZATION KINETICS

Table 3.4 summarizes the apparent polymerization rates (k_p) for a series of MMA homo and copolymerizations. The values of k_p were obtained from linear plots of $\ln([MMA]_o/[MMA])$ versus time. In all cases, k_p increases with increasing amount of added Lewis acid. Further, the enhancement in k_p is larger in the copolymerization reactions. This observation, together with the decrease in r_1 in the presence of a Lewis acid (tables 3.2 and 3.3) clearly indicates that Lewis acid promotes cross-propagation more than MMA self-propagation.

Table 3.4 Apparent (co)polymerization rates for MMA in the presence of $AlCl_3$[a]

Entry	$AlCl_3$/MMA molar ratio	Olefin	k_p(MMA) (min^{-1})
1	0	0	0.00117
2	0.1	0	0.00127
3	0.2	0	0.00140
4	0.5	0	0.00184
5	0	1-hexene	0.00110
6	0.1	1-hexene	0.00186
7	0.2	1-hexene	0.00278
8	0.5	1-hexene	0.00356
9	0	norbornene	0.00252
10	0.1	norbornene	0.00322
11	0.2	norbornene	0.00339

[a]Conditions: MMA, 0.3 g; 1-hexene, 0.44 g; norbornene, 0.28 g; AIBN, 0.005 g; toluene, 5 mL; tetrachloroethane, 0.05 g; $AlCl_3$, 0.04 g (0.1 equiv. to MMA), 0.08 g (0.2 equiv. to MMA), 0.2 g (0.5 equiv. to MMA); 60 ^oC; 4 h (copolymerization), 2 h (homopolymerization).

3.2.3 NMR STUDY OF THE INTERACTION OF METHACRYLATE MONOMER AND POLYMER WITH LEWIS ACIDS

In order to understand why a sub-stoichiometric (i.e., catalytic) amount of Lewis acid is sufficient to strongly influence the copolymerization reactions, we examined the interaction of Lewis acids with both MMA and the corresponding polymer PMMA. As shown in Fig. 3.4, the addition of $AlCl_3$ to a solution of MMA resulted in a gradual downfield shift in the carbonyl group in the ^{13}C-NMR spectrum until $AlCl_3$/MMA ratio reaches 1. At that point, all the MMA carbonyl groups are expected to be bonded to $AlCl_3$. Cooling a solution in which the $AlCl_3$/MMA ratio is ~ 0.5 to – 90 ^oC did not result in the observation of separate resonances for free and $AlCl_3$-bound carbonyl groups suggesting an extremely fast exchange rate between the two.

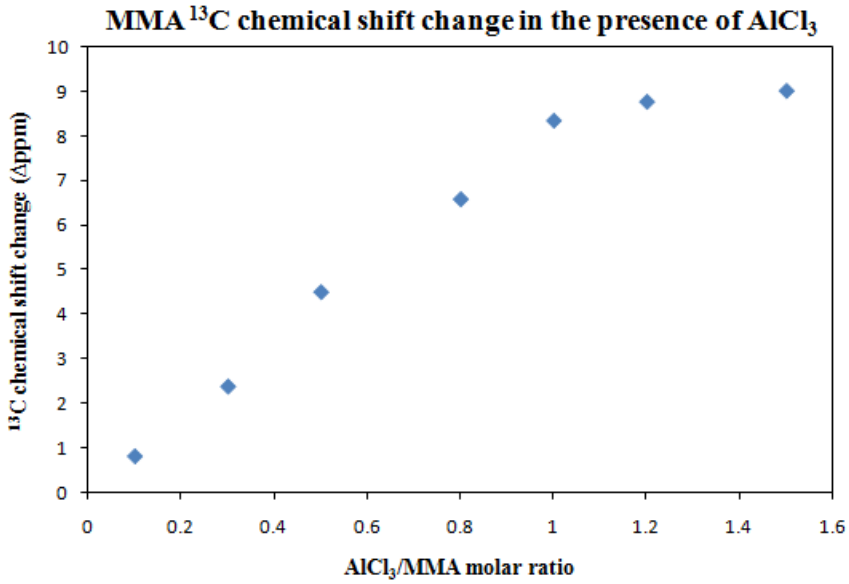

Figure 3.4 Change in ^{13}C-NMR chemical shift ($CDCl_3$, 50 ^{o}C) of the carbonyl carbon of MMA versus $AlCl_3$/MMA molar ratio.

We also observed a pronounced preference for Lewis acids to coordinate to the carbonyl group of the monomer MMA over those in a polymer (see table 3.5). Thus, we hypothesize a facile Lewis acid exchange between MMA units in the polymer and monomeric MMA as shown below (figure 3.5), consistent with the large effect of Lewis acids even when added in catalytic amounts.

Table 3.5 Shift in ^{13}C-NMR carbonyl resonances of PMMA and MMA in the presence of Lewis acids[a]

	PMMA/MMA/$TiCl_4$ molar ratio = 1/1/0.5		PMMA/MMA/$AlCl_3$ molar ratio = 1/1/0.5	
Shift in ^{13}C-NMR carbonyl resonance (Δ ppm)	PMMA	MMA	PMMA	MMA
	1.09	3.80	0.60	3.12

[a]Conditions: MMA, 0.05 g; PMMA, 0.05 g; $TiCl_4$, 0.047 g; $AlCl_3$, 0.033 g; 25 ^{o}C; $CDCl_3$.

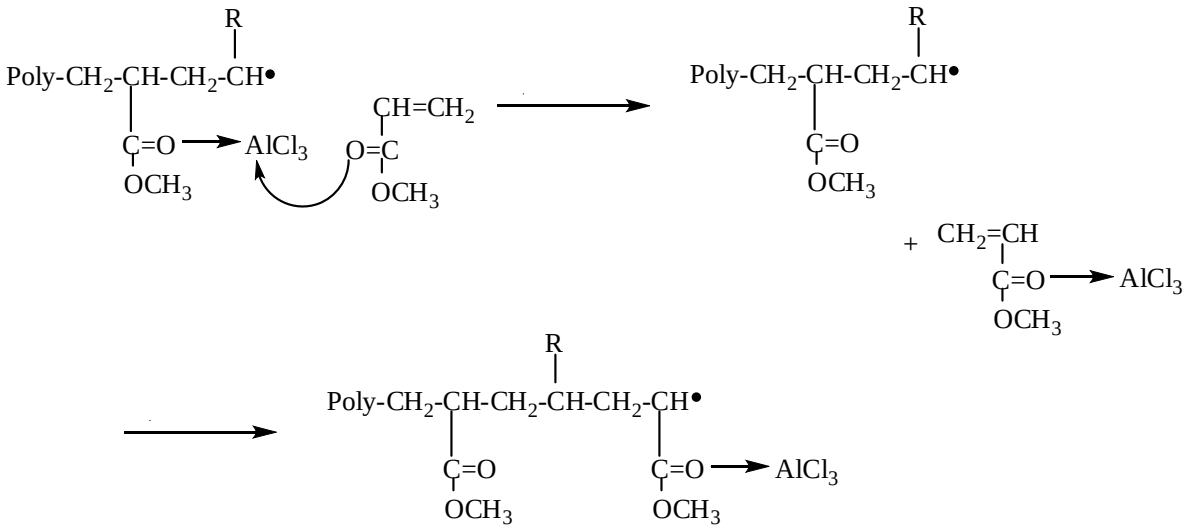

Figure 3.5 Lewis acid exchange between MMA units in the polymer and monomeric MMA.

3.2.4 THE EFFECT OF LEWIS ACID ON MONOMER REACTIVITY RATIOS IN METHYL ACRYLATE (MA)/OLEFIN COPOLYMERIZATION

As with copolymerizations involving MMA, we observed enhanced polymerization rate[1] and enhanced olefin incorporation in the copolymerization of MA with 1-hexene in the presence of Lewis acids (fig. 3.6 and table 3.6). Two Lewis acids, $AlCl_3$ and $Sc(OTf)_3$, were employed. For the latter, due to poor solubility in toluene, 1,2-dichlorobenzene was used as solvent. The copolymer microstructure was determined by ^{13}C-NMR and ^{13}C DEPT135-NMR spectroscopy. The copolymers synthesized with $AlCl_3$ are nearly alternating; with the predominant presence of MA-hexene dyads.[14] Resonance at 35 and 33.5 ppm due to the CH groups of MA-MA and hexene-hexene dyads were not obviously visible (figure 3.7). The nearly alternating nature of the copolymer obtained is also consistent with both r_1 and r_2 values being near-zero (see table 3.6). For both Lewis acids, the MA cross-propagation is clearly promoted much more so than MA self-propagation. As with MMA/hexene copolymers, there was complete overlap of the gel permeation chromatographic (GPC) traces using the refractive index (RI) and ultraviolet (UV, 254 nm) detectors thereby establishing that the materials obtained were true copolymers rather than a mixtures of homopolymers.

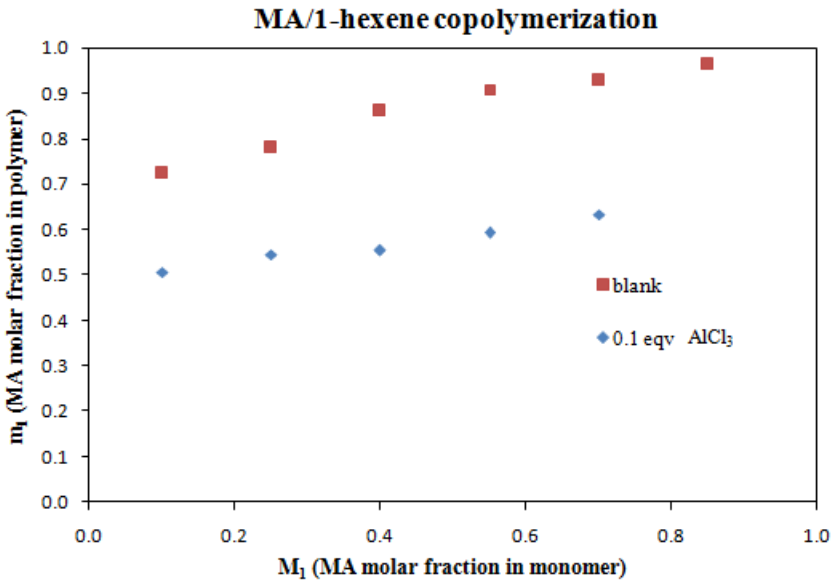

Figure 3.6 Copolymer composition versus monomer feed ratio in MA/1-hexene copolymerization**.** Conditions: MA, 0.3 g; AIBN, 0.005 g; toluene, 5 mL; $AlCl_3$, 0.04 g (0.1 equiv. to MA); 60 ^{o}C.

Table 3.6 Reactivity ratios for MA/1-hexene copolymerization in the presence of Lewis acids[a]

Entry	Lewis acid	LA/MA molar ratio	Kelen-Tudos		NLLS	
			r_1 (MA)	r_2 (1-hexene)	r_1 (MA)	r_2 (1-hexene)
1[b]	None	0	3.87	-0.24	9.56	0
2[b]	$AlCl_3$	0.1	0.19	-0.035	0.35	0
3[c]	None	0	4.66	-0.26	7.60	0
4[c]	$Sc(OTf)_3$	0.1	1.50	-0.18	2.73	0

[a]Conditions: MA, 0.3 g; AIBN, 0.005 g; 60 ^{o}C. [b]Toluene, 5 mL. [c]1,2-Dichlorobenzene, 5 mL.

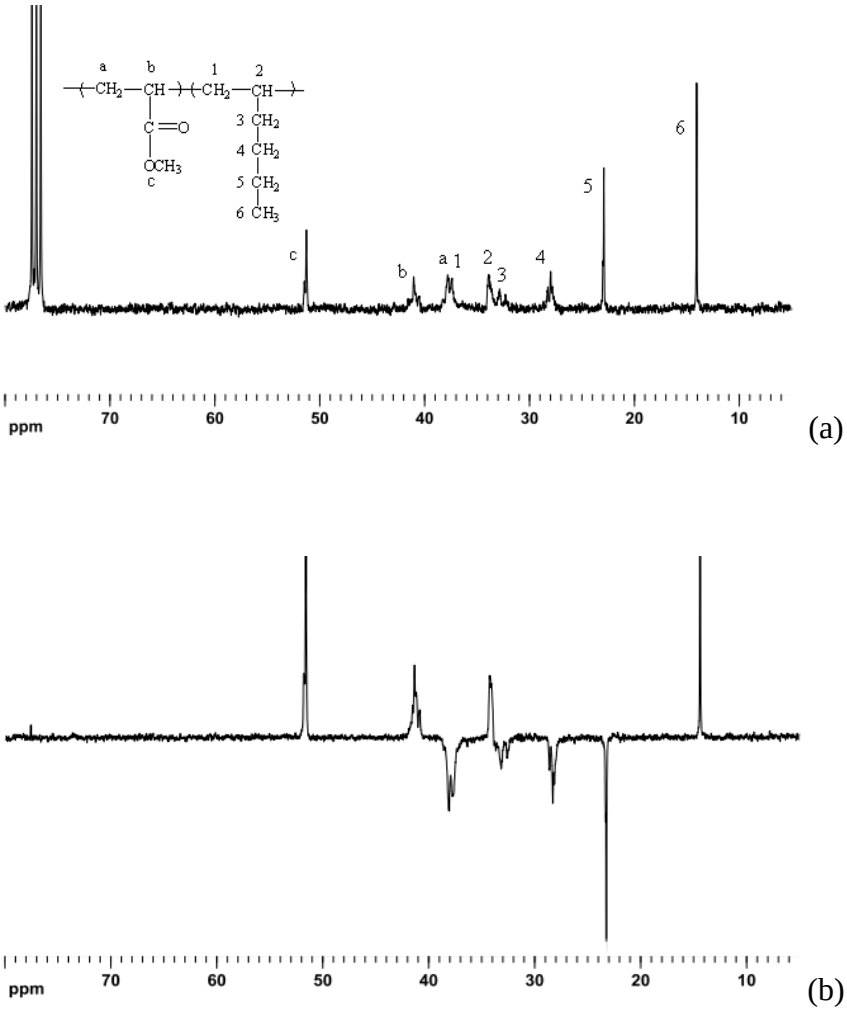

Figure 3.7 NMR of MA/1-hexene copolymer (25 ^{o}C, $CDCl_3$, MA molar fraction 55 %). (a) ^{13}C NMR, (b) ^{13}C DEPT135 NMR.

3.3 CONCLUSIONS

The effect of Lewis acids on the reactivity ratios for (meth)acrylate/non-polar olefin radical copolymerizations was investigated. The reactivity ratio r_1 for both MA and MMA decreases in the presence of Lewis acids; olefin reactivity ratio r_2 is close to zero. The substantial decrease in r_1 values and an increased polymerization rate demonstrate that Lewis acids promote (meth)acrylate cross-propagation significantly more than self-propagation, especially for MA. Furthermore, due to (a) enhanced binding of the Lewis acid to the carbonyl group on the monomer compared to those on the polymer and (b) the facile exchange of the Lewis acid between the monomer and the polymer, only a catalytic amount to Lewis acid is required to strongly influence alkene uptake and copolymerization rate.

Consistent with an r_2 value of zero, hexene and norbornene do not undergo self-propagation under our conditions. This limits the highest incorporation of these and related non-polar olefin in the copolymers with (meth)acrylates to 50 mol%. At the other extreme, Brookhart, Drent, and others have shown that metal-catalyzed insertion polymerization of alkenes with acrylates (but not methacrylates) can lead to copolymers with alkene content of 100-85 mol%.[15-18] This leaves a "35 mol% gap" in the compositions that are not readily accessible through the copolymerization of acrylates with olefin.[19] The composition gap is even higher for methacrylates since they do not participate in metal-catalyzed insertion polymerizations due to rapid β-hydrogen elimination following insertion.[20-22]

3.4 EXPERIMENTAL SECTION

3.4.1 MATERIALS

All chemicals and reagents were obtained from Aldrich unless otherwise stated. Methyl acrylate (MA, 99%), methyl methacrylate (MMA, 99%), 1-hexene (97%) and cyclohexene (99%) were passed through basic alumina column to remove the inhibitor and impurities, then degassed and stored under N_2. Tetrachloroethane was degassed and stored under N_2. 2,2'-Azobis(isobutyronitrile) (AIBN, 98%), titanium chloride ($TiCl_4$, 99.9%), aluminum chloride ($AlCl_3$, anhydrous, 99.99%, Strem Chemicals), and scandium(III) trifluoromethanesulfonate ($Sc(OTf)_3$, Alfa Aesar, 98%) were used as received.

3.4.2 INSTRUMENTATION

NMR spectra were recorded using a Bruker 300-DPX spectrometer at ambient temperature (^{1}H-NMR, 300MHz; ^{13}C-NMR, 75 MHz). Chemical shifts are referenced to $CDCl_3$. Gas chromatography analysis was performed on an Agilent 5890 Series II GC. The samples were heated from 40 ^{o}C to 100 ^{o}C at a ramp rate of 5 ^{o}C/min. Molecular weights and molecular weight distributions were determined on a Shimadzu gel permeation chromatography (GPC) chromatograph containing a three-column bed (styragel HR 7.8 × 300 mm columns with 5 μm beads size; 100-5000, 500-30,000, and 2,000-4 × 10^6 Da), a Shimadzu RDI-10A differential refractometer, and a Shimadzu SPD-10A tunable absorbance detector (254 nm). GPC samples were run in tetrahydrofuran at a flow rate of 1 ml/min at 35 ^{o}C and calibrated against polystyrene standards. Analysis was done using EZSTART 7.2 software.

3.4.3 COPOLYMERIZATION OF (METH)ACRYLATE WITH NON-POLAR OLEFIN

In a typical experiment, in a N_2-filled glove box, AIBN (0.005 g), MMA (0.3 g), $AlCl_3$ (0.04 g), 1-hexene (2.27 g) and toluene (5 mL) were added into a 20 mL scintillation vial. The vial was sealed, removed from glove box. Then the reaction mixture was allowed to stir in a 60 ^oC oil bath for a certain amount of time until it reaches desired monomer conversion (< 8%). The resulting polymer was precipitated in 200 mL methanol and collected by centrifugation, then dissolved in dichloromethane and precipitated again in methanol to remove impurities. The product was finally dried under high vacuum overnight. The copolymer composition was determined from ^1H-NMR integration of the methoxy protons versus all the aliphatic resonances. Other copolymerization reactions were conducted similarly by varying the feed of 1-hexene or norbornene, while keeping MMA feed constant.

3.4.4 KINETIC STUDY OF METHACRYLATE HOMOPOLYMERIZATION IN THE PRESENCE OF LEWIS ACIDS

In a N_2-filled glove box, MMA (0.3 g), AIBN (0.005 g), $AlCl_3$ (0.04 g), toluene (5 mL) and tetrachloroethane (0.05 g) as internal standard were added into a reaction vessel equipped with a magnetic stirring bar. The reaction was stirred in 60 ^oC oil bath for 2 h. GC samples were taken every half hour to determine MMA conversion.

3.4.5 KINETIC STUDY OF METHACRYLATE/OLEFIN COPOLYMERIZATION IN THE PRESENCE OF LEWIS ACIDS

In a N_2-filled glove box, a reaction vessel equipped with a stirring bar was charged with MMA (0.3 g), 1-hexene (0.44 g), AIBN (0.005 g), $AlCl_3$ (0.04 g), toluene (5 mL) and

tetrachloroethane (0.05 g). The reaction vessel was sealed and stirred in 60 ^{o}C oil bath for 4 hours. GC samples were taken at a regular interval to determine MMA and hexene conversions.

3.5 REFERENCES

1. Luo, R.; Sen, A. *Macromolecules* **2007**, *40*, 154-156.
2. Nagel, M.; Poli, D.; Sen, A. *Macromolecules* **2005**, *38*, 7262-7265.
3. Liu, S.; Sen, A. *J. Polym. Sci. Part A: Polym. Chem.* **2004**, *42*, 6175-6192.
4. Luo, R.; Chen, Y.; Sen, A. *J. Polym. Sci Part A* **2008**, *46*, 5499-5505.
5. Lee, H.-Y.; Herman, M. S.; Padias, A. B.; Hall, H. K.; Tack, J. R. D. Acta Polymerica **1994**, *45*, 413-418.
6. Braun, D.; Manger, E. *Angew. Makromolekulare Chemie* **1986**, *145*, 101-124.
7. Lutz, J. F.; Kirci, B.; Matyjaszewski, K. *Macromolecules* **2003**, *36*, 3136-3145.
8. Lutz, J.-F.; Neugebauer, D.; Matyjaszewski, K. *J. Am. Chem. Soc.* **2003**, *125*, 6986-6993.
9. Ray, B.; Isobe, Y.; Matsumoto, K.; Habaue, S.; Okamoto, Y.; Kamigaito, M.; Sawamoto, M. *Macromolecules* **2004**, *37*, 1702-1710.
10. Yutaka Isobe, T. N. Y. O. *J. Polym. Sci., Part A: Polym. Chem.* **2001**, *39*, 1463-1471.
11. Tüdős, F.; Kelen, T.; Földes-Berezhnykh, T.; Turcsányi, B. *Reaction Kinetics and Catalysis Letters* **1975**, *2*, 439-447.
12. van Herk, A. M.; Dröge, T. *Macromol. Theory Simul.* **1997**, *6*, 1263-1276.
13. Subramanyam, U.; Rajamohanan, P. R.; Sivaram, S. *Polymer* **2004**, *45*, 4063-4076.
14. Liu, S.; Gu, B.; Rowlands, H.; Sen, A. *Macromolecules* **2004**, *37*, 7924-7929.
15. Gibson, V. C.; Spitzmesser, S. K. *Chem. Rev.* **2003**, *103*, 283-316.
16. Ittel, S. D.; Johnson, L. K.; Brookhart, M. *Chem. Rev.* **2000**, *100*, 1169-1204.
17. Mecking, S.; Johnson, L. K.; Wang, L.; Brookhart, M. *J. Am. Chem. Soc.* **1998**, *120*, 888-899.

18. Drent, E.; van Dijk, R.; van Ginkel, R.; van Oort, B.; Pugh, R. I. *Chem. Commun*. **2002**, 744-745.

19. Sen A.; Borkar, S. *J. Organomet. Chem.*, **2007**, *692*, 3291-3299.

20. Elia, C.; Elyashiv-Barad, S.; Sen, A.; Lopez-Fernandez, R.; Albeniz, A. C.; Espinet, P. *Organometallics*, **2002**, *21*, 4249-4256.

21. Gibson, V. C.; Tomov, A. *Chem. Commun*. **2001**, 1964-1965.

22. Borkar, S.; Yennawar, H.; Sen, A. *Organometallics*, **2007**, *26*, 4711-4714.

CHAPTER 4. SYNTHESIS OF ASYMMETRIC PALLADIUM COMPLEXES AND THEIR USE IN ETHYLENE HOMOPOLYMERIZATION AND FUNCTIONAL NORBORNENE COPOLYMERIZATION

4.1 INTRODUCTION

Cyclic olefin copolymers (COC) are a class of amorphous, transparent copolymers comprised of cyclic olefins and linear olefins. Among them, ethylene/norbornene (E-N) copolymer is one of the most commercialized copolymers. Due to its unique properties, such as high transparency, excellent water vapor barrier property, biocompatibility, high rigidity and strength, E-N copolymer is used in pharmaceuticals packaging, diagnostic disposable, moldings for optical lenses and etc. Generally group 4 metallocenes/MAO[1] and late transition metal[2-4] (Ni and Pd) catalysts were used to synthesize E-N copolymers, and recently cationic rare-earth metal complexes[5] have been reported for the synthesis of such copolymers. However, to copolymerize ethylene with polar functional norbornenes, group 4 catalysts require a pretreatment of the polar functional norbornene[6-8] or a post reaction conversion[9], only late transition metal catalysts have the tolerance toward polar functional norbornenes[2,3,10-13]. Studying late transition metal systems would extend the E-N copolymer properties by directly incorporating functional groups into this copolymer. In this study, two asymmetric palladium catalysts have been synthesized, characterized and tested on their catalyst activities for ethylene/functional norbornene copolymerizations, ethylene homopolymerizations as well as CO/norbornene copolymerizations. Both catalysts exhibited high activity in ethylene/functional norbornene copolymerizations, resulting nearly alternating copolymer product. Reaction mechanism was probed by studying the ^{13}C NMR

spectra of CO/norbornene step by step insertion, and by studying the relationship between monomer feed and product molecular weight. Furthermore, these two catalysts can serve as a scaffold to synthesize novel asymmetric late transition metal catalysts.

4.2 RESULTS AND DISCUSSION

4.2.1 SYNTHESIS AND CHARACTERIZATION OF ASYMMETRIC PALLADIUM CATALYSTS

The synthesis routes of three palladium complexes are shown in figure 4.1. These Pd complexes were characterized by ^{1}H NMR spectra and X-ray crystallography. Figure 4.2 to figure 4.5 shows the crystal structure of the three complexes and ligand **1**. Under N_2 atmosphere, complex **a** and **c** are stable at room temperature for weeks, but complex **b** would decompose at R.T. within 3 days. Regarding to their activity in polymerization, complex **c** showed no activity in ethylene homo- or copolymerization, possibly because the bonding between TMEDA and Pd center was so strong that it prevented ethylene insertion to occur. The polymerization experiment results of complex **a** and **b** are discussed in the following sections.

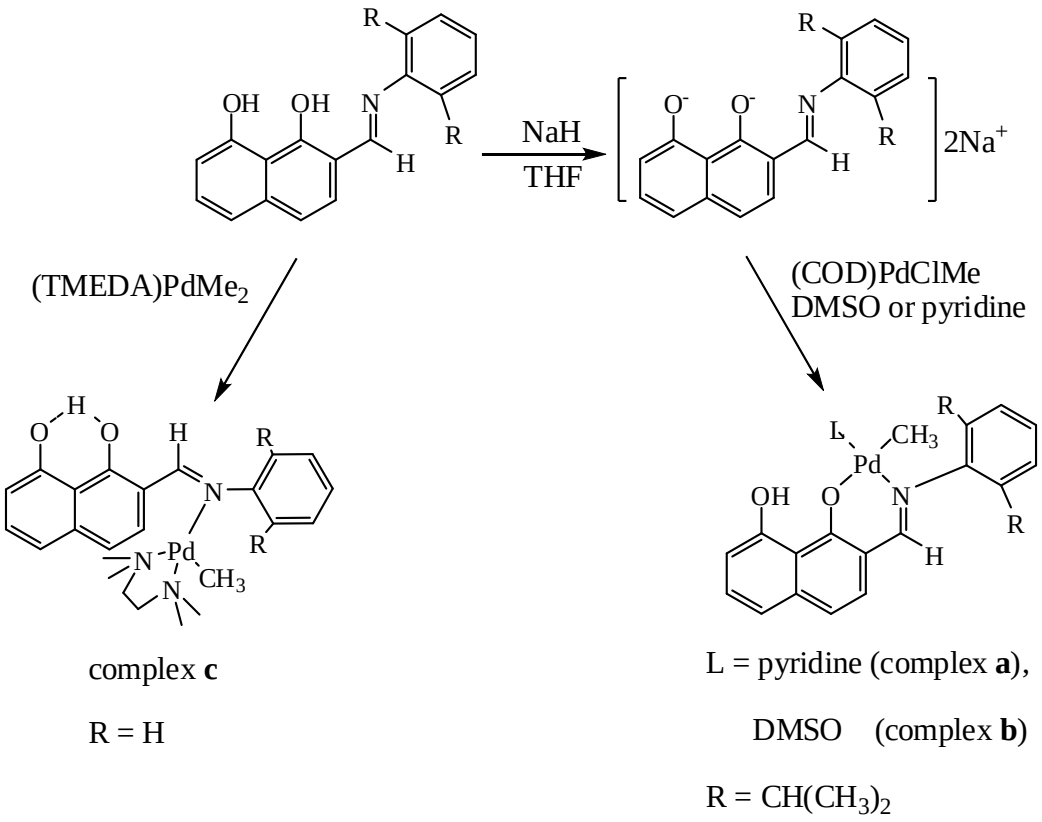

Figure 4.1 Synthesis of asymmetric Palladium complexes **a**, **b** and **c**

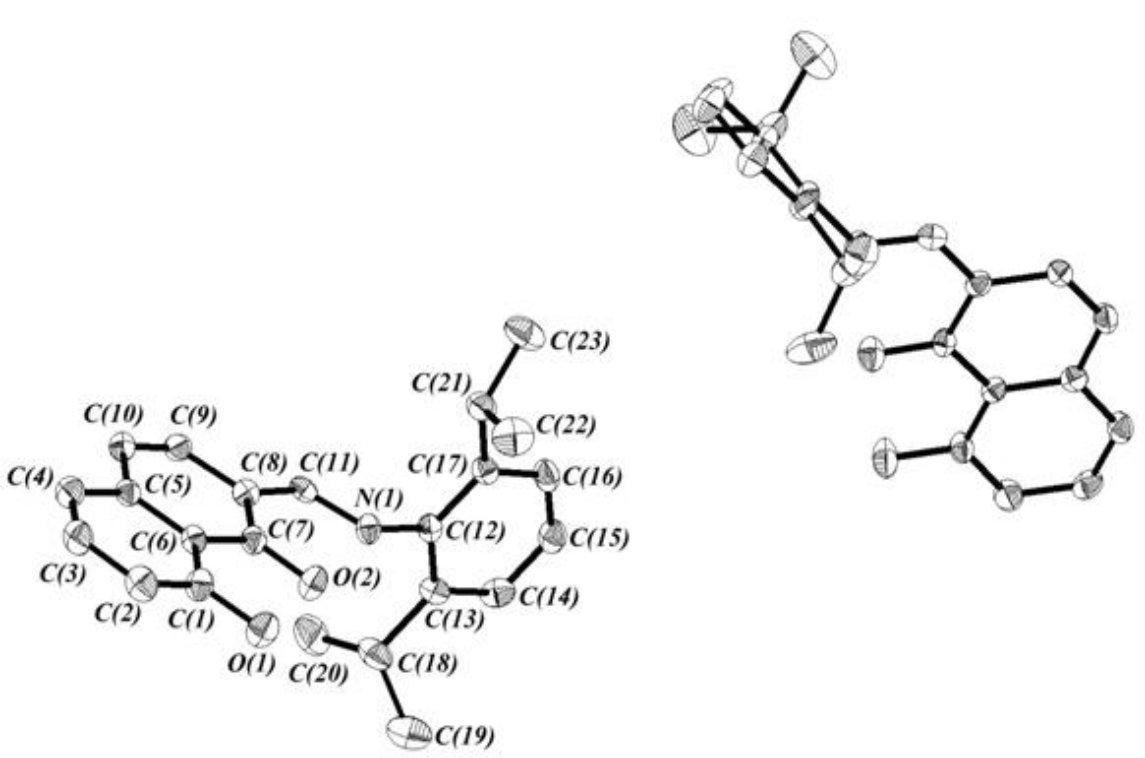

Figure 4.2 ORTEP diagram of ligand **1** (Thermal ellipsoids are given at 50% probability).

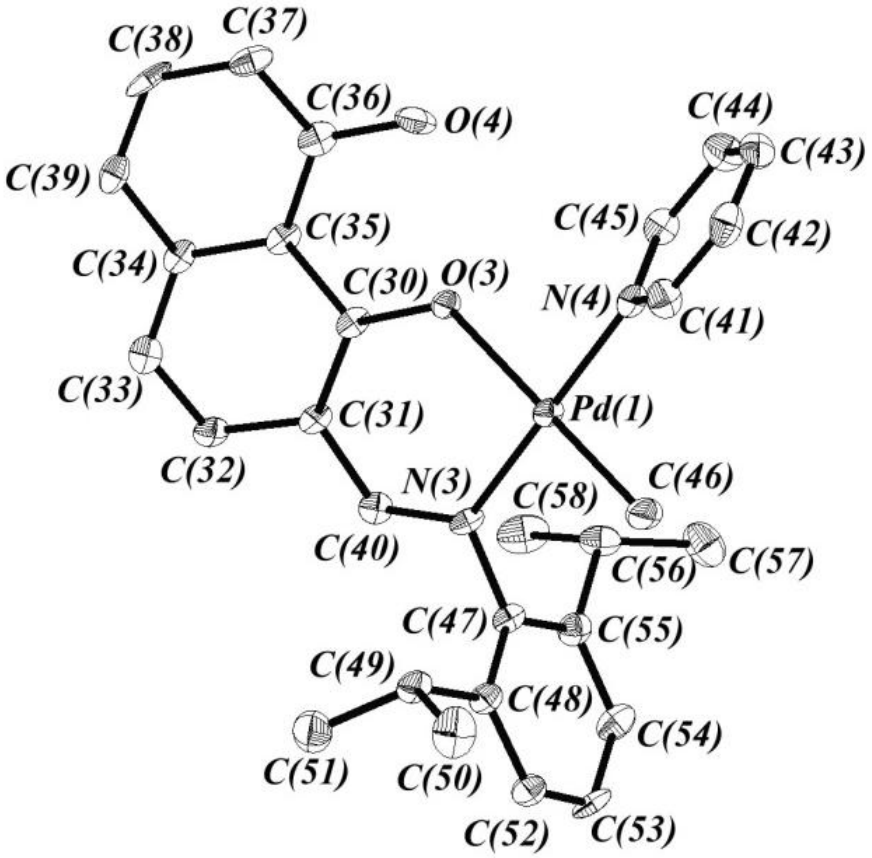

Figure 4.3 ORTEP diagram of complex **a** (Thermal ellipsoids are given at 50% probability).

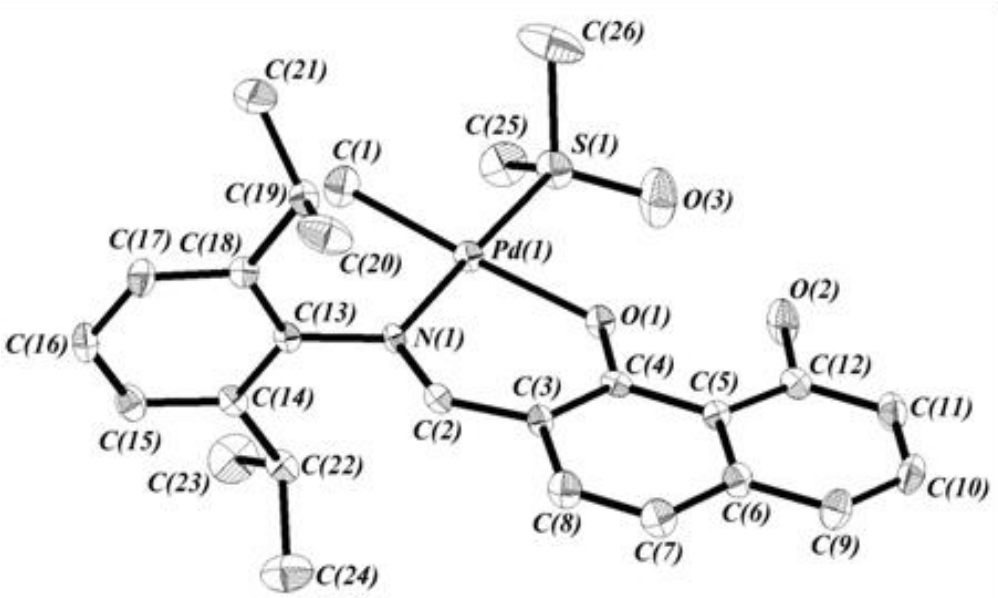

Figure 4.4 ORTEP diagram of complex **b** (Thermal ellipsoids are given at 50% probability).

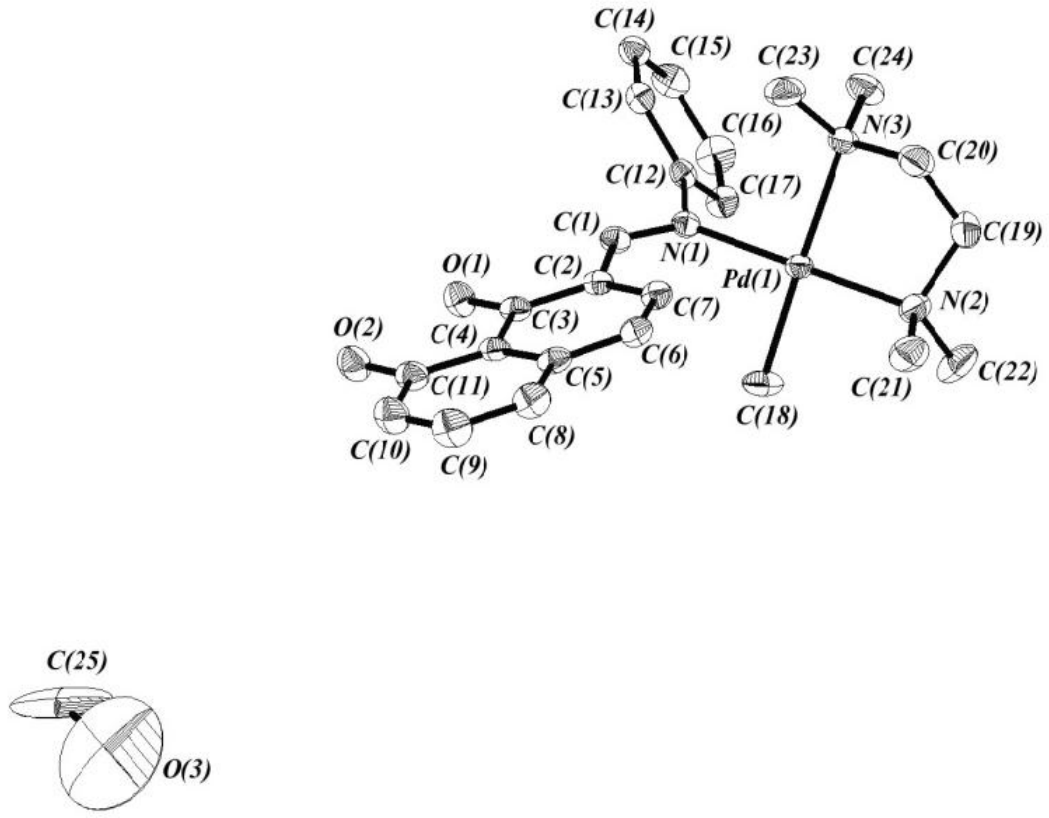

Figure 4.5 ORTEP diagram of complex **c** with a CH_3OH molecule (Thermal ellipsoids are given at 50% probability).

4.2.2 ETHYLENE HOMOPOLYMERIZATION

Due to the poor stability of complex **b**, the reactions with **b** as catalyst were conducted at 30 ^{o}C. Table 4.1 summarizes the experiment results of ethylene polymerization with complex **a** and **b**. The activity of complex **a** increased at higher reaction temperature. However, complex **a** only produced ethylene oligomers with molecular weight (M_n) less than 700, and the addition of co-catalyst BPh_3 did not increase catalyst activity. The presence of ethylene accelerated the decomposition of complex **b**, after 2 hours complex **b** turned black and ethylene polymerization did not happen. The oligomers synthesized in entry 1-3 (table 4.1) were highly branched[14-16], as proven by ^{13}C NMR in figure 4.6. It suggested that "chain walking" and β-H elimination occurred in the polymerization process[15].

Table 4.1 Ethylene homopolymerization experiments with Pd complex **a** and **b**[a]

Entry	Catalyst	Co-catalyst	T (^{o}C)	Yield (g)	Activity (kg/mol[Pd] h)	Mn[b]	PDI[b]
1	a	--	60	0.15	2.6	631	1.3
2	a	--	90	0.95	15.8	340	1.6
3	a	BPh_3	90	0.29	5.0	172	1.7
4	b	--	30	0	---	---	---

[a]Conditions: Pd complex, 0.03 mmol; toluene, 5 mL; BPh_3, 0.06 mmol; ethylene, 300 psi; reaction time, 2 hours. [b]Determined by GPC using polystyrene standards.

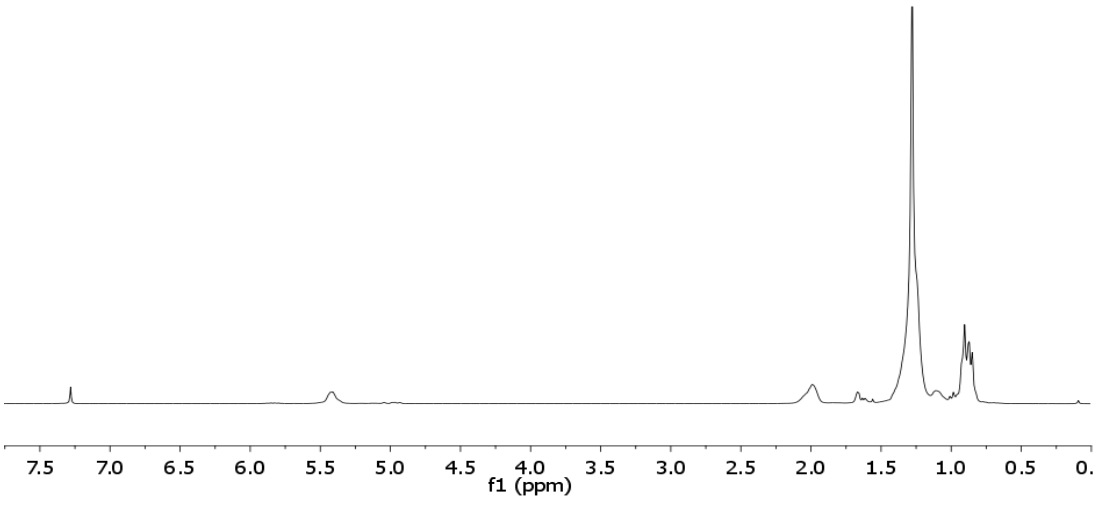

(a)

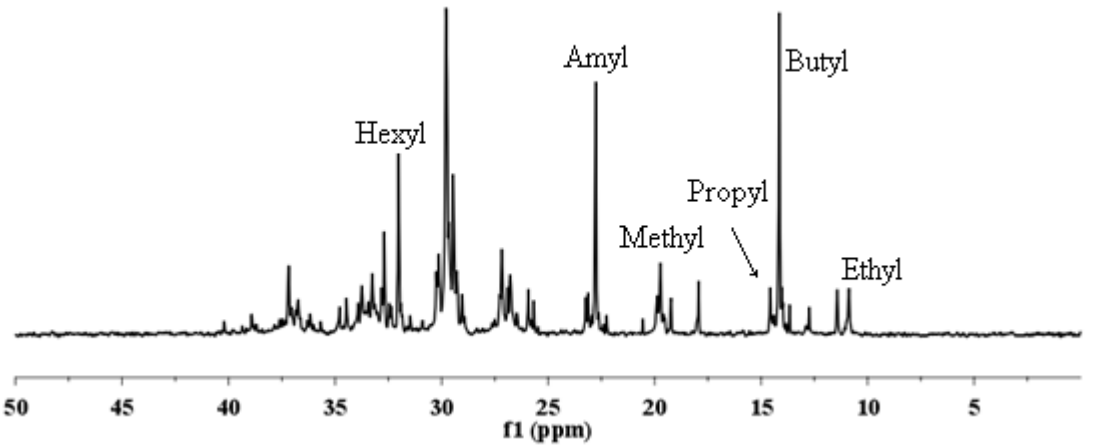

(b)

Figure 4.6 ^{1}H and ^{13}C NMR spectra of ethylene oligomers synthesized by complex **a**. (a) ^{1}H NMR; (b) ^{13}C NMR (Samples from entry 2, table 4.1; NMR was performed in $CDCl_3$ at 25 ^{o}C).

4.2.3 ETHYLENE/NORBORNENE COPOLYMERIZATION

Both complex **a** and **b** demonstrated much higher activity in ethylene/norbornene copolymerization than in ethylene or norbornene homopolymerizations. Table 4.2 presents some selected copolymerization experiment results. Depending on the solubility of the copolymers, their NMR spectra were performed in either $CDCl_3$ or toluene-d_8 at 25 ^oC, or in tetrachloroethene-d_4 at elevated temperature. Ethylene/5-norbornene-2-methanol copolymer was integrated by ^1H NMR spectrum against $-CH_2$-OH proton integration; the rest of the copolymers were integrated by ^{13}C NMR spectra, and figure 4.7 provides a typical ^{13}C NMR spectrum of ethylene/norbornene copolymer. From the simple ethylene unit peak at 31 ppm, it could be determined that the copolymer had a linear structure. Both catalysts had low activity toward norbornene homopolymerization, as seen in entry 1 and 10 in table 4.2. The low activity was likely due to the bulkiness of norbornene monomer, which made sequential norbornene unites hard to obtain. By a controlled experiment with radical trap galvinoxyl (entry 2, table 4.2), the radical mechanism of norbornene homopolymerization was ruled out. Because the presense of galvinoxyl did not reduce the product yield. Compare entry 1 and 4 in table 4.2, the addition of ethylene resulted in more than 30-fold increase of activity. This suggested that in norbornene copolymerization, the bulkiness of norbornene inhibited another norbornene monomer to insert, but ethylene insertion was allowed. The insertion of ethylene relived the crowdness near Pd center, thus enabling next norbornene or ethylene insertion to occur. Compare entry 3 and 4, a four times increase in norbornene feed only boosted norbornene mole incorporation from 42.3% to 43.5%, which proved that sequential norbornene insertion was unlikely to happen. Besides, given the same reaction conditions, the copolymer yield and composition appeared closely related to norbornene feed rather than

reaction temperature (entry 4 and 5, table 4.2). Ethylene/functional norbornene copolymerizations were also investigated. For non-polar norbornene derivative and norbornene, both catalyst **a** and **b** provided similar activity. Catalyst **a** showed better tolerance toward polar norbornene derivatives. In all the cases, norbornene incorporation was less than 50%. Propene/norbornene copolymerization was studied using complex **a**, however, the product yield and norbornene incorporation were lower than ethylene/norbornene copolymerization results.

Table 4.2 Ethylene/functional norbornene copolymerization[a]

Entry	Catalyst	Ethylene (psi)	NB derivative (g)	T (^oC)	Yield (g)	NB incorp. (mol%)[b]	Activity (kg/mol[Pd] h)
1	a	0	Nb, 2	30	0.07	---	1.2
2[c]	a	0	Nb, 2	30	0.06	---	1.0
3	a	300	Nb, 0.5	30	0.63	42.3	10.5
4	a	300	Nb, 2	30	2.67	43.5	44.5
5	a	300	Nb, 2	90	2.34	42.0	39.0
6[d]	a	300	5-Nb-2-nC_4H_9, 2	90	2.29	42.4	38.2
7[d]	a	300	5-Nb-2-tBu ester, 2	90	1.20	32.6	20.0
8	a	300	5-Nb-2-CH_2OH, 2	90	1.00	34.7	16.7
9	a	Propene 125 psi	Nb, 2g	90	0.11	18.1	1.9
10	b	0	Nb, 2	30	0.16	--	2.7
11	b	300	Nb, 2	30	2.53	48.5	42.2
12[d]	b	300	5-Nb-2-nC_4H_9, 2	30	2.35	42.2	39.2
13[d]	b	300	5-Nb-2-tBu ester, 2	30	0.30	32.1	5.0
14	b	300	5-Nb-2-CH_2OH, 2	30	0.45	34.8	7.5

[a]Conditions: Pd complex, 0.03 mmol; toluene 5 mL; reaction time, 2 hours. [b]Entry 8 and 14 were determined by ^1H NMR in $C_2D_2Cl_4$ at 115 ^oC; entry 3 and 11 were determined by ^{13}C NMR in $C_2D_2Cl_4$ at 115 ^oC; entry 6, 7, 12 and 13 were determined by ^{13}C NMR in $CDCl_3$ at 25 ^oC; entry 4 and 5 were determined by ^{13}C NMR in toluene-d_8 at 25 ^oC; entry 9 was determined by CHN analysis provided by Galbraith Laboratories. [c]In the presence of 1.5

equivalents of galvinoxyl to Pd. [d]Molecular weight (M_n) and PDI were determined by GPC using polystyrene standards, entry 6, $M_n = 17 \times 10^3$, PDI = 2.33; entry 7, $M_n = 28 \times 10^3$, PDI = 1.55; entry 12, $M_n = 65 \times 10^3$, PDI = 1.27; entry 13, $M_n = 18 \times 10^3$, PDI = 1.65.

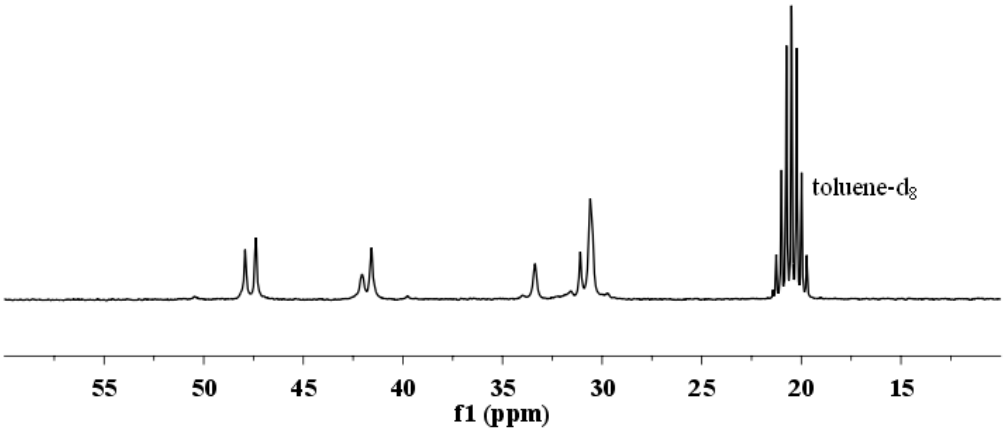

Figure 4.7 ^{13}C NMR spectrum of ethylene/norbornene copolymer (Samples from entry 4, table 4.2, norbornene 43.5 mol%; NMR was performed in toluene-d_8 at 25 ^{o}C).

4.2.4 COPOLYMERIZATION OF POLAR MONOMERS WITH NON-POLAR OLEFIN

Catalysts **a** is active to copolymerize CO/ethylene and CO/norbornene, and the product copolymers are likely to have an alternating structure. Methyl acrylate (MA)/norbornene copolymerization and MA homopolymerization were studied using complex **a** catalyst, the mechanism was radical polymerization[3,17], the addition of radical trap galvinoxyl would shut down these reactions (entry 5 and 7, table 4.3). The MA/norbornene copolymer structure was confirmed by ^{13}C NMR, the existence of 37 ppm (non-sequential MA CH_2 carbon) peak proved that it had MA-norbornene units[18]. For norbornene/CO copolymerization, the mechanism was insertion, the addition of galvinoxyl hardly effected the reaction (entry 2, table 4.3). The copolymerization process was studied by ^{1}H and ^{13}C NMR as following.

Table 4.3 Copolymerization of polar monomers with non-polar olefin[a]

Entry	Catalyst	Polar monomer (psi or g)	Olefin (psi or g)	T (^{o}C)	Yield (g)	Olefin incorp.[b] (mol%)	Activity (kg/mol[Pd] h)
1	a	CO, 50	Nb, 2	90	0.77	53.8	12.9
2[c]	a	CO, 50	Nb, 2	90	0.64	--	--
3	a	CO, 50	C_2H_4, 300	90	0.40	50.0	6.7
4	a	MA, 2	Nb, 2	50	0.20	21.5	---
5[c]	a	MA, 2	Nb, 2	50	0.02	96.5	---
6	a	MA, 3	0	50	0.84	---	---
7[c]	a	MA, 3	0	50	0	---	---

[a]Conditions: Pd complex, 0.03 mmol; toluene 5 mL; reaction time, 2 hours (entry 1-3), 15 hours (entry 4-7). [b]Entry 1 and 2 were determined by CHN analysis provided by Galbraith Laboratories; entry 3 was determined by ^{1}H NMR in $CDCl_3$ at 25 ^{o}C, and 1,1,1,3,3,3-hexafluoro-2-propanol was added to dissolve the copolymer; entry 4-5 was determined by ^{1}H NMR in C_6D_6 at 25 ^{o}C. [c]In the presence of 1.5 equivalents of galvinoxyl to Pd.

In CO/norbornene copolymerization ^{1}H NMR study, regular CO (40 psi) was added to a high pressure NMR tube containing complex **a** (0.01 mmol) solution in acetone-d_6. Intermediate of one step CO insertion was observed, as shown in figure 4.8. The Pd-CH_3 proton peak (0.06 ppm) disappeared after CO was added, and a new Pd-CO-CH_3 peak showed up at 1.7 ppm. In ^{13}C NMR study, ^{13}CO was used and multiple insertion steps could be observed as shown in figure 4.9. In the first step, ^{13}CO (40 psi) was added to a high pressure NMR tube containing complex **a** (0.01 mmol) solution in C_6D_6, and ^{13}C-NMR spectrum was taken. The ^{13}C NMR spectrum (figure 4.10 (a)) shows the inserted ^{13}CO (C^1) at 230.5 ppm and free ^{13}CO at 184.4 ppm. At the same time, ^{1}H NMR indicates that the originally coordinated pyridine was freed from Pd center. In the second step, free ^{13}CO was released and then around 0.5 equivalent norbornene to Pd was added to the solution. When the norbornene insertion was complete, ^{13}C NMR spectrum (figure 4.10 (b)) was taken and it provided a new carbon peak (C^2) at 235.1 ppm. The facts, that C^2 had a very downfield chemical shift and the absence of coordinated pyridine peak in ^{1}H NMR, suggested that C^2 was bonding with Pd center. After the second step, ^{13}CO (40 psi) was added again into the solution. In ^{13}C NMR spectrum (figure 4.10 (c)), C^2 was replaced by C^3 (231.7 ppm) and C^4 (206.7 ppm). The insertion of CO was a reversible process, as proved by step 4. The release of free ^{13}CO promoted the formation of C^2, so the C^2 (235.0 ppm) peak appeared again in figure 4.10 (d). In the last step, extra norbornene (2 equivalents to Pd) was added into the solution. Due to the stereo bulkiness of norbornene, the formation of sequential norbornene unites was not favored, therefore only two kinds of Pd compounds existed. And newly formed C^5 (239.5 ppm) and C^6 (207.3 ppm) replaced C^3 and C^4. The ^{13}C NMR spectra

illustrate the synthesis of alternation norbornene/CO copolymer, also prove that it is unlikely to have sequential CO or sequential norbornene unites.

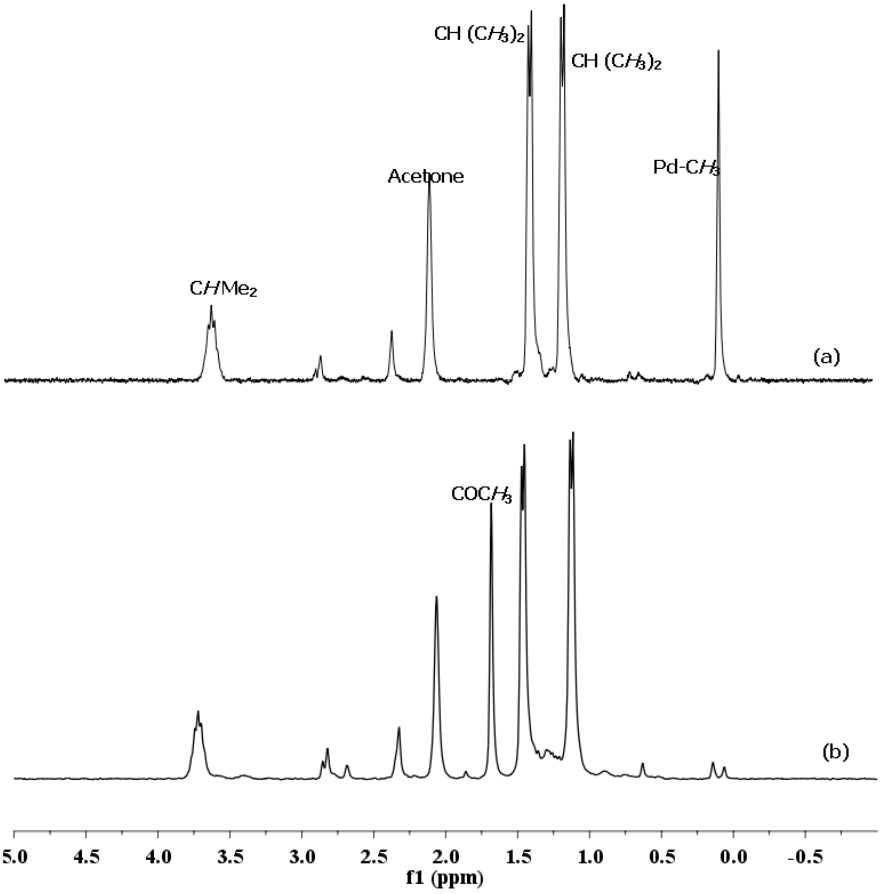

Figure 4.8 ^{1}H NMR spectra of CO insertion to complex **a**. (a) before CO insertion; (b) after CO insertion (NMR was conducted in acetone-d_6 at 25 ^{o}C).

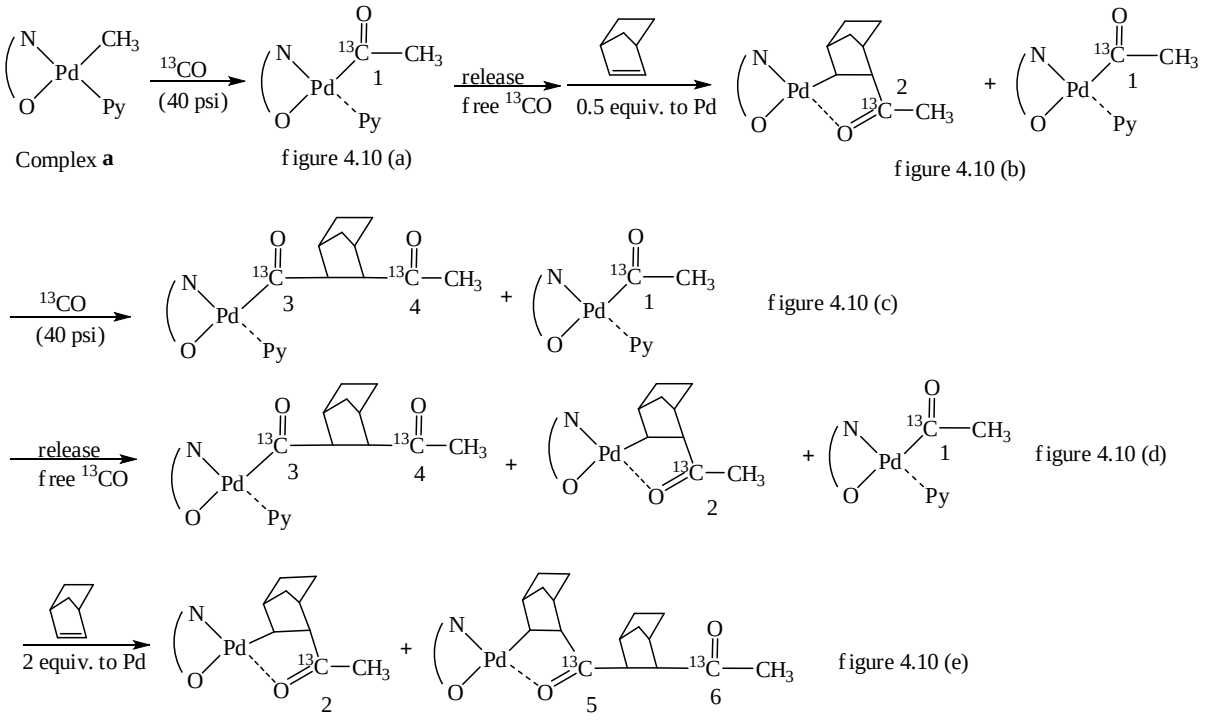

Figure 4.9 Illustration of step by step insertion of ^{13}CO and norbornene to complex **a**.

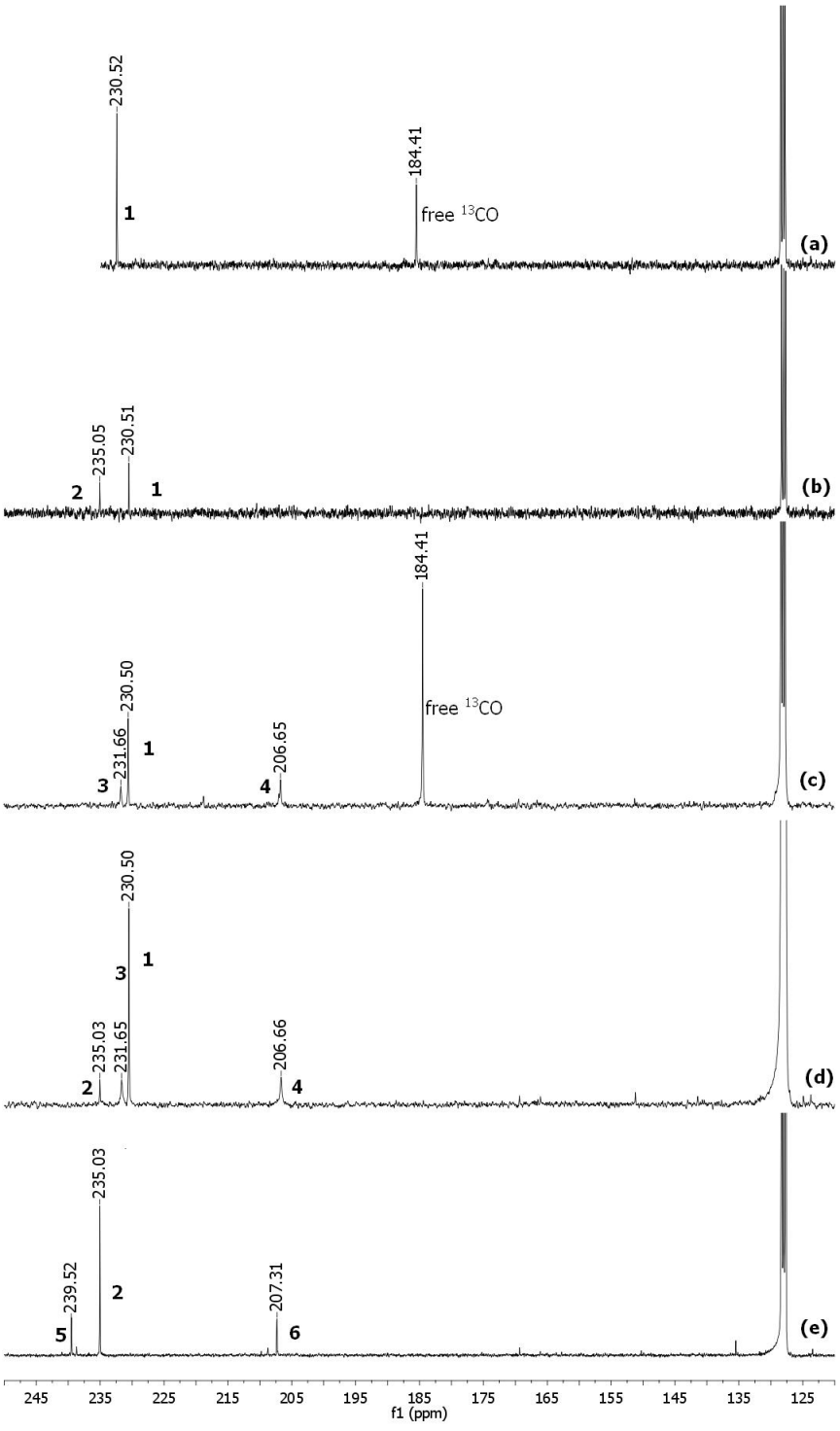

Figure 4.10 ^{13}C NMR spectra of ^{13}CO and norbornene step by step insertion to complex **a** (Insertion sequence was given in figure 4.9, and NMR was conducted in C_6D_6 at 25 ^oC).

4.2.5 THE INFLUENCE OF NORBORNENE FEED AND ETHYLENE PRESSURE ON COPOLYMER M_N USING CATALYST b

Ethylene/5-Nb-2-nC_4H_9 copolymerization was studied in this case, considering the solubility of the copolymer in GPC solvent THF at room temperature. The experiment results are summarized in table 4.4. Compare entry 1-3, the increase in norbornene feed lead to an increase in copolymer molecular weight M_n. On the other hand, compare entry 4-6, the decrease of ethylene pressure also lead to higher M_n. Taking this fact and previous ethylene polymerization data, the following polymerization mechanism was proposed as figure 4.11. By increasing ethylene pressure, the chance of β-H elimination became larger, hence lower M_n of the copolymer. Conversely, when norbornene feed was increased the chance of β-H elimination became smaller, which gave longer polymer chain. The β-H elimination resulted catalyst **b** decomposition was the reason that complex **b** could not catalyze ethylene homopolymerization.

Table 4.4 Influence of norbornene feed and ethylene pressure on copolymer molecular weight (M_n) using catalyst **b**[a]

Entry	Ethylene (psi)	Norbornene (g)	Yield (g)	Nb incorp.[b] (mol%)	M_n[c] ($x10^{-3}$)	PDI[c]
1	300	5-Nb-2-nC_4H_9, 0.5	0.57	30.6	22	1.21
2	300	5-Nb-2-nC_4H_9, 1	1.13	41.2	47	1.11
3	300	5-Nb-2-nC_4H_9, 2	2.35	42.2	64	1.25
4	500	5-Nb-2-nC_4H_9, 2	2.39	36.5	61	1.38
5	300	5-Nb-2-nC_4H_9, 2	2.35	42.2	64	1.25
6	100	5-Nb-2-nC_4H_9, 2	2.57	43.5	89	1.22

[a]Conditions: complex **b**, 0.03 mmol; toluene, 5 mL; reaction temperature, 30 ^oC; reaction time, 2 hours. [b]Determined by ^{13}C NMR spectrum in $CDCl_3$ at 25 ^oC. [c]Determined by GPC using polystyrene standards.

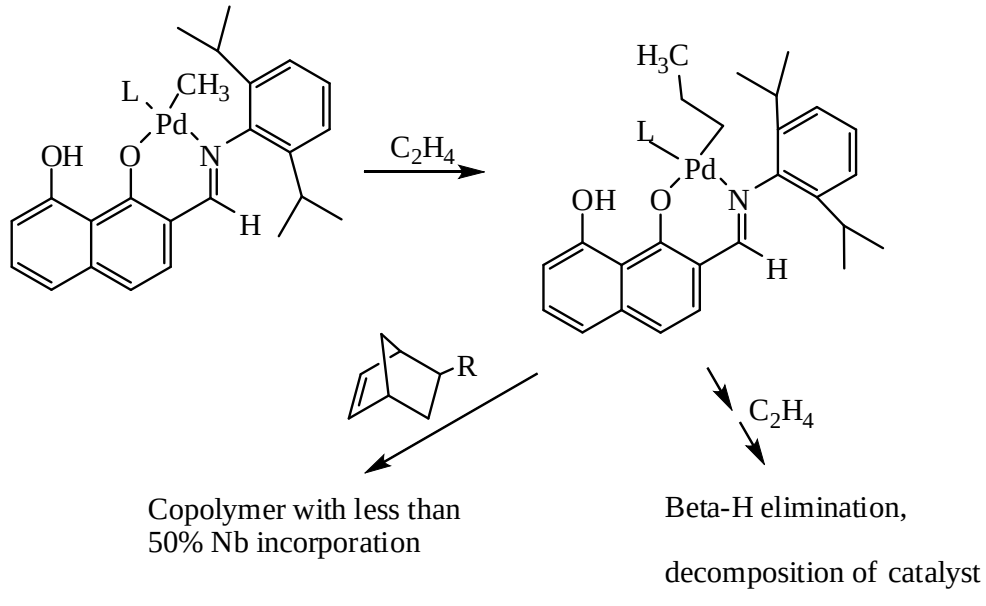

Figure 4.11 Possible polymerization mechanism for catalyst **b**

4.2.6 STUDY OF THE CATALYST PREFERENCE OF *ENDO/EXO* ISOMERS

The relative uptake of *endo/exo* norbornene derivative isomers was investigated by gas chromatograph. Some selected data are presented in table 4.5. Similar to many other palladium catalysts[3], catalyst **a** and **b** showed a small preference over *exo* isomers. When the monomer conversion is less than 40%, the selectivity was negligible. However, when monomer conversion was high (90%), the *endo* isomer would be left over.

Table 4.5 *Endo/exo* ratio of norbornene derivatives before and after ethylene/norbornene copolymerization[a]

Entry	Catalyst	Norbornene derivative	T (^{o}C)	Nb conversion (mol %)[b]	*Endn/Exo* before reaction[b]	*Endn/Exo* after reaction[b]
1	a	5-Nb-2-tBu ester	90	44	63/37	66/34
2	a	5-Nb-2-CH_2OH	90	35	60/40	69/31
3	a	5-Nb-2-nC_4H_9	90	92	67/33	100/0
4	b	5-Nb-2-tBu ester	30	15	63/67	65/35
5	b	5-Nb-2-CH_2OH	30	16	60/40	68/32

[a]Conditions: palladium complex, 0.03 mmol; ethylene, 300 psi; norbornene derivative, 2 g; toluene, 5 mL; chlorobenzene, 0.15 g as internal standard for GC; reaction time, 2 hours. [b]Determined by GC.

4.3 CONCLUSIONS

In conclusion, the synthesis, characterization and polymerization activity of three novel asymmetric palladium complexes are presented. Catalysts **a** and **b** showed high activity toward ethylene/functional norbornene copolymerizations, and they have small preference to *exo* isomers. Step by step CO/norbornene insertion to catalyst **a** was observed by ^{13}C NMR spectra. It was also proven that the M_n of the copolymer could be adjusted by changing norbornene or ethylene feed. Furthermore, the existence of hydroxyl group on the catalysts provide us many opportunities to modify the catalysts and to explore their catalytic capabilities.

4.4 EXPERIMENTAL SECTION

4.4.1 MATERIALS

All chemicals and reagents were obtained from Aldrich unless otherwise stated. Methyl acrylate (MA, 99%) was passed through basic alumina column to remove the inhibitor and impurities, then degassed and dried with CaH_2. 5-Norbornene-2-carboxylic t-butyl ester (BF Goodrich, 98%), 5-norbornene-2-methanol (98%) and 5-norbornene-2-butyl (BF, Goodrich) were degassed and dried with molecular sieves. Norbornene was degassed. Palladium chloride ($PdCl_2$, 99.9%), pyridine (anhydrous, 99.8%), triphenylphosphine (PPh_3, 99%), galvinoxyl, 2,6-diisopropylaniline (97%) and sodium hydride (NaH, dry, 95%) were used as received. (COD)PdMeCl, (TMEDA)$PdMe_2$[19] and 2-formyl-1,8-naphthalenediol[20,21] were synthesized as literature. All the manipulations of air-sensitive materials were performed in a N_2-filled dry box.

4.4.2 INSTRUMENTATION

^{1}H-NMR (300MHz) and ^{13}C-NMR (75MHz) spectra were recorded using a Bruker 300-DPX spectrometer. Gas chromatography analysis was performed on an Agilent 5890 Series II GC using a RTX-5 split capillary column (Restek) connected to an FID detector. Molecular weights and molecular weight distributions were determined on a Shimadzu gel permeation chromatography (GPC) chromatograph containing a three-column bed (styragel HR 7.8 × 300 mm columns with 5 μm beads size; 100-5000, 500-30,000, and 2,000-4 × 10^6 Da), a Shimadzu RDI-10A differential refractometer, and a Shimadzu SPD-10A tunable absorbance detector (254 nm). GPC samples were run in tetrahydrofuran at a flow rate of 1

ml/min at 35 ^{o}C and calibrated against polystyrene standards. Analysis was done using EZSTART 7.2 software.

4.4.3 SYNTHESIS OF 2-(2,6-DIISOPROPYLPHENYL)IMINO-1,8-DIHYDROXYNAPHTHALENE (LIGAND 1)

2-formyl-1,8-naphthalenediol (361 mg, 1.92 mmol) was dissolved in ethanol (70 ml). Then one drop of formic acid and 2,6-diisopropylaniline (340 mg, 1.92 mmol) were added into the solution. After that the solution was refluxed for 5 hours. Ligand **1** precipitated out while cooling down the ethanol, then it was collected by filtration and washed with cold ethanol. Yield, 90%. ^{1}H NMR (acetone-d_6, 25 ^{o}C, ppm): 14.0 (s, 1H, O-*H*), 13.4 (s, 1H, O-*H*), 8.1 (d, 1H, N=C*H*), 7.5-6.7 (m, 8H, aromatic), 3.2 (m, 2H, C*H*Me$_2$), 1.3 (d, 12H, CH*Me*$_2$).

4.4.4 SYNTHESIS OF 2-(PHENYL)IMINO-1,8-DIHYDROXYNAPHTHALENE (LIGAND 2)

Ligand **2** was synthesized similarly as above by 2-formyl-1,8-naphthalenediol and aniline. Yield, 93%. ^{1}H NMR (acetone-d_6, 25 ^{o}C, ppm): 14.0 (s, 1H, O-*H*), 13.8 (s, 1H, O-*H*), 8.2 (d, 1H, N=C*H*), 7.5-6.7 (m, 10H, aromatic).

4.4.5 SYNTHESIS OF 2-[(2,6-DIISOPROPYLPHENYL)IMINO]-1,8-DIHYDROXYNAPHTHALENEDIOLATE SODIUM SALT (1-Na)

To a solution of **1** (347 mg, 1 mmol) in dry THF (10 ml) was added NaH (240 mg, 10 mmol). The resulting mixture was stirred at room temperature for 2 hours, filtered by a syringe membrane. The solvent was removed, leaving a yellow residue. This salt was immediately used. Yield, 80%. ^{1}H NMR (acetone-d_6, 25 ^{o}C, ppm): 7.4 (s, 1H, N=C*H*), 7.5-

6.7 (m, 8H, aromatic), 3.6 (broad, 2H, C*H*Me_2), 1.3 (broad, 6H, CH*Me*), 1.0 (broad, 6H, CH*Me*).

4.4.6 SYNTHESIS OF PALLADIUM COMPLEX A

To a solution of **1-Na** (295 mg, 0.8 mmol) in toluene (10 ml) was added pyridine (127 mg, 1.6 mmol), then (COD)PdMeCl (424 mg, 1.6 mmol). The mixture was stirred at room temperature for 15 hours, filtered by a syringe membrane. The solvent was removed by vacuum, and complex **a** was obtained as an orange powder. Yield, 85%. ^{1}H NMR (acetone-d_6, 25 ^{o}C, ppm): 13.2 (s, 1H, O-*H*), 8.9 (d, 2H, pyridine), 8.1 (m, 1H, pyridine), 7.9 (s, 1H, N=C*H*), 7.7 (m, 2H, pyridine), 7.4-6.5 (m, 8H, aromatic), 3.6 (m, 2H, C*H*Me), 1.4 (d, 6H, CH*Me_2*), 1.2 (d, 6H, CH*Me_2*), 0.06 (s, 3H, Pd-*Me*).

4.4.7 SYNTHESIS OF PALLADIUM COMPLEX B

To a solution of **1-Na** (147 mg, 0.4 mmol) in toluene (5 ml) was added DMSO (34 mg, 0.44 mmol), then (COD)PdMeCl (212 mg, 0.8 mmol). The mixture was stirred at room temperature for 15 hours, filtered by a syringe membrane. The solvent was removed by vacuum, and complex **b** was obtained as a yellow powder. Yield, 80%. ^{1}H NMR (acetone-d_6, 25 ^{o}C, ppm): 12.8 (s, 1H, O-*H*), 8.1 (s, 1H, N=C*H*), 7.5-6.6 (m, 8H, aromatic), 3.4 (m, 2H, C*H*Me), 3.3 (s, 6H, DMSO), 1.3 (d, 6H, CH*Me_2*), 1.1 (d, 6H, CH*Me_2*), 0.07 (s, 3H, Pd-*Me*).

4.4.8 SYNTHESIS OF PALLADIUM COMPLEX C

(TMEDA)$PdMe_2$ (253 mg, 1 mmol) and ligand **2** (263 mg, 1mmol) were stirred in toluene (10 mL) overnight at 40 ^{o}C. After that the solvent was removed by vacuum, and the solid was washed by hexanes. Complex **c** was obtained as an amber powder. Yield, 88%. ^{1}H

NMR (acetone-d_6, 25 ^{o}C, ppm): 10.3 (d, 1H, N=C*H*), 8.9 (s, 1H, O-*H*), 7.8-6.4 (m, 10H, aromatic), 2.3-2.9 (m, 16H, TMEDA), 0.1 (s, 3H, Pd-*Me*).

4.4.9 GENERAL PROCEDURE FOR ETHYLENE POLYMERIZATION BY PALLADIUM CATALYSTS

In a typical experiment, in a N_2-filled glove box, a glass-lined stainless steel autoclave was charged with palladium complex **a** (16.2 mg, 0.03 mmol) and toluene (5 ml). The autoclave was sealed, removed from glove box, heated in oil bath to desired temperature, then it was charged with ethylene (300 psi constant). The resulting polymer was precipitated out in methanol/HCl, collected and dried in vacuum oven overnight. Ethylene copolymerization procedures were similar to homo-polymerizations.

4.4.10 DETERMINATION OF THE RELATIVE UPTAKE OF *ENDO* VERSUS *EXO* ISOMERS OF FUNCTIONALIZED NORBORNENE

In a typical experiment, in a N_2-filled glove box, a glass-lined stainless steel autoclave was charged with palladium complex **a** (16.2 mg, 0.03 mmol), t-butyl ester norbornene (2g), chlorobenzene (100 mg, as internal reference) and toluene (5 ml). The autoclave was sealed, removed from glove box, heated in oil bath to 90 ^{o}C, and charged with ethylene (300 psi constant). The amounts of unreacted *exo* and *endo* isomers before and after the reaction were determined by GC analysis.

4.4.11 X-RAY CRYSTALLOGRAPHY

Crystals suitable for X-ray analysis were obtained by slowly evaporating their solution in toluene, and for complex **c** small amount of methanol was added into toluene to help dissolve the complex. Crystal data for ligand **1** and complexes **a**, **b** and **c** were given in

table 4.6 to table 4.17. CCDC 750324-750327 contains the supplementary crystallographic data for this paper. These data can be obtained free of charge from The Cambridge Crystallographic Data Centre via www.ccdc.cam.ac.uk/data_request/cif.

The single crystal diffraction data were collected on a Bruker APEX diffractometer with a CCD area detector at 120 K. The X-ray generator was operated at 50 kV and 32 mA using Mo K (λ = 0.71073 Å) radiation. Data were collected with ω scan width of 0.3°. A total 600, 430, 235 and 50 frames were collected in three different settings of φ (0°, 90°, 180°, 270°), keeping the sample-to-detector distance fixed at 6.03 cm and the detector position (2θ) fixed at -25°. The data were reduced using SAINTPLUS1x and an empirical absorption correction was applied using the SADABS2x program. The crystal structure was solved by direct methods using SHELXS97 and refined using SHELXL97 present in the SHELXTL V6.143x package. Because of the disorder, the hydrogen atoms to methanol molecule of compound **c** were unable to be located. The location of hydrogen positions for this molecule was not feasible. All non-hydrogen atoms were easily found from the different Fourier maps was refined anisotropically. For the final refinement, the hydrogen atoms were placed in geometrically ideal positions and refined using the riding mode. Isotropic refinement was employed for the disordered atoms. The last cycles of the refinement included atomic positions, anisotropic thermal parameters for all the non-hydrogen atoms, and isotropic thermal parameters for all the hydrogen atoms. Full-matrix-least-squares structure refinement against F^2 was carried out using the SHELXTL V6.14 package of programs.

Table 4.6 Crystal data and structure refinement for ligand **1**

Identification code	Ligand **1**
Empirical formula	$C_{46}\ H_{50}\ N_2\ O_4$
Formula weight	694.88
Temperature	293(2) K
Wavelength	0.71073 Å
Crystal system	Orthorhombic
Space group	*Pca*2(1) (no. 29)
Unit cell dimensions	a = 15.333(4) Å alpha = 90°
	b = 9.790(3) Å beta = 90°
	c = 25.859(7) Å gamma = 90°
Volume	3882.0(17) $Å^3$
Z	4
Calculated density	1.189 mg/m^3
Absorption coefficient	0.075 mm^{-1}
F(000)	1488
Crystal size	0.10 x 0.08 x 0.08 mm^3
Theta range for data collection	1.57 to 28.29°
Limiting indices	-16<=h<=20, -13<=k<=12, -24<=l<=33
Reflections collected	24315
Unique reflections	7550 [R(int) = 0.0833]
Completeness to theta = 28.29°	98.4 %

Table 4.6, continued

Max. and min. transmission	0.9940 and 0.9925
Refinement method	Full-matrix least-squares on F^2
Data / restraints / parameters	7550 / 1 / 481
Goodness-of-fit on F^2	0.973
Final R indices [I>2sigma(I)]	R1 = 0.0625, wR2 = 0.1189
R indices (all data)	R1 = 0.1134, wR2 = 0.1341
Absolute structure parameter	-1.1(15)
Largest diff. peak and hole	0.427 and -0.281 e.$Å^{-3}$

Table 4.7 Atomic coordinates ($x10^4$) and equivalent isotropic displacement parameters ($Å^2x10^3$) for ligand **1**

	x	y	z	U(eq)
C(1)	1924(2)	2619(4)	4413(1)	28(1)
C(2)	1636(3)	2287(4)	4905(1)	33(1)
C(3)	892(2)	2902(4)	5099(1)	33(1)
C(4)	417(2)	3836(3)	4813(1)	30(1)
C(5)	693(2)	4187(3)	4308(1)	22(1)
C(6)	1457(2)	3571(3)	4104(1)	21(1)
C(7)	1746(2)	3926(3)	3588(1)	24(1)
C(8)	1265(2)	4899(3)	3296(1)	21(1)
C(9)	494(2)	5474(3)	3519(1)	25(1)
C(10)	220(2)	5148(3)	3997(1)	27(1)
C(11)	1548(2)	5308(3)	2808(1)	23(1)
C(12)	2579(2)	5221(3)	2074(1)	20(1)
C(13)	2426(2)	4299(3)	1669(1)	23(1)
C(14)	2793(2)	4618(3)	1189(1)	29(1)
C(15)	3284(2)	5773(3)	1122(1)	30(1)
C(16)	3430(2)	6653(3)	1531(1)	28(1)
C(17)	3084(2)	6392(3)	2018(1)	23(1)
C(18)	1905(3)	3011(3)	1751(1)	35(1)
C(19)	2247(3)	1815(4)	1437(2)	52(1)

Table 4.7, continued

C(20)	940(3)	3279(4)	1629(2)	57(1)
C(21)	3297(2)	7308(3)	2479(1)	29(1)
C(22)	4054(3)	6679(4)	2790(2)	43(1)
C(23)	3530(3)	8781(4)	2332(2)	44(1)
C(24)	9450(2)	7529(3)	2441(1)	25(1)
C(25)	9738(2)	6992(3)	1979(1)	29(1)
C(26)	10530(2)	7437(3)	1774(1)	27(1)
C(27)	11029(2)	8399(3)	2026(1)	26(1)
C(28)	10753(2)	8962(3)	2496(1)	21(1)
C(29)	9959(2)	8501(3)	2710(1)	19(1)
C(30)	9664(2)	9012(3)	3209(1)	20(1)
C(31)	10190(2)	10010(3)	3468(1)	21(1)
C(32)	10975(2)	10472(3)	3229(1)	26(1)
C(33)	11252(2)	9975(3)	2772(1)	27(1)
C(34)	9926(2)	10525(3)	3953(1)	22(1)
C(35)	8924(2)	10673(3)	4689(1)	20(1)
C(36)	8229(2)	11588(3)	4673(1)	24(1)
C(37)	7918(2)	12089(4)	5144(1)	32(1)
C(38)	8281(2)	11664(4)	5604(1)	32(1)
C(39)	8968(2)	10766(3)	5607(1)	27(1)
C(40)	9313(2)	10236(3)	5150(1)	23(1)

Table 4.7, continued

C(41)	7814(2)	12052(4)	4163(1)	30(1)
C(42)	6838(3)	11877(5)	4160(2)	57(1)
C(43)	8065(3)	13502(4)	4054(2)	58(1)
C(44)	10048(2)	9210(4)	5150(1)	34(1)
C(45)	10608(2)	9245(4)	5639(1)	41(1)
C(46)	9683(3)	7767(4)	5060(2)	52(1)
N(1)	2265(2)	4840(3)	2583(1)	23(1)
N(2)	9225(2)	10108(3)	4201(1)	22(1)
O(1)	2665(2)	2028(2)	4228(1)	36(1)
O(2)	2439(2)	3363(2)	3404(1)	30(1)
O(3)	8680(2)	7098(3)	2632(1)	38(1)
O(4)	8962(2)	8563(2)	3415(1)	29(1)

Table 4.8 Bond lengths [Å] and angles [^{o}] for ligand **1**

C(1)-O(1)	1.361(4)
C(1)-C(2)	1.387(5)
C(1)-C(6)	1.421(5)
C(2)-C(3)	1.383(5)
C(2)-H(2)	0.9300
C(3)-C(4)	1.383(5)
C(3)-H(3)	0.9300
C(4)-C(5)	1.415(4)
C(4)-H(4)	0.9300
C(5)-C(6)	1.419(4)
C(5)-C(10)	1.435(4)
C(6)-C(7)	1.448(4)
C(7)-O(2)	1.288(4)
C(7)-C(8)	1.422(4)
C(8)-C(11)	1.394(4)
C(8)-C(9)	1.432(4)
C(9)-C(10)	1.342(4)
C(9)-H(9)	0.9300
C(10)-H(10)	0.9300
C(11)-N(1)	1.325(4)
C(11)-H(11)	0.9300
C(12)-C(17)	1.392(4)

Table 4.8, continued

C(12)-C(13)	1.402(4)
C(12)-N(1)	1.450(4)
C(13)-C(14)	1.399(4)
C(13)-C(18)	1.507(4)
C(14)-C(15)	1.370(5)
C(14)-H(14)	0.9300
C(15)-C(16)	1.382(5)
C(15)-H(15)	0.9300
C(16)-C(17)	1.389(4)
C(16)-H(16)	0.9300
C(17)-C(21)	1.528(5)
C(18)-C(19)	1.518(5)
C(18)-C(20)	1.534(6)
C(18)-H(18)	0.9800
C(19)-H(19A)	0.9600
C(19)-H(19B)	0.9600
C(19)-H(19C)	0.9600
C(20)-H(20A)	0.9600
C(20)-H(20B)	0.9600
C(20)-H(20C)	0.9600
C(21)-C(23)	1.533(5)

Table 4.8, continued

C(21)-C(22)	1.540(5)
C(21)-H(21)	0.9800
C(22)-H(22A)	0.9600
C(22)-H(22B)	0.9600
C(22)-H(22C)	0.9600
C(23)-H(23A)	0.9600
C(23)-H(23B)	0.9600
C(23)-H(23C)	0.9600
C(24)-O(3)	1.348(4)
C(24)-C(25)	1.377(4)
C(24)-C(29)	1.414(4)
C(25)-C(26)	1.395(5)
C(25)-H(25)	0.9300
C(26)-C(27)	1.378(5)
C(26)-H(26)	0.9300
C(27)-C(28)	1.399(4)
C(27)-H(27)	0.9300
C(28)-C(29)	1.412(4)
C(28)-C(33)	1.442(5)
C(29)-C(30)	1.456(4)
C(30)-O(4)	1.279(4)

Table 4.8, continued

C(30)-C(31)	1.434(4)
C(31)-C(34)	1.411(4)
C(31)-C(32)	1.427(4)
C(32)-C(33)	1.347(4)
C(32)-H(32)	0.9300
C(33)-H(33)	0.9300
C(34)-N(2)	1.315(4)
C(34)-H(34)	0.9300
C(35)-C(36)	1.392(4)
C(35)-C(40)	1.402(4)
C(35)-N(2)	1.454(4)
C(36)-C(37)	1.397(4)
C(36)-C(41)	1.532(5)
C(37)-C(38)	1.379(5)
C(37)-H(37)	0.9300
C(38)-C(39)	1.372(5)
C(38)-H(38)	0.9300
C(39)-C(40)	1.394(4)
C(39)-H(39)	0.9300
C(40)-C(44)	1.510(5)
C(41)-C(43)	1.498(5)

Table 4.8, continued

C(41)-C(42)	1.507(5)
C(41)-H(41)	0.9800
C(42)-H(42A)	0.9600
C(42)-H(42B)	0.9600
C(42)-H(42C)	0.9600
C(43)-H(43A)	0.9600
C(43)-H(43B)	0.9600
C(43)-H(43C)	0.9600
C(44)-C(45)	1.528(5)
C(44)-C(46)	1.538(5)
C(44)-H(44)	0.9800
C(45)-H(45A)	0.9600
C(45)-H(45B)	0.9600
C(45)-H(45C)	0.9600
C(46)-H(46A)	0.9600
C(46)-H(46B)	0.9600
C(46)-H(46C)	0.9600
O(1)-H(1)	0.8200
O(2)-H(2A)	0.8200
O(3)-H(3A)	0.8200
O(4)-H(4A)	0.8200

Table 4.8, continued

O(1)-C(1)-C(2)	119.3(3)
O(1)-C(1)-C(6)	120.1(3)
C(2)-C(1)-C(6)	120.6(3)
C(3)-C(2)-C(1)	119.6(3)
C(3)-C(2)-H(2)	120.2
C(1)-C(2)-H(2)	120.2
C(4)-C(3)-C(2)	121.9(3)
C(4)-C(3)-H(3)	119.0
C(2)-C(3)-H(3)	119.0
C(3)-C(4)-C(5)	119.7(3)
C(3)-C(4)-H(4)	120.1
C(5)-C(4)-H(4)	120.1
C(4)-C(5)-C(6)	119.2(3)
C(4)-C(5)-C(10)	121.7(3)
C(6)-C(5)-C(10)	119.1(3)
C(5)-C(6)-C(1)	119.1(3)
C(5)-C(6)-C(7)	119.5(3)
C(1)-C(6)-C(7)	121.4(3)
O(2)-C(7)-C(8)	121.1(3)
O(2)-C(7)-C(6)	119.4(3)
C(8)-C(7)-C(6)	119.5(3)

Table 4.8, continued

C(11)-C(8)-C(7)	120.9(3)
C(11)-C(8)-C(9)	120.6(3)
C(7)-C(8)-C(9)	118.5(3)
C(10)-C(9)-C(8)	122.4(3)
C(10)-C(9)-H(9)	118.8
C(8)-C(9)-H(9)	118.8
C(9)-C(10)-C(5)	121.0(3)
C(9)-C(10)-H(10)	119.5
C(5)-C(10)-H(10)	119.5
N(1)-C(11)-C(8)	123.7(3)
N(1)-C(11)-H(11)	118.1
C(8)-C(11)-H(11)	118.1
C(17)-C(12)-C(13)	123.0(3)
C(17)-C(12)-N(1)	119.5(3)
C(13)-C(12)-N(1)	117.1(3)
C(14)-C(13)-C(12)	116.9(3)
C(14)-C(13)-C(18)	121.6(3)
C(12)-C(13)-C(18)	121.5(3)
C(15)-C(14)-C(13)	121.2(3)
C(15)-C(14)-H(14)	119.4
C(13)-C(14)-H(14)	119.4

Table 4.8, continued

C(14)-C(15)-C(16)	120.4(3)
C(14)-C(15)-H(15)	119.8
C(16)-C(15)-H(15)	119.8
C(15)-C(16)-C(17)	121.2(3)
C(15)-C(16)-H(16)	119.4
C(17)-C(16)-H(16)	119.4
C(16)-C(17)-C(12)	117.3(3)
C(16)-C(17)-C(21)	121.3(3)
C(12)-C(17)-C(21)	121.3(3)
C(13)-C(18)-C(19)	112.8(3)
C(13)-C(18)-C(20)	109.8(3)
C(19)-C(18)-C(20)	110.8(3)
C(13)-C(18)-H(18)	107.7
C(19)-C(18)-H(18)	107.7
C(20)-C(18)-H(18)	107.7
C(18)-C(19)-H(19A)	109.5
C(18)-C(19)-H(19B)	109.5
H(19A)-C(19)-H(19B)	109.5
C(18)-C(19)-H(19C)	109.5
H(19A)-C(19)-H(19C)	109.5
H(19B)-C(19)-H(19C)	109.5

Table 4.8, continued

C(18)-C(20)-H(20A)	109.5
C(18)-C(20)-H(20B)	109.5
H(20A)-C(20)-H(20B)	109.5
C(18)-C(20)-H(20C)	109.5
H(20A)-C(20)-H(20C)	109.5
H(20B)-C(20)-H(20C)	109.5
C(17)-C(21)-C(23)	114.1(3)
C(17)-C(21)-C(22)	109.5(3)
C(23)-C(21)-C(22)	109.2(3)
C(17)-C(21)-H(21)	108.0
C(23)-C(21)-H(21)	108.0
C(22)-C(21)-H(21)	108.0
C(21)-C(22)-H(22A)	109.5
C(21)-C(22)-H(22B)	109.5
H(22A)-C(22)-H(22B)	109.5
C(21)-C(22)-H(22C)	109.5
H(22A)-C(22)-H(22C)	109.5
H(22B)-C(22)-H(22C)	109.5
C(21)-C(23)-H(23A)	109.5
C(21)-C(23)-H(23B)	109.5
H(23A)-C(23)-H(23B)	109.5

Table 4.8, continued

C(21)-C(23)-H(23C)	109.5
H(23A)-C(23)-H(23C)	109.5
H(23B)-C(23)-H(23C)	109.5
O(3)-C(24)-C(25)	118.7(3)
O(3)-C(24)-C(29)	120.9(3)
C(25)-C(24)-C(29)	120.5(3)
C(24)-C(25)-C(26)	119.3(3)
C(24)-C(25)-H(25)	120.4
C(26)-C(25)-H(25)	120.4
C(27)-C(26)-C(25)	121.2(3)
C(27)-C(26)-H(26)	119.4
C(25)-C(26)-H(26)	119.4
C(26)-C(27)-C(28)	120.8(3)
C(26)-C(27)-H(27)	119.6
C(28)-C(27)-H(27)	119.6
C(27)-C(28)-C(29)	118.4(3)
C(27)-C(28)-C(33)	122.7(3)
C(29)-C(28)-C(33)	118.9(3)
C(28)-C(29)-C(24)	119.9(3)
C(28)-C(29)-C(30)	120.4(3)
C(24)-C(29)-C(30)	119.8(3)

Table 4.8, continued

O(4)-C(30)-C(31)	120.8(3)
O(4)-C(30)-C(29)	120.9(3)
C(31)-C(30)-C(29)	118.3(3)
C(34)-C(31)-C(32)	120.9(3)
C(34)-C(31)-C(30)	119.9(3)
C(32)-C(31)-C(30)	119.2(3)
C(33)-C(32)-C(31)	122.2(3)
C(33)-C(32)-H(32)	118.9
C(31)-C(32)-H(32)	118.9
C(32)-C(33)-C(28)	121.0(3)
C(32)-C(33)-H(33)	119.5
C(28)-C(33)-H(33)	119.5
N(2)-C(34)-C(31)	123.8(3)
N(2)-C(34)-H(34)	118.1
C(31)-C(34)-H(34)	118.1
C(36)-C(35)-C(40)	123.2(3)
C(36)-C(35)-N(2)	117.6(3)
C(40)-C(35)-N(2)	119.1(3)
C(35)-C(36)-C(37)	117.5(3)
C(35)-C(36)-C(41)	122.3(3)
C(37)-C(36)-C(41)	120.3(3)

Table 4.8, continued

C(38)-C(37)-C(36)	120.6(3)
C(38)-C(37)-H(37)	119.7
C(36)-C(37)-H(37)	119.7
C(39)-C(38)-C(37)	120.5(3)
C(39)-C(38)-H(38)	119.7
C(37)-C(38)-H(38)	119.7
C(38)-C(39)-C(40)	121.7(3)
C(38)-C(39)-H(39)	119.2
C(40)-C(39)-H(39)	119.2
C(39)-C(40)-C(35)	116.5(3)
C(39)-C(40)-C(44)	122.0(3)
C(35)-C(40)-C(44)	121.5(3)
C(43)-C(41)-C(42)	111.2(3)
C(43)-C(41)-C(36)	109.7(3)
C(42)-C(41)-C(36)	112.6(3)
C(43)-C(41)-H(41)	107.7
C(42)-C(41)-H(41)	107.7
C(36)-C(41)-H(41)	107.7
C(41)-C(42)-H(42A)	109.5
C(41)-C(42)-H(42B)	109.5
H(42A)-C(42)-H(42B)	109.5

Table 4.8, continued

C(41)-C(42)-H(42C)	109.5
H(42A)-C(42)-H(42C)	109.5
H(42B)-C(42)-H(42C)	109.5
C(41)-C(43)-H(43A)	109.5
C(41)-C(43)-H(43B)	109.5
H(43A)-C(43)-H(43B)	109.5
C(41)-C(43)-H(43C)	109.5
H(43A)-C(43)-H(43C)	109.5
H(43B)-C(43)-H(43C)	109.5
C(40)-C(44)-C(45)	113.9(3)
C(40)-C(44)-C(46)	109.9(3)
C(45)-C(44)-C(46)	110.5(3)
C(40)-C(44)-H(44)	107.5
C(45)-C(44)-H(44)	107.5
C(46)-C(44)-H(44)	107.5
C(44)-C(45)-H(45A)	109.5
C(44)-C(45)-H(45B)	109.5
H(45A)-C(45)-H(45B)	109.5
C(44)-C(45)-H(45C)	109.5
H(45A)-C(45)-H(45C)	109.5
H(45B)-C(45)-H(45C)	109.5

Table 4.8, continued

C(44)-C(46)-H(46A)	109.5
C(44)-C(46)-H(46B)	109.5
H(46A)-C(46)-H(46B)	109.5
C(44)-C(46)-H(46C)	109.5
H(46A)-C(46)-H(46C)	109.5
H(46B)-C(46)-H(46C)	109.5
C(11)-N(1)-C(12)	125.7(3)
C(34)-N(2)-C(35)	124.3(3)
C(1)-O(1)-H(1)	109.5
C(7)-O(2)-H(2A)	109.5
C(24)-O(3)-H(3A)	109.5
C(30)-O(4)-H(4A)	109.5

Symmetry transformations used to generate equivalent atoms.

Table 4.9 Crystal data and structure refinement for complex **a**

Identification code	complex **a**	
Empirical formula	$C_{29}\ H_{32}\ N_2\ O_2\ Pd$	
Formula weight	546.97	
Temperature	293(2) K	
Wavelength	0.71073 Å	
Crystal system	Monoclinic	
Space group	P2(1)/*n* (no. 14)	
Unit cell dimensions	a = 9.605(2) Å	alpha = 90^o
	b = 30.963(7) Å	beta = $96.724(4)^o$
	c = 17.097(4) Å	gamma = 90^o
Volume	5049.7(18) $Å^3$	
Z	4	
Calculated density	1.439 mg/m^3	
Absorption coefficient	0.763 mm^{-1}	
F(000)	2256	
Crystal size	0.20 x 0.10 x 0.08 mm^3	
Theta range for data collection	1.78 to 28.38^o	
Limiting indices	-12<=h<=12, -35<=k<=41, -22<=l<=20	
Reflections collected	36782	
Unique reflections	12143 [R(int) = 0.0804]	
Completeness to theta = 28.38^o	95.9 %	

Table 4.9, continued

Refinement method	Full-matrix least-squares on F^2
Data / restraints / parameters	12143 / 0 / 625
Goodness-of-fit on F^2	1.112
Final R indices [I>2sigma(I)]	R1 = 0.0838, wR2 = 0.1736
R indices (all data)	R1 = 0.1213, wR2 = 0.1888
Largest diff. peak and hole	2.443 and -1.770 e.$Å^{-3}$

Table 4.10 Atomic coordinates ($x10^4$) and equivalent isotropic displacement parameters ($Å^2x10^3$) for complex **a**

	x	y	z	U(eq)
C(1)	8085(6)	7957(2)	8700(3)	19(1)
C(2)	7460(7)	7582(2)	8953(4)	27(2)
C(3)	7921(8)	7418(2)	9724(4)	35(2)
C(4)	8947(8)	7609(2)	10212(4)	37(2)
C(5)	9616(7)	7982(2)	9973(4)	25(1)
C(6)	9179(6)	8162(2)	9216(4)	24(1)
C(7)	9863(6)	8540(2)	8974(4)	23(1)
C(8)	10893(7)	8732(2)	9489(4)	34(2)
C(9)	11312(8)	8552(3)	10210(4)	38(2)
C(10)	10710(8)	8183(2)	10451(4)	37(2)
C(11)	6388(7)	7337(2)	8500(4)	28(2)
C(12)	5148(6)	8790(2)	6506(4)	23(1)
C(13)	5278(7)	9223(2)	6298(4)	29(2)
C(14)	6593(7)	9381(2)	6234(4)	28(2)
C(15)	7727(7)	9104(2)	6356(4)	30(2)
C(16)	7519(6)	8684(2)	6569(3)	23(1)
C(17)	4478(8)	7782(2)	6309(4)	34(2)
C(18)	4729(7)	7077(2)	7552(4)	24(1)
C(19)	5113(7)	6746(2)	7053(4)	25(1)

Table 4.10, continued

C(20)	4153(7)	6420(2)	6874(4)	31(2)
C(21)	2876(7)	6419(2)	7167(4)	32(2)
C(22)	2488(7)	6760(2)	7597(4)	33(2)
C(23)	3362(6)	7103(2)	7791(4)	24(1)
C(24)	2925(8)	7487(2)	8233(5)	36(2)
C(25)	1489(9)	7644(3)	7897(6)	55(2)
C(26)	2960(11)	7391(3)	9119(5)	59(3)
C(27)	6537(7)	6752(2)	6739(4)	28(2)
C(28)	6458(9)	6575(3)	5916(4)	44(2)
C(29)	7636(7)	6522(3)	7290(4)	40(2)
C(30)	8362(5)	559(2)	4077(3)	14(1)
C(31)	8372(5)	853(2)	3450(3)	15(1)
C(32)	8795(6)	1288(2)	3613(3)	18(1)
C(33)	9157(6)	1436(2)	4355(4)	19(1)
C(34)	9182(5)	1153(2)	5000(3)	15(1)
C(35)	8815(5)	711(2)	4874(3)	15(1)
C(36)	8881(6)	426(2)	5528(4)	20(1)
C(37)	9257(6)	577(2)	6278(4)	23(1)
C(38)	9607(6)	1013(2)	6400(3)	24(1)
C(39)	9576(6)	1291(2)	5782(4)	21(1)
C(40)	8038(5)	743(2)	2631(3)	16(1)

Table 4.10, continued

C(41)	4676(6)	-670(2)	3701(4)	24(1)
C(42)	4312(7)	-1024(2)	4118(4)	27(1)
C(43)	5350(7)	-1280(2)	4498(4)	24(1)
C(44)	6721(7)	-1170(2)	4456(4)	27(2)
C(45)	7021(6)	-810(2)	4042(3)	20(1)
C(46)	5357(8)	-288(2)	2061(4)	32(2)
C(47)	7230(6)	377(2)	1483(3)	15(1)
C(48)	6164(6)	609(2)	1037(3)	18(1)
C(49)	5168(6)	904(2)	1420(4)	21(1)
C(50)	3650(7)	839(2)	1098(5)	36(2)
C(51)	5586(8)	1376(2)	1335(4)	33(2)
C(52)	6053(6)	569(2)	225(3)	21(1)
C(53)	6940(6)	314(2)	-136(3)	23(1)
C(54)	7972(7)	77(2)	316(4)	25(1)
C(55)	8132(6)	106(2)	1130(4)	20(1)
C(56)	9265(6)	-149(2)	1627(4)	22(1)
C(57)	9613(7)	-578(2)	1265(4)	34(2)
C(58)	10605(7)	127(2)	1777(4)	33(2)
N(1)	5743(5)	7405(2)	7796(3)	23(1)
N(2)	6240(5)	8528(2)	6643(3)	23(1)
N(3)	7384(5)	404(2)	2329(3)	14(1)

Table 4.10, continued

N(4)	6019(5)	-561(2)	3655(3)	17(1)
O(1)	7697(4)	8136(1)	8009(2)	25(1)
O(2)	9535(5)	8711(2)	8256(3)	32(1)
O(3)	7950(4)	162(1)	3986(2)	18(1)
O(4)	8548(5)	6(1)	5416(3)	26(1)
Pd(1)	6659(1)	-71(1)	2987(1)	15(1)
Pd(2)	6025(1)	7945(1)	7172(1)	21(1)

Table 4.11 Bond lengths [Å] and angles [^{o}] for complex **a**

C(1)-O(1)	1.318(7)
C(1)-C(2)	1.400(9)
C(1)-C(6)	1.438(8)
C(2)-C(11)	1.431(8)
C(2)-C(3)	1.432(9)
C(3)-C(4)	1.350(9)
C(4)-C(5)	1.406(10)
C(5)-C(10)	1.400(9)
C(5)-C(6)	1.426(9)
C(6)-C(7)	1.429(9)
C(7)-O(2)	1.339(7)
C(7)-C(8)	1.380(9)
C(8)-C(9)	1.370(10)
C(9)-C(10)	1.365(10)
C(11)-N(1)	1.305(8)
C(12)-N(2)	1.326(8)
C(12)-C(13)	1.396(9)
C(13)-C(14)	1.371(9)
C(14)-C(15)	1.383(9)
C(15)-C(16)	1.371(9)
C(16)-N(2)	1.340(8)

Table 4.11, continued

C(17)-Pd(2)	2.030(6)
C(18)-C(19)	1.408(9)
C(18)-C(23)	1.423(9)
C(18)-N(1)	1.435(8)
C(19)-C(20)	1.379(9)
C(19)-C(27)	1.527(9)
C(20)-C(21)	1.378(10)
C(21)-C(22)	1.363(10)
C(22)-C(23)	1.370(9)
C(23)-C(24)	1.495(9)
C(24)-C(25)	1.510(11)
C(24)-C(26)	1.539(11)
C(27)-C(28)	1.505(9)
C(27)-C(29)	1.509(9)
C(30)-O(3)	1.294(6)
C(30)-C(31)	1.406(8)
C(30)-C(35)	1.460(7)
C(31)-C(32)	1.427(8)
C(31)-C(40)	1.441(8)
C(32)-C(33)	1.354(8)
C(33)-C(34)	1.407(8)

Table 4.11, continued

C(34)-C(35)	1.422(8)
C(35)-C(36)	1.421(8)
C(36)-O(4)	1.348(7)
C(36)-C(37)	1.373(8)
C(37)-C(38)	1.401(9)
C(38)-C(39)	1.360(9)
C(40)-N(3)	1.299(7)
C(41)-N(4)	1.345(8)
C(41)-C(42)	1.376(9)
C(42)-C(43)	1.376(9)
C(43)-C(44)	1.371(9)
C(44)-C(45)	1.367(9)
C(45)-N(4)	1.346(7)
C(46)-Pd(1)	2.016(6)
C(47)-C(55)	1.394(8)
C(47)-C(48)	1.401(8)
C(47)-N(3)	1.438(7)
C(48)-C(52)	1.386(8)
C(48)-C(49)	1.525(8)
C(49)-C(50)	1.510(8)
C(49)-C(51)	1.527(9)

Table 4.11, continued

C(52)-C(53)	1.362(9)
C(53)-C(54)	1.392(9)
C(54)-C(55)	1.385(9)
C(55)-C(56)	1.521(8)
C(56)-C(57)	1.517(9)
C(56)-C(58)	1.541(9)
N(1)-Pd(2)	2.018(5)
N(2)-Pd(2)	2.040(5)
N(3)-Pd(1)	2.024(5)
N(4)-Pd(1)	2.037(5)
O(1)-Pd(2)	2.108(4)
O(3)-Pd(1)	2.117(4)
O(1)-C(1)-C(2)	122.7(5)
O(1)-C(1)-C(6)	118.3(5)
C(2)-C(1)-C(6)	119.0(6)
C(1)-C(2)-C(11)	125.4(6)
C(1)-C(2)-C(3)	118.7(6)
C(11)-C(2)-C(3)	115.9(6)
C(4)-C(3)-C(2)	122.6(7)
C(3)-C(4)-C(5)	120.3(6)
C(10)-C(5)-C(4)	122.2(6)

Table 4.11, continued

C(10)-C(5)-C(6)	118.5(6)
C(4)-C(5)-C(6)	119.2(6)
C(5)-C(6)-C(7)	119.1(6)
C(5)-C(6)-C(1)	120.1(6)
C(7)-C(6)-C(1)	120.7(6)
O(2)-C(7)-C(8)	119.3(6)
O(2)-C(7)-C(6)	121.5(5)
C(8)-C(7)-C(6)	119.2(6)
C(9)-C(8)-C(7)	120.8(7)
C(10)-C(9)-C(8)	121.6(7)
C(9)-C(10)-C(5)	120.7(7)
N(1)-C(11)-C(2)	130.5(6)
N(2)-C(12)-C(13)	122.7(6)
C(14)-C(13)-C(12)	118.3(6)
C(13)-C(14)-C(15)	118.9(6)
C(16)-C(15)-C(14)	119.4(6)
N(2)-C(16)-C(15)	122.2(6)
C(19)-C(18)-C(23)	122.1(6)
C(19)-C(18)-N(1)	118.3(6)
C(23)-C(18)-N(1)	119.5(6)
C(20)-C(19)-C(18)	116.9(6)

Table 4.11, continued

C(20)-C(19)-C(27)	122.3(6)
C(18)-C(19)-C(27)	120.8(6)
C(21)-C(20)-C(19)	121.4(7)
C(22)-C(21)-C(20)	120.4(6)
C(21)-C(22)-C(23)	122.2(7)
C(22)-C(23)-C(18)	116.4(6)
C(22)-C(23)-C(24)	122.6(6)
C(18)-C(23)-C(24)	121.0(6)
C(23)-C(24)-C(25)	111.2(6)
C(23)-C(24)-C(26)	111.6(6)
C(25)-C(24)-C(26)	110.5(7)
C(28)-C(27)-C(29)	111.5(6)
C(28)-C(27)-C(19)	112.0(6)
C(29)-C(27)-C(19)	111.4(6)
O(3)-C(30)-C(31)	123.5(5)
O(3)-C(30)-C(35)	118.2(5)
C(31)-C(30)-C(35)	118.3(5)
C(30)-C(31)-C(32)	119.3(5)
C(30)-C(31)-C(40)	124.6(5)
C(32)-C(31)-C(40)	116.0(5)
C(33)-C(32)-C(31)	122.5(6)

Table 4.11, continued

C(32)-C(33)-C(34)	120.2(6)
C(33)-C(34)-C(39)	122.1(5)
C(33)-C(34)-C(35)	119.9(5)
C(39)-C(34)-C(35)	118.0(5)
C(36)-C(35)-C(34)	119.4(5)
C(36)-C(35)-C(30)	121.0(5)
C(34)-C(35)-C(30)	119.6(5)
O(4)-C(36)-C(37)	119.6(6)
O(4)-C(36)-C(35)	120.1(5)
C(37)-C(36)-C(35)	120.4(6)
C(36)-C(37)-C(38)	120.0(6)
C(39)-C(38)-C(37)	120.8(5)
C(38)-C(39)-C(34)	121.4(6)
N(3)-C(40)-C(31)	128.2(5)
N(4)-C(41)-C(42)	122.2(6)
C(43)-C(42)-C(41)	119.4(6)
C(44)-C(43)-C(42)	118.6(6)
C(45)-C(44)-C(43)	119.5(6)
N(4)-C(45)-C(44)	122.6(6)
C(55)-C(47)-C(48)	121.7(5)
C(55)-C(47)-N(3)	118.3(5)

Table 4.11, continued

C(48)-C(47)-N(3)	120.0(5)
C(52)-C(48)-C(47)	117.7(5)
C(52)-C(48)-C(49)	120.3(5)
C(47)-C(48)-C(49)	121.9(5)
C(50)-C(49)-C(48)	113.0(5)
C(50)-C(49)-C(51)	110.2(5)
C(48)-C(49)-C(51)	110.4(5)
C(53)-C(52)-C(48)	121.8(6)
C(52)-C(53)-C(54)	119.8(6)
C(55)-C(54)-C(53)	120.8(6)
C(54)-C(55)-C(47)	118.2(6)
C(54)-C(55)-C(56)	121.1(6)
C(47)-C(55)-C(56)	120.7(5)
C(57)-C(56)-C(55)	113.9(5)
C(57)-C(56)-C(58)	109.4(5)
C(55)-C(56)-C(58)	109.5(5)
C(11)-N(1)-C(18)	112.8(5)
C(11)-N(1)-Pd(2)	122.8(4)
C(18)-N(1)-Pd(2)	124.1(4)
C(12)-N(2)-C(16)	118.4(6)
C(12)-N(2)-Pd(2)	120.1(4)

Table 4.11, continued

C(16)-N(2)-Pd(2)	120.3(4)
C(40)-N(3)-C(47)	115.7(5)
C(40)-N(3)-Pd(1)	123.2(4)
C(47)-N(3)-Pd(1)	121.0(4)
C(41)-N(4)-C(45)	117.6(5)
C(41)-N(4)-Pd(1)	125.0(4)
C(45)-N(4)-Pd(1)	117.2(4)
C(1)-O(1)-Pd(2)	127.1(4)
C(30)-O(3)-Pd(1)	124.2(3)
C(46)-Pd(1)-N(3)	91.6(2)
C(46)-Pd(1)-N(4)	89.5(2)
N(3)-Pd(1)-N(4)	177.37(18)
C(46)-Pd(1)-O(3)	177.5(3)
N(3)-Pd(1)-O(3)	89.65(16)
N(4)-Pd(1)-O(3)	89.37(16)
N(1)-Pd(2)-C(17)	92.7(2)
N(1)-Pd(2)-N(2)	173.7(2)
C(17)-Pd(2)-N(2)	90.1(2)
N(1)-Pd(2)-O(1)	90.73(18)
C(17)-Pd(2)-O(1)	176.1(2)
N(2)-Pd(2)-O(1)	86.75(18)

Table 4.12 Crystal data and structure refinement for complex **b**

Identification code	complex **b**	
Empirical formula	C_{26} H_{33} N O_3 Pd S	
Formula weight	545.99	
Temperature	293(2) K	
Wavelength	0.71073 Å	
Crystal system	Monoclinic	
Space group	*P2*(1)/n (no. 14)	
Unit cell dimensions	a = 9.628(3) Å	alpha = 90^o
	b = 15.109(4) Å	beta = $95.874(4)^o$
	c= 17.184(5) Å	gamma = 90^o
Volume	2486.5(11) $Å^3$	
Z	4	
Calculated density	1.459 mg/m^3	
Absorption coefficient	0.857 mm^{-1}	
F(000)	1128	
Crystal size	0.20 x 0.12 x 0.10 mm^3	
Theta range for data collection	1.80 to 28.36^o.	
Limiting indices	-12<=h<=12, -17<=k<=20, -22<=l<=19	
Reflections collected	18386	
Unique reflections	6042 [R(int) = 0.0476]	
Completeness to theta = 28.36^o	97.2 %	

Table 4.12, continued

Refinement method	Full-matrix least-squares on F^2
Data / restraints / parameters	6042 / 0 / 297
Goodness-of-fit on F^2	1.069
Final R indices [I>2sigma(I)]	R1 = 0.0493, wR2 = 0.1174
R indices (all data)	R1 = 0.0628, wR2 = 0.1233
Largest diff. peak and hole	1.316 and -1.098 e.$Å^{-3}$

Table 4.13 Atomic coordinates ($x10^4$) and equivalent isotropic displacement parameters ($Å^2x10^3$) for complex **b**

	x	y	z	U(eq)
C(1)	910(4)	5722(3)	844(2)	27(1)
C(2)	4933(3)	6010(2)	2053(2)	14(1)
C(3)	5756(3)	6773(2)	1954(2)	15(1)
C(4)	5396(3)	7453(2)	1403(2)	13(1)
C(5)	6356(3)	8180(2)	1339(2)	14(1)
C(6)	7617(4)	8214(2)	1845(2)	19(1)
C(7)	7958(4)	7505(3)	2379(2)	24(1)
C(8)	7071(4)	6825(3)	2431(2)	23(1)
C(9)	8536(4)	8936(3)	1792(2)	24(1)
C(10)	8211(4)	9599(3)	1255(2)	24(1)
C(11)	6997(4)	9572(2)	755(2)	24(1)
C(12)	6081(4)	8870(2)	784(2)	18(1)
C(13)	3200(3)	4932(2)	1954(2)	13(1)
C(14)	3487(3)	4187(2)	1518(2)	15(1)
C(15)	3073(4)	3366(2)	1777(2)	21(1)
C(16)	2384(4)	3292(2)	2449(2)	23(1)
C(17)	2069(4)	4046(2)	2848(2)	21(1)
C(18)	2450(3)	4887(2)	2608(2)	16(1)
C(19)	2062(4)	5712(2)	3038(2)	19(1)

Table 4.13, continued

C(20)	3055(5)	5878(3)	3752(3)	39(1)
C(21)	564(4)	5684(3)	3260(3)	35(1)
C(22)	4226(4)	4262(2)	781(2)	19(1)
C(23)	3469(5)	3767(3)	94(3)	37(1)
C(24)	5745(4)	3968(3)	926(3)	36(1)
C(25)	625(4)	6892(3)	-832(2)	32(1)
C(26)	1(5)	7897(4)	418(3)	51(1)
N(1)	3697(3)	5787(2)	1719(2)	12(1)
O(1)	4237(2)	7454(2)	942(1)	17(1)
O(2)	4918(3)	8884(2)	274(2)	28(1)
O(3)	2256(4)	8166(2)	-279(2)	47(1)
Pd(1)	2591(1)	6561(1)	893(1)	15(1)
S(1)	1441(1)	7438(1)	5(1)	24(1)

Table 4.14 Bond lengths [Å] and angles [^{o}] for complex **b**

C(1)-Pd(1)	2.051(4)
C(2)-N(1)	1.311(4)
C(2)-C(3)	1.419(5)
C(3)-C(4)	1.415(5)
C(3)-C(8)	1.438(5)
C(4)-O(1)	1.300(4)
C(4)-C(5)	1.446(5)
C(5)-C(12)	1.419(5)
C(5)-C(6)	1.421(5)
C(6)-C(9)	1.413(5)
C(6)-C(7)	1.427(5)
C(7)-C(8)	1.346(5)
C(9)-C(10)	1.376(5)
C(10)-C(11)	1.378(6)
C(11)-C(12)	1.384(5)
C(12)-O(2)	1.350(4)
C(13)-C(14)	1.394(5)
C(13)-C(18)	1.399(5)
C(13)-N(1)	1.449(4)
C(14)-C(15)	1.391(5)
C(14)-C(22)	1.519(5)

Table 4.14, continued

C(15)-C(16)	1.392(5)
C(16)-C(17)	1.379(5)
C(17)-C(18)	1.397(5)
C(18)-C(19)	1.515(5)
C(19)-C(20)	1.497(6)
C(19)-C(21)	1.530(5)
C(22)-C(23)	1.519(5)
C(22)-C(24)	1.525(5)
C(25)-S(1)	1.770(4)
C(26)-S(1)	1.763(5)
N(1)-Pd(1)	2.051(3)
O(1)-Pd(1)	2.077(2)
O(3)-S(1)	1.464(3)
Pd(1)-S(1)	2.2276(10)
N(1)-C(2)-C(3)	130.5(3)
C(4)-C(3)-C(2)	124.6(3)
C(4)-C(3)-C(8)	118.9(3)
C(2)-C(3)-C(8)	116.4(3)
O(1)-C(4)-C(3)	123.0(3)
O(1)-C(4)-C(5)	117.9(3)
C(3)-C(4)-C(5)	119.2(3)

Table 4.14, continued

C(12)-C(5)-C(6)	118.2(3)
C(12)-C(5)-C(4)	122.2(3)
C(6)-C(5)-C(4)	119.6(3)
C(9)-C(6)-C(5)	119.4(3)
C(9)-C(6)-C(7)	121.1(3)
C(5)-C(6)-C(7)	119.5(3)
C(8)-C(7)-C(6)	120.7(3)
C(7)-C(8)-C(3)	122.1(4)
C(10)-C(9)-C(6)	120.2(4)
C(9)-C(10)-C(11)	121.1(3)
C(10)-C(11)-C(12)	120.2(4)
O(2)-C(12)-C(11)	117.0(3)
O(2)-C(12)-C(5)	122.2(3)
C(11)-C(12)-C(5)	120.8(3)
C(14)-C(13)-C(18)	122.7(3)
C(14)-C(13)-N(1)	118.7(3)
C(18)-C(13)-N(1)	118.6(3)
C(15)-C(14)-C(13)	118.0(3)
C(15)-C(14)-C(22)	120.5(3)
C(13)-C(14)-C(22)	121.5(3)
C(14)-C(15)-C(16)	120.8(3)

Table 4.14, continued

C(17)-C(16)-C(15)	119.7(3)
C(16)-C(17)-C(18)	121.7(3)
C(17)-C(18)-C(13)	117.0(3)
C(17)-C(18)-C(19)	121.3(3)
C(13)-C(18)-C(19)	121.7(3)
C(20)-C(19)-C(18)	111.7(3)
C(20)-C(19)-C(21)	109.8(3)
C(18)-C(19)-C(21)	112.6(3)
C(14)-C(22)-C(23)	112.5(3)
C(14)-C(22)-C(24)	111.4(3)
C(23)-C(22)-C(24)	111.0(3)
C(2)-N(1)-C(13)	114.7(3)
C(2)-N(1)-Pd(1)	122.7(2)
C(13)-N(1)-Pd(1)	122.5(2)
C(4)-O(1)-Pd(1)	128.9(2)
C(1)-Pd(1)-N(1)	91.58(13)
C(1)-Pd(1)-O(1)	177.64(13)
N(1)-Pd(1)-O(1)	90.13(10)
C(1)-Pd(1)-S(1)	90.25(11)
N(1)-Pd(1)-S(1)	178.10(8)
O(1)-Pd(1)-S(1)	88.02(7)

Table 4.14, continued

O(3)-S(1)-C(26)	108.0(3)
O(3)-S(1)-C(25)	106.7(2)
C(26)-S(1)-C(25)	102.1(2)
O(3)-S(1)-Pd(1)	115.43(13)
C(26)-S(1)-Pd(1)	108.33(18)
C(25)-S(1)-Pd(1)	115.31(16)

Table 4.15 Crystal data and structure refinement for complex **c**

Identification code	complex **c**	
Empirical formula	$C_{25}\ H_{31}\ N_3\ O_3\ Pd$	
Formula weight	527.93	
Temperature	108(2) K	
Wavelength	0.71073 Å	
Crystal system	Monoclinic	
Space group	*P2*(1)/*n* (no. 14)	
Unit cell dimensions	a = 8.3518(13) Å	alpha = 90^o
	b = 11.9400(18) Å	beta = $91.688(3)^o$
	c = 26.064(4) Å	gamma = 90^o
Volume	2598.0(7) $Å^3$	
Z	4	
Calculated density	1.350 mg/m^3	
Absorption coefficient	0.743 mm^{-1}	
F(000)	1088	
Crystal size	0.16 x 0.10 x 0.08 mm^3	
Theta range for data collection	2.31 to 28.35^o	
Limiting indices	-9<=h<=11, -15<=k<=15, -34<=l<=33	
Reflections collected	18512	
Unique reflections	6249 [R(int) = 0.0299]	
Completeness to theta = 28.35^o	96.3 %	

Table 4.15, continued

Refinement method	Full-matrix least-squares on F^2
Data / restraints / parameters	6249 / 0 / 295
Goodness-of-fit on F^2	1.085
Final R indices [I>2sigma(I)]	R1 = 0.0448, wR2 = 0.1122
R indices (all data)	R1 = 0.0510, wR2 = 0.1164
Largest diff. peak and hole	1.905 and -0.900 e.$Å^{-3}$

Table 4.16 Atomic coordinates ($x10^4$) and equivalent isotropic displacement parameters ($Å^2x10^3$) for complex **c**

	x	y	z	U(eq)
C(1)	501(3)	2827(2)	2237(1)	21(1)
C(2)	888(4)	2480(2)	2751(1)	21(1)
C(3)	-420(4)	2449(2)	3089(1)	21(1)
C(4)	-69(4)	2152(2)	3623(1)	23(1)
C(5)	1522(4)	1921(2)	3792(1)	24(1)
C(6)	2786(4)	1987(2)	3438(1)	26(1)
C(7)	2466(4)	2246(2)	2937(1)	23(1)
C(8)	1807(5)	1623(3)	4312(1)	33(1)
C(9)	538(5)	1564(3)	4642(1)	38(1)
C(10)	-1011(5)	1815(3)	4485(1)	38(1)
C(11)	-1338(4)	2112(3)	3977(1)	27(1)
C(12)	672(3)	3233(2)	1371(1)	21(1)
C(13)	159(3)	4339(3)	1377(1)	23(1)
C(14)	-558(4)	4818(3)	941(1)	26(1)
C(15)	-769(4)	4183(3)	502(1)	31(1)
C(16)	-220(5)	3091(3)	487(1)	34(1)
C(17)	510(4)	2606(3)	918(1)	27(1)
C(18)	2159(4)	427(3)	1835(1)	35(1)
C(19)	6728(4)	1855(3)	1463(2)	39(1)

Table 4.16, continued

C(20)	6502(4)	2975(3)	1711(2)	35(1)
C(21)	6179(5)	600(3)	2173(1)	38(1)
C(22)	5514(5)	52(3)	1311(1)	43(1)
C(23)	4553(5)	4301(3)	1992(1)	36(1)
C(24)	4603(4)	3829(3)	1103(1)	33(1)
N(1)	1333(3)	2720(2)	1825(1)	21(1)
N(2)	5582(3)	1017(2)	1668(1)	28(1)
N(3)	4851(3)	3387(2)	1625(1)	24(1)
O(1)	-1876(3)	2656(2)	2940(1)	28(1)
O(2)	-2841(3)	2360(2)	3820(1)	34(1)
Pd(1)	3412(1)	1868(1)	1745(1)	19(1)
C(25)	180(20)	618(4)	-368(2)	175(6)
O(3)	1854(18)	-11(11)	74(6)	333(8)

Table 4.17 Bond lengths [Å] and angles [^{o}] for complex **c**

C(1)-N(1)	1.302(4)
C(1)-C(2)	1.430(4)
C(2)-C(7)	1.419(4)
C(2)-C(3)	1.424(4)
C(3)-O(1)	1.289(4)
C(3)-C(4)	1.457(4)
C(4)-C(5)	1.415(4)
C(4)-C(11)	1.426(4)
C(5)-C(8)	1.415(4)
C(5)-C(6)	1.424(5)
C(6)-C(7)	1.361(4)
C(8)-C(9)	1.387(5)
C(9)-C(10)	1.378(6)
C(10)-C(11)	1.391(4)
C(11)-O(2)	1.342(4)
C(12)-C(13)	1.389(4)
C(12)-C(17)	1.399(4)
C(12)-N(1)	1.431(3)
C(13)-C(14)	1.392(4)
C(14)-C(15)	1.379(4)
C(15)-C(16)	1.383(5)

Table 4.17, continued

C(16)-C(17)	1.389(4)
C(18)-Pd(1)	2.031(3)
C(19)-N(2)	1.495(4)
C(19)-C(20)	1.500(5)
C(20)-N(3)	1.475(4)
C(21)-N(2)	1.481(4)
C(22)-N(2)	1.482(4)
C(23)-N(3)	1.477(4)
C(24)-N(3)	1.470(4)
N(1)-Pd(1)	2.029(2)
N(2)-Pd(1)	2.092(3)
N(3)-Pd(1)	2.203(2)
N(1)-C(1)-C(2)	129.2(3)
C(7)-C(2)-C(3)	120.3(2)
C(7)-C(2)-C(1)	124.0(3)
C(3)-C(2)-C(1)	115.5(3)
O(1)-C(3)-C(2)	122.9(2)
O(1)-C(3)-C(4)	119.7(3)
C(2)-C(3)-C(4)	117.4(3)
C(5)-C(4)-C(11)	120.0(3)
C(5)-C(4)-C(3)	120.4(3)

Table 4.17, continued

C(11)-C(4)-C(3)	119.6(3)
C(4)-C(5)-C(8)	118.5(3)
C(4)-C(5)-C(6)	119.7(3)
C(8)-C(5)-C(6)	121.8(3)
C(7)-C(6)-C(5)	120.3(3)
C(6)-C(7)-C(2)	121.8(3)
C(9)-C(8)-C(5)	119.8(3)
C(10)-C(9)-C(8)	122.2(3)
C(9)-C(10)-C(11)	119.6(3)
O(2)-C(11)-C(10)	120.1(3)
O(2)-C(11)-C(4)	120.1(3)
C(10)-C(11)-C(4)	119.8(3)
C(13)-C(12)-C(17)	119.7(3)
C(13)-C(12)-N(1)	120.6(3)
C(17)-C(12)-N(1)	119.6(3)
C(12)-C(13)-C(14)	120.4(3)
C(15)-C(14)-C(13)	119.6(3)
C(14)-C(15)-C(16)	120.4(3)
C(15)-C(16)-C(17)	120.5(3)
C(16)-C(17)-C(12)	119.2(3)
N(2)-C(19)-C(20)	110.6(3)

Table 4.17, continued

N(3)-C(20)-C(19)	111.2(3)
C(1)-N(1)-C(12)	116.0(2)
C(1)-N(1)-Pd(1)	127.9(2)
C(12)-N(1)-Pd(1)	116.10(18)
C(21)-N(2)-C(22)	107.6(3)
C(21)-N(2)-C(19)	110.0(3)
C(22)-N(2)-C(19)	108.0(3)
C(21)-N(2)-Pd(1)	110.4(2)
C(22)-N(2)-Pd(1)	114.8(2)
C(19)-N(2)-Pd(1)	105.97(19)
C(24)-N(3)-C(20)	111.5(3)
C(24)-N(3)-C(23)	108.2(3)
C(20)-N(3)-C(23)	108.9(3)
C(24)-N(3)-Pd(1)	111.33(19)
C(20)-N(3)-Pd(1)	102.46(19)
C(23)-N(3)-Pd(1)	114.5(2)
N(1)-Pd(1)-C(18)	88.12(13)
N(1)-Pd(1)-N(2)	178.82(10)
C(18)-Pd(1)-N(2)	92.91(13)
N(1)-Pd(1)-N(3)	94.24(9)
C(18)-Pd(1)-N(3)	177.34(13)

Table 4.17, continued

N(2)-Pd(1)-N(3)	84.75(10)

4.5 REFERENCES

1. Tritto, I.; Boggioni, L.; Jansen, J. C.; Thorshaug, K.; Sacchi, M. C.; Ferro, D. R. *Macromolecules* **2001**, *35*, 616-623.
2. Sen, A.; Lai, T.-W. *J. Am. Chem. Soc.* **1982**, *104*, 3520-3522.
3. Liu, S.; Borkar, S.; Newsham, D.; Yennawar, H.; Sen, A. *Organometallics* **2006**, *26*, 210-216.
4. Hung-Ren, W.; Yi-Hung, L.; Shie-Ming, P.; Shiuh-Tzung, L. *Eur. J. Inorg. Chem.* **2003**, *2003*, 3152-3159.
5. Ravasio, A.; Zampa, C.; Boggioni, L.; Tritto, I.; Hitzbleck, J.; Okuda, J. *Macromolecules* **2008**, *41*, 9565-9569.
6. Radhakrishnan, K.; Sivaram, S. *Macromol. Rapid Commun.* **1998**, *19*, 581-584.
7. Ralf Alexander, W.; Gerhard, F. *Macromol. Chem. Phys.* **2000**, *201*, 1365-1373.
8. Ralf Alexander, W.; Klaus, A.; Vidar, J.; Walter, T.; Gerhard, F. *Macomol. Chem. Phys.* **2004**, *205*, 308-318.
9. Marathe, S.; Sivaram, S. *Macromolecules* **1994**, *27*, 1083-1086.
10. Kang, M.; Sen, A. *Organometallics* **2005**, *24*, 3508-3515.
11. Benedikt, G. M.; Elce, E.; Goodall, B. L.; Kalamarides, H. A.; McIntosh, L. H.; Rhodes, L. F.; Selvy, K. T.; Andes, C.; Oyler, K.; Sen, A. *Macromolecules* **2002**, *35*, 8978-8988.
12. Makovetskii, K.; Bykov, V.; Finkel'shtein, E. *Kinetics and Catalysis* **2006**, *47*, 241-244.
13. Younkin, T. R.; Connor, E. F.; Henderson, J. I.; Friedrich, S. K.; Grubbs, R. H.; Bansleben, D. A. *Science* **2000**, *287*, 460-462.

14. Subramanyam, U.; Rajamohanan, P. R.; Sivaram, S. *Polymer* **2004**, *45*, 4063-4076.

15. Ittel, S. D; Johnson, L. K.; Brookhart, M. *Chem. Rev.* **2000**, *100*. 1169-1203.

16. Galland, G. B.; de Souza, R. F.; Mauler, R. S.; Nunes, F. F. *Macromolecules* **1999**, *32*, 1620-1625.

17. Lopez-Fernandez, R.; Carrera, N.; Albeniz, A. C.; Espinet, P. *Organometallics* **2009**, *28*, 4996-5001.

18. Chen, Y.; Sen, A. *Macromolecues* **2009**, *42*, 3951-3957.

19. de Graaf, W. *Organometallics* **1989**, *8*, 2907-2917.

20. Glaser, T.; Liratzis, I.; Frohlich, R. *Dalton Trans.* **2005**, 2892-2898.

21. Rodriguez, B. A.; Delferro, M.; Marks, T. J. *J. Am. Chem. Soc.* **2009**, *131*, 5902-5919.

CHAPTER 5. CATALYTIC ETHYLENE OLIGOMERIZATION WITH SIMPLE NICKEL CHLORIDE/ALUMINUM TRICHLORIDE-BASED SYSTEMS

5.1 INTRODUCTION

Since the discovery of the "nickel effect" by Ziegler[1] in 1953, the past a few decades witnessed a great endeavor and progress in designing and developing catalysts for ethylene oligomerization and polymerization. Both industry and academia showed enormous interest in discovering active and selective catalysts. Most research was focused on ligand design, because the chelated ligands controll the catalyst property. Some recent studies on the activities of various nickel catalysts were reviewed in detail[2-7]. Four coordinated nickel complexes with P-O[8-10], P-N[11-14], N-N[15,16] or N-O[9,17,18] ligands were commonly used, these ligands could leave potential coordination sites for ethylene insertion. An alkyl aluminum based activator, such as MAO and $AlEtCl_2$, was usually present in the nickel system, whose function was to create an unsaturated active species. Still some nickel catalysts did not require a cocatalyst, such as the P-O chelated nickel catalyst used in SHOP process.

In this chapter, we present a simple $NiCl_2/AlCl_3$ system that has high productivities for ethylene oligomerization. TOF of 3×10^4 mol of C_2H_4 (mol of Ni)$^{-1}$ h^{-1} and around 70 wt.% butene yield have been observed. As a cocatalyst, $AlCl_3$ gives higher productivity than MAO and $AlEtCl_2$, and it is easier to handle and store than alkyl aluminum compounds. Ni(pyridine)$_2$Cl$_2$, Ni(2,2'-bipyridyl)Cl$_2$ and Ni(2,6-lutidine)$_2$Cl$_2$ can also be used as catalyst for ethylene oligomerization with cocatalyst $AlCl_3$, although they are less active than $NiCl_2$. However, Ni(4-tert-butylpyridine)$_2$Cl$_2$ shows fairly higher productivity, possibly due to its solubility in chlorobenzene.

5.2 RESULTS AND DISCUSSION

5.2.1 EFFECT OF DIFFERENT COCATALYSTS ON ETHYLENE OLIGOMERIZATION USING NICKEL CHLORIDE AS CATALYST

In the presence of $NiCl_2$, the effects of the type and amount of cocatalysts are summarized in table 5.1. The property of cocatalyst made a significant role in ethylene oligomerization. Distinct from most nickel systems that utilized MAO or $AlEtCl_2$, in this system $AlCl_3$ is the most effective cocatalyst. The cocatalyst amount required for maximum butene yield is around 10 equivalents to $NiCl_2$, much lower than normally needed for MAO or $AlEtCl_2$. Increasing $AlCl_3$ feed to 20 equivalents to $NiCl_2$ increased C_6-C_{12} olefin yield, but not drastically for the yield of butenes (compare entry 3 and entry 4 in table 5.1). Generally, catalyst activity increased as ethylene pressure rose in the range of 100 psi ~ 500 psi. Keeping other reaction conditions the same, higher ethylene pressure resulted more C_4 products, lower ethylene pressure lead to more C_6-C_{12} and Friedel-Crafts products. During the reaction, a sudden temperature raise (1^oC to 10^oC) was observed as a result of exothermic reaction. The reactions performed in chlorobenzene produced higher yield for oligomerization products than those in toluene. Toluene was more reactive for Friedel-Crafts alkylation, it reacted with the olefin synthesized by $NiCl_2/AlCl_3$ and converted 19 wt.% ~ 95 wt.% olefin to Friedel-Crafts products. With chlorobenzene as the solvent, less than 10 wt.% of olefin was converted to Friedel-Crafts products, therefore chlorobenzene was a better solvent for ethylene oligomerization in this system. ^1H and ^{13}C NMR spectra (figure 5.1) were collected to study the product composition for a fresh sample (entry 3, table 5.1). Around 75 mol% of the olefin products were internal olefin, majorly trans-2-butene. Small

amount (<0.5 g) of ethylene oily oligomers (M_n = 420, PDI = 2.3) formed by $AlCl_3$ induced ethylene cationic polymerization were also found in the olefin mixture.

Table 5.1 Effect of different cocatalysts on ethylene oligomerization using nickel chloride as catalyst[a]

Entry	Co-catalyst	Cocatalyst/ $NiCl_2$ (mol/mol)	Ethylene (psi)	Solvent	Mass of all product (g)[b]	Distribution of olefin (mass %)						Productivity[d]	TON[e]
						C_4	C_6	C_8	C_{10}	C_{12}	F-C[c]		
1	$AlCl_3$	2	500	PhCl	0.9	29.6	8.6	0	0	0	61.9	37	1314
2	$AlCl_3$	6	500	PhCl	9.4	69.6	19.7	3.7	1.5	0	5.5	377	13471
3	$AlCl_3$	10	500	PhCl	20.4	70.4	17.4	4.6	2.7	0.2	4.7	816	29143
4	$AlCl_3$	20	500	PhCl	30.9	61.1	20.0	6.4	5.0	0.9	6.6	1235	44121
5	$AlCl_3$	10	300	PhCl	14.8	58.7	23.6	6.8	4.3	0.7	6.1	592	21143
6	$AlCl_3$	10	100	PhCl	2.9	38.1	25.0	15.2	12.5	0.5	8.6	115	4114
7	$AlCl_3$	10	500	toluene	23.0	55.2	15.0	8.6	2.1	0.0	19.1	920	32857
8	$AlCl_3$	10	300	toluene	10.8	31.9	9.1	9.2	0.7	0.0	49.0	432	15429
9	$AlCl_3$	10	100	toluene	3.8	3.6	0.9	0.3	0.1	0.0	95.2	151	5387
10	MAO	10	500	PhCl	3.5	C_4-C_{12}: 94 %; polymer: 6%						140	5000
11	$AlEtCl_2$	10	500	PhCl	<0.1	-	-	-	-	-	-	0	0
12	$AlEt_2Cl$	10	500	PhCl	0.1	-	-	-	-	-	-	0	0
13	$TiCl_4$	10	500	PhCl	<0.1	-	-	-	-	-	-	0	0

[a]Conditions: $NiCl_2$, 0.05 mmol; chlorobenzene or toluene, 5 mL; 50 ^oC; reaction time, 30 minutes; ethylene pressure kept constant; olefin composition was determined by GC and calibrated by standard solution. [b]Mass [(before reaction)-(after reaction)]. [c]Friedel-Crafts products. [d]In units of kg of C_2H_4 (mol of Ni)$^{-1}$ h^{-1}. [e]In units of mol of C_2H_4 (mol of Ni)$^{-1}$ h^{-1}.

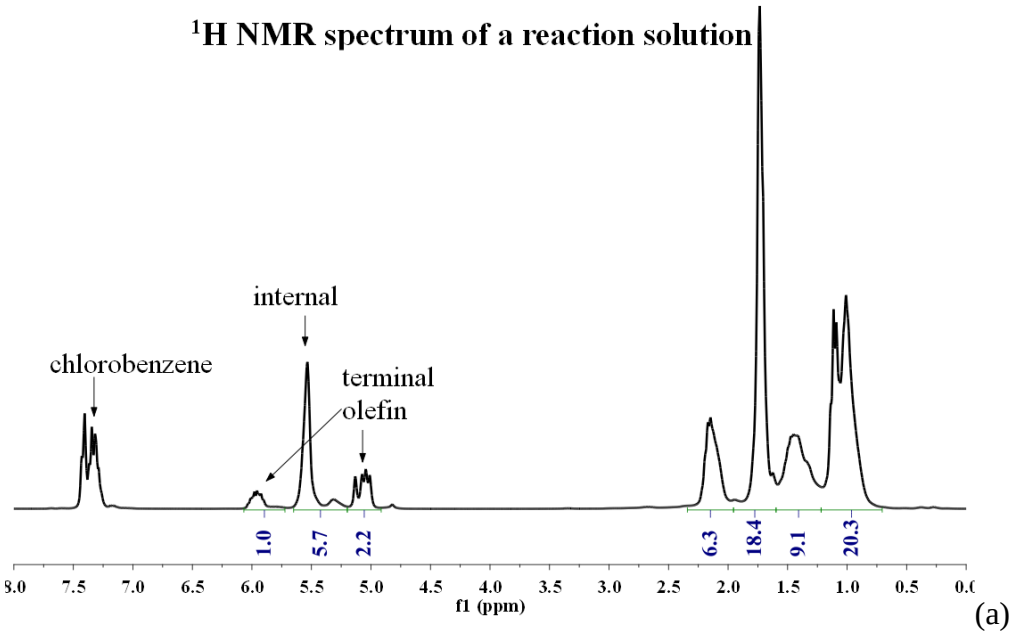

Figure 5.1 ^{1}H (a) and ^{13}C (b) NMR spectra of a reaction solution (Sample from entry 3, table 5.1; NMR was conducted in $CDCl_3$ at 25^{o}C).

5.2.2 THE EFFECT OF NICKEL COMPLEXES AS CATALYSTS

Besides $NiCl_2$, five different nickel complexes were used for ethylene oligomerization with cocatalyst $AlCl_3$. Not surprisingly, Brookhart's nickel diimine catalyst could not be activated by $AlCl_3$ (entry 5, table 5.2). Ni(4-tert-butylpyridine)$_2$$Cl_2$ was the only nickel complex soluble in chlorobenzene. It showed the highest activity (entry 1, table 5.2), possibly because of its solubility. Comparing entry 2, 3, 4 (table 5.2) with $NiCl_2$, adding N-ligand to $NiCl_2$ did not significantly improve the ethylene oligomerization activity of this system.

Table 5.2 Effect of the type of nickel complex[a]

Entry	Catalyst	Mass of all product (g)[b]	C_4 (mass %)	C_6-C_{12} (mass %)	F-C[c] (mass %)	Productivity[d]	TON[e]
1	Ni(4-t-butylpyridine)$_2$Cl$_2$	24.5	63.0	34.4	2.6	980	35000
2	Ni(pyridine)$_2$Cl$_2$	15.0	63.7	30.2	6.1	602	21486
3	Ni(2,6-lutidine)$_2$Cl$_2$	13.1	70.2	24.4	5.4	522	18643
4	Ni(2,2'-bipyridyl)Cl$_2$	16.5	68.4	25.7	5.9	661	23619
5	(diimine)NiBr$_2$[f]	0.17		polyethylene		3	100

[a]Conditions: Nickel complex, 0.05 mmol; $AlCl_3$, 0.5 mmol; chlorobenzene, 5 mL; 50 ^oC; reaction time, 30 minutes; ethylene pressure kept 500 psi constantly; olefin composition is determined by GC and calibrated by standard solution. [b]Mass [(before reaction)-(after reaction)]. [c]Friedel-Crafts products. [d]In units of kg of C_2H_4 (mol of Ni)$^{-1}$ h^{-1}. [e]In units of mol of C_2H_4 (mol of Ni)$^{-1}$ h^{-1}. [f]ArN=C(An)-C(An)=NAr)NiBr$_2$ (Ar = 2,6-C_6H_3(*i*-Pr)$_2$).

5.2.3 REACTION MECHANISM STUDY

By comparing these oligomerization reactions with $AlCl_3$ induced ethylene and 2-butene cationic polymerizations (table 5.3), it could be concluded that these olefin products come from ethylene insertion rather than cationic mechanism. In the absence of nickel complex, ethylene cationic polymerization only generated oily oligomers, no C_4-C_{12} olefin was detected. For 2-butene cationic polymerization with only $AlCl_3$, no C_6-C_{12} olefin was detected either. Therefore, the olefin products were made by an insertion mechanism. The identity of the real active species was also investigated. First, it was a long-lived active system. After continuous reaction for 7 days, the active species was still very reactive for ethylene oligomerization. Second, the active species was soluble in chlorobenzene. Although both $NiCl_2$ and $AlCl_3$ were insoluble in chlorobenzene, there was not any insoluble residue left after a reaction. Third, ^{27}Al NMR spectrum (figure 5.2) indicated a four coordinated aluminum center, possibly $AlCl_4^-$ or $AlRCl_3^-$. Unfortunately, due to the oily nature of the reaction residue, crystallographic analysis was unable to be done.

Table 5.3 $AlCl_3$ induced cationic polymerization[a]

Entry	Monomer	$AlCl_3$	C_4-C_{12}[b]	oily product		
				yield/g	Mn[c]	PDI[c]
1	ethylene, 500 psi	0.5 mmol	0	0.07	420	2.3
2	trans-2-butene, 0.4 g	0.5 mmol	0	0.08	450	1.7

[a]Conditions: chlorobenzene, 5 mL; 50 ^oC; reaction time, 30 minutes. [b]Determined by GC, and C_4 was excluded for entry 2. [c]By GPC using polystyrene standards.

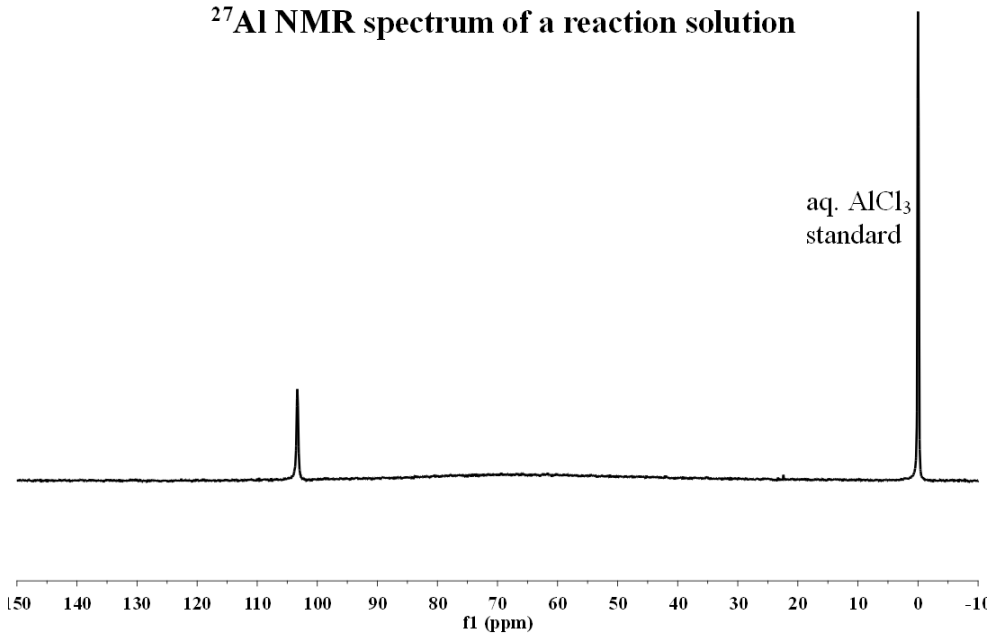

Figure 5.2 ^{27}Al NMR spectrum of a reaction solution (Sample from entry 3, table 5.1; aqueous $AlCl_3$ (1M) was used as external standard).

5.3 CONCLUSIONS

In conclusion, ethylene oligomerization with $NiCl_2/AlCl_3$ based system was investigated. This system is not only simple, but also has high activity for producing internal olefin, e.g. trans-2-butene, however, further study on its activation process and active component is still needed.

5.4 EXPERIMENTAL SECTION

5.4.1 MATERIALS

All chemicals and reagents were obtained from Aldrich unless otherwise stated. Aluminum chloride ($AlCl_3$, anhydrous, 99.99%, Alfa Aesar), ethylaluminum dichloride ($AlEtCl_2$, 1.0 M in hexanes), diethylaluminum chloride ($AlEt_2Cl$, 1.0 M in hexanes), methylaluminoxane (MAO, 10 wt.% in toluene), nickel(II) chloride ($NiCl_2$, anhydrous, 98%, Strem Chemicals), ethylene (polymer grade, Matheson Co.), 2,2'-bipyridyl (98%) and nickel(II) chloride ethylene glycol dimethyl ether complex ((DME)$NiCl_2$, 98%) were used as received. Pyridine (anhydrous, 99.8%), 2,6-lutidine (99%) and 4-tert-butylpyridine (95%, TCI America) were degassed and stored under N_2. Nickel complex ArN=C(An)-C(An)=NAr)$NiBr_2$, Ni(2,2'-bipyridyl)Cl_2, Ni(pyridine)$_2Cl_2$, Ni(4-tert-butylpyridine)$_2Cl_2$ and Ni(2,6-lutidine)$_2Cl_2$ were synthesized as literature[19,20].

5.4.2 INSTRUMENTATION

NMR spectra were recorded using a Bruker 300-DPX spectrometer at ambient temperature (^{1}H-NMR, 300MHz; ^{13}C-NMR, 75 MHz). Gas chromatography analysis was performed on an Agilent 5890 Series II GC using a RTX-5 split capillary column (Restek) connected to an FID detector. The samples were heated from 40 ^{o}C to 200 ^{o}C at a ramp rate of 5 ^{o}C/min. Molecular weights and molecular weight distributions were determined on a Shimadzu gel permeation chromatography (GPC) chromatograph containing a three-column bed (styragel HR 7.8 × 300 mm columns with 5 μm beads size; 100-5000, 500-30,000, and 2,000-4 × 10^6 Da), a Shimadzu RDI-10A differential refractometer, and a Shimadzu SPD-10A tunable absorbance detector (254 nm). GPC samples were run in tetrahydrofuran at a flow rate of 1 ml/min at 35 ^{o}C and calibrated against polystyrene standards. Analysis was

done using EZSTART 7.2 software. GC-MS measurements were performed using a Waters GC-TOF with Agilent 6890 GC; 20 meter 150 um i.d., 0.15 um 95% dimethyl/ 5% diphenyl-polysiloxane film column; 70 eV electron ionization.

5.4.3 GENERAL PROCEDURE FOR ETHYLENE OLIGOMERIZATION

In a N_2-filled glove box, a glass-lined Parr high-pressure reactor was charged with $NiCl_2$ (6.5 mg, 0.05 mmol), $AlCl_3$ (66 mg, 0.5 mmol) and chlorobenzene (5 mL). The reactor was sealed, removed from glove box and immersed in an oil bath at 50 ^oC. When the reactor reached the desired temperature, it was charged with ethylene (500 psi, constant pressure) for 30 minutes. The oligomerization was stopped by cooling the reactor in ice bath immediately and degassing unreacted ethylene. After that, the product was weighed and analyzed by NMR, GC or GC-MS. And the liquid solution was quenched by adding a small amount of methanol.

5.4.4 ETHYLENE CATIONIC POLYMERIZATION

In a N_2-filled glove box, a glass-lined Parr high-pressure reactor was charged with $AlCl_3$ (66 mg, 0.5 mmol) and chlorobenzene (5 mL). The reactor was sealed, removed from glove box and immersed in an oil bath at 50 ^oC. When the reactor reached the desired temperature, it was charged with ethylene (500 psi, constant pressure) for 30 minutes. The cationic polymerization was stopped by cooling the reactor in ice bath, degassing unreacted ethylene, and followed by adding a small amount of methanol. After that, the reaction mixture was filtered and analyzed by GC, the solvent was removed by vacuum resulting in a clear oil liquid.

5.5 REFERENCES

1. Ziegler, K.; Gellert, H. G.; Holzkamp, E.; Wilke, G. *Brennst. Chem.* **1954**, *35*, 321.
2. Braunstein, P. *Chem. Rev.* **2006**, *106*, 134-159.
3. Gibson, V. C.; Spitzmesser, S. K. *Chem. Rev.* **2003**, *103*, 283-316.
4. Britovsek, G. J. P.; Gibson, V. C.; Wass, D. F. *Angew. Chem., Int. Ed.* **1999**, *38*, 428-447.
5. Wilhelm, K. *Angew. Chem., Int. Ed.* **1990**, *29*, 235-244.
6. Ittel, S. D.; Johnson, L. K.; Brookhart, M. *Chem. Rev.* **2000**, *100*, 1169-1204.
7. Mecking, S. *Coord. Chem. Rev.* **2000**, *203*, 325-351.
8. Keim, W.; Kowaldt, F. H.; Goddard, R.; Kruger, C. *Angew. Chem., Int. Ed.* **1978**, *17*, 466-467.
9. Wang, C.; Friedrich, S.; Younkin, T. R.; Li, R. T.; Grubbs, R. H.; Bansleben, D. A.; Day, M. W. *Organometallics* **1998**, *17*, 3149-3151.
10. Liu, W.; Malinoski, J. M.; Brookhart, M. *Organometallics* **2002**, *21*, 2836-2838.
11. Weng, Z.; Teo, S.; Lin, L.; S., K. T.; Hor, A. *Angew. Chem., Int. Ed.* **2005**, *44*, 7560-7564.
12. Dyer, P. W.; Fawcett, J.; Hanton, M. J. *Organometallics* **2008**, *27*, 5082-5087.
13. Speiser, F.; Braunstein, P.; Saussine, L. *Acc. Chem. Res.* **2005**, *38*, 784-793.
14. Flapper, J.; Kooijman, H.; Lutz, M.; Spek, A. L.; van Leeuwen, P. W. N. M.; Elsevier, C. J.; Kamer, P. C. J. *Organometallics* **2009**, *28*, 1180-1192.
15. Svejda, S. A.; Brookhart, M. *Organometallics* **1999**, *18*, 65-74.
16. Killian, C. M.; Tempel, D. J.; Johnson, L. K.; Brookhart, M. *J. Am. Chem. Soc.* **1996**, *118*, 11664-11665.

17. Kermagoret, A.; Braunstein, P. *Dalton Trans.* **2008**, 1564-1573.

18. Hu, T.; Tang, L.; Li, X.; Li, Y.; Hu, N. *Organometallics* **2005**, *24*, 2628-2632.

19. Allan, J. R.; Brown, D. H.; Nuttall, R. H.; Sharp, D. W. A. *J. Inorg. Nucl. Chem* **1965**, *27*, 1305-1309.

20. Johnson, L. K.; Killian, C. M.; Brookhart, M. *J. Am. Chem. Soc.* **1995**, *117*, 6414-6415.

CHAPTER 6. MOLECULAR WEIGHT CONTROL OF PMMA IN NICKEL(II) ACETYLACETONATE/MAO SYSTEM BY USING OLEFIN AS CHAIN TRANSFER AGENTS

6.1 INTRODUCTION

As one of the most important commercial polymers, poly(methyl methacrylate) (PMMA) possesses many desirable properties, such as optical clarity, high strength and impact resistance, therefore substantial effects have been made on the synthesis of well-defined PMMA polymers in terms of molecular weight, polydispersity, tacticity, end-group functionalization and etc[1].

Nickel(II) acetylacetonate ($Ni(acac)_2$)/MAO catalyst is well known for producing PMMA and some other polyolefin[2-4]. Compared to other metallocene catalysts, $Ni(acac)_2$ is easier to synthesize and still has high activity. Endo[2] and Continho[3,4] have reported distinct results of the polydispersity of PMMA obtained from this system, and they also investigated the parameters that affected polymer tacticity. An insertion mechanism was proposed for $Ni(acac)_2$/MAO system, however, no direct evidence or details were provided.

To achieve better molecular weight control of the synthesized PMMA and to understand the polymerization mechanism, we studied the effects of several different olefin as chain transfer agents. Further, we compared the polymer microstructure with those prepared by free radical route, and the microstructure difference proved its insertion mechanism.

6.2 RESULTS AND DISCUSSION

6.2.1 OLEFIN AS CHAIN TRANSFER AGENT

MMA polymerization results via $Ni(acac)_2$/MAO catalyst in the presence of different olefin are summarized in table 6.1. In all cases, the olefin incorporation to the polymer backbone was less than 1 mol%, so the product obtained here could be treated as a PMMA homopolymer regarding tacticity calculation and molecular weight. Figure 6.1 shows the ^{1}H and ^{13}C NMR spectra of PMMA synthesized in the presence of one equivalent 1-hexene (entry 6, table 6.1), and no noticeable 1-hexene peaks are observed. Due to the fact that the products had high molecular weight, the polymer chain end group was unable to be identified in NMR spectrum.

Most olefin studied here, except 1,5-hexadiene, were proved effective as chain transfer agents. When gradually increasing olefin/MMA ratio, the product's tacticity and yield remained almost the same, and the PMMA molecular weight dropped as increasing olefin feed. Cyclopentene was the least effective among these olefin; its insertion might be hindered by the ring structure. In the case of 1,5-hexadiene, the PMMA molecular weight increased as increasing 1,5-hexadiene/MMA ratio, possibly due to the diene crosslink. The presence of hydrogen also lead to a decrease in polymer molecular weight (table 6.2), however the yield dropped as more H_2 present. It is worth noting that most polymer molecular weights, including the blank PMMA sample (entry 1, table 6.1), showed a bimodal distribution.

Table 6.1 Polymerization of methyl methacrylate (MMA) in the presence and absence of different olefin[a]

Entry	Olefin	Olefin/MMA molar ratio	Yield (g)	mm/mr/rr[b]	M_n[c] ($\times 10^{-3}$)	PDI[c]
1	blank	0	0.58	8/23/69	1052	1.96
2	1-hexene	0.05	0.56	7/23/70	971	2.11
3	1-hexene	0.10	0.53	8/22/70	908	1.65
4	1-hexene	0.20	0.62	8/22/71	778	2.18
5	1-hexene	0.40	0.57	7/23/70	711	2.22
6	1-hexene	1.00	0.49	7/23/70	680	2.20
7	1-decene	0.05	0.52	8/22/70	1046	1.73
8	1-decene	0.10	0.58	7/22/71	988	1.71
9	1-decene	0.20	0.56	7/23/70	909	1.63
10	1-decene	0.40	0.56	8/23/69	830	1.86
11	1-decene	1.00	0.58	7/23/70	710	1.98
12	cyclopentene	0.05	0.53	7/23/70	898	1.80
13	cyclopentene	0.10	0.51	7/22/71	879	2.09
14	cyclopentene	0.20	0.51	8/23/69	737	2.15
15	cyclopentene	0.40	0.48	8/23/69	740	2.08
16	cyclopentene	1.00	0.48	8/23/69	734	2.36
17	styrene	0.05	0.56	8/22/70	783	2.48
18	styrene	0.10	0.55	7/22/71	732	2.63
19	styrene	0.20	0.59	7/22/71	684	2.66

Table 6.1, continued

20	styrene	0.40	0.60	7/23/70	545	3.54
21	isoprene	0.05	0.48	8/24/68	811	2.37
22	isoprene	0.10	0.47	8/23/69	679	1.98
23	isoprene	0.20	0.50	8/23/69	635	2.16
24	isoprene	0.40	0.49	8/24/68	573	2.14
25	isoprene	1.00	0.48	6/21/73	562	2.14
26	1,5-hexadiene	0.10	0.40	8/22/70	1092	1.78
27	1,5-hexadiene	0.20	0.34	8/21/71	1329	1.56
28	1,5-hexadiene	0.40	0.33	6/20/74	1639	1.44
29	1,5-hexadiene	1.00	0.14	7/20/74	1777	1.44

[a]Conditions: $Ni(acac)_2$, 0.0376 mmol; MAO, 1.88 mmol; MMA, 9.4 mmol (Ni/MAO/MMA = 1/50/250); toluene, 20 mL; reaction time, 2 hours; 25 ^{o}C. [b]Determined by ^{1}H NMR. [c]Determined by GPC, using polystyrene standards.

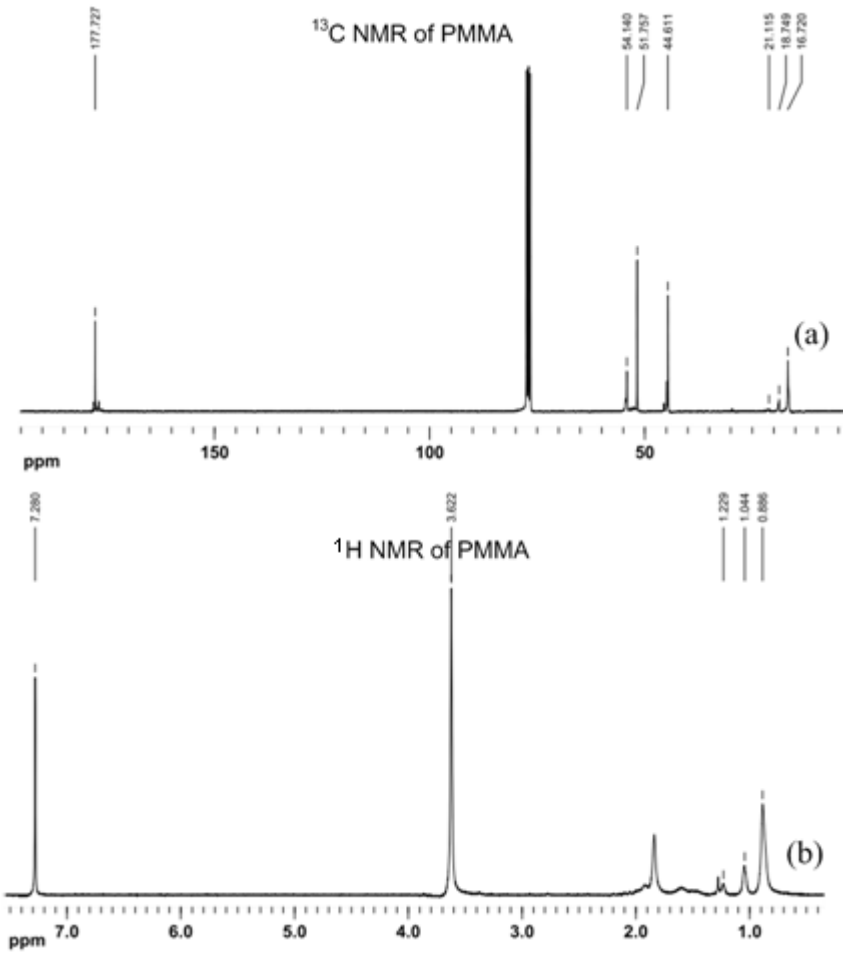

Figure 6.1 ^{13}C (a) and ^{1}H (b) NMR spectra of PMMA (Sample from entry 6, table 6.1; NMR was conducted in $CDCl_3$ at 25 ^{o}C).

Table 6.2 Polymerization of methyl methacrylate (MMA) in the presence of H_2[a]

Entry	H_2 (psi)	Reaction time (h)	Yield (g)	mm/mr/rr[b]	M_n[c] ($\times 10^{-3}$)	PDI[c]
1	15	2	0.29	9/23/68	320	2.75
2	50	2	0.14	12/23/65	303	2.76
3	200	2	0.08	7/19/74	238	2.94

[a]Conditions: $Ni(acac)_2$, 0.0376 mmol; MAO, 1.88 mmol; MMA, 9.4 mmol (Ni/MAO/MMA = 1/50/250); toluene, 20 mL; 25 ^{o}C. [b]Determined by ^{1}H NMR. [c]Determined by GPC using polystyrene standards.

6.2.2 COMPARISON OF NI(ACAC)$_2$/MAO SYSTEM WITH RADICAL POLYMERIZATION

In order to verify that Ni(acac)$_2$/MAO catalyzed polymerization followed an insertion route, radical scavenger galvinoxyl and TEMPO were added to the reactions (table 6.3). Neither of the two scavengers could completely shut down the polymerization, although TEMPO slowed down the reaction more drastically than galvinoxyl did. However, a decrease in polymerization rate could not prove the reaction went through a radical route, because the scavengers might have induced the catalyst's decomposition. The best evidence of its mechanism is the product's microstructures, such as tacticity and composition[5].

Table 6.3 Polymerization of methyl methacrylate (MMA) in the presence of radical scavenger[a]

Entry	Radical scavenger	Scavenger/Ni molar ratio	Monomer	Yield (g)	mm/mr/rr[b]
1	none	0	MMA	0.58	8/23/69
2	galvinoxyl	2	MMA	0.42	7/23/70
3	TEMPO	2	MMA	0.27	9/25/66

[a]Conditions: $Ni(acac)_2$, 0.0376 mmol; MAO, 1.88 mmol; MMA, 9.4 mmol (Ni/MAO/MMA = 1/50/250); galvinoxyl, 0.0752 mmol; TEMPO, 0.0752 mmol; toluene, 20 mL; reaction time, 2 hours; 25 ^{o}C. [b]Determined by ^{1}H NMR.

Therefore the polymer products prepared from the following three different routes were compared (table 6.4): $Ni(acac)_2$/MAO system, AIBN initiated free radical polymerization and AIBN free radical polymerization in the presence of MAO. The polymers made by Ni catalyst demonstrated a huge distinction in their composition and tacticity from those made by free radical polymerization (table 6.4). For the homopolymerization of MMA, Ni catalyst gave the highest syndiotacticity; for the polymerization of MMA in the presence of 1-hexene, Ni catalyst only produced homo PMMA. On the other hand, AIBN free radical polymerization would make a MMA/1-hexene copolymer when 1-hexene was present, and the copolymer showed only one peak with both refractive index (RI) and UV detector on GPC. Cocatalyst MAO was acting as Lewis acid in these reactions, so the olefin incorporation was higher in the presence of MAO[6,7]. In all the cases, the polymers made by Ni catalyst and free radical polymerization were distinct, it was more likely that Ni catalyst went through an insertion mechanism rather than radical polymerization.

Table 6.4 Comparison of polymer products from different synthesis routes[a]

Entry	Olefin	Olefin/MMA molar ratio		$Ni(acac)_2$/MAO[b]	AIBN[c]	AIBN + MAO[d]
1	none	0	mm/mr/rr	8/23/69	5/34/61	11/34/55
			yield (g)	0.26	0.10	0.14
2	1-hexene	1/1	olefin incorp.[e]	0	3.1	6.4
			yield (g)	0.39	0.09	0.13
3	1-hexene	4/1	olefin incorp.[e]	0	7.6	12.9
			yield (g)	0.40	0.05	0.06

[a]Conditions: [b]$Ni(acac)_2$, 0.0376 mmol; MAO, 1.88 mmol; MMA, 9.4 mmol (Ni/MAO/MMA = 1/50/250); toluene, 20 mL; 2 hours; 60 ^{o}C. [c]AIBN, 0.3 mmol; MMA, 9.4 mmol; toluene, 20 mL; 5 hours; 60 ^{o}C. [d]AIBN, 0.3 mmol; MAO, 1.88 mmol; MMA, 9.4 mmol; toluene, 20 mL; 2 hours; 60 ^{o}C. [e]Olefin mole incorporation determined by ^{1}H NMR.

6.2.3 METHYL ACRYLATE (MA) POLYMERIZATION VIA NI(ACAC)$_2$/MAO SYSTEM

Surprisingly, Ni(acac)$_2$/MAO system had little activity toward methyl acrylate (MA) polymerization. For MA/1-hexene free radical copolymerization, the addition of MAO increased the olefin incorporation as the data shown in table 6.5.

Table 6.5 Methyl acrylate (MA) (co)polymerization via different synthesis routes[a]

Entry	Olefin	Olefin/MA molar ratio		$Ni(acac)_2$ /MAO[b]	AIBN[c]	AIBN + MAO[d]
1	none	---	yield	0	0.18	0.10
2	1-hexene	1/1	olefin incorp.[e]	0	12.8	21.5
			yield (g)	0	0.0032	0.098

[a]Conditions: [b]$Ni(acac)_2$, 0.0376 mmol; MAO, 1.88 mmol; MA, 9.4 mmol (Ni/MAO/MA = 1/50/250); toluene, 20 mL; 2 hours; 60 ^{o}C. [c]AIBN, 0.3 mmol; MA, 9.4 mmol; toluene, 20 mL; 5 hours; 60 ^{o}C. [d]AIBN, 0.3 mmol; MAO, 1.88 mmol; MA, 9.4 mmol; toluene, 20 mL; 2 hours; 60 ^{o}C. [e]Olefin mole incorporation determined by ^{1}H NMR.

6.3 CONCLUSIONS

In the polymerization of MMA via $Ni(acac)_2$/MAO catalyst, the addition of olefin had a chain transfer effect. By varying the olefin/MMA ratio, the polymer molecular weight and end group could be controlled, which provided another way to modify the synthesized polymer. The polymer products had been compared with those synthesized by radical route, and the distinctions in both polymer tacticity and composition ruled out the possibility that the Ni system went through a radical mechanism.

6.4 EXPERIMENTAL SECTION

6.4.1 MATERIALS

All chemicals and reagents were obtained from Aldrich unless otherwise stated. Methyl methacrylate (MMA, 99%) and styrene (99%) were passed through basic alumina column to remove inhibitor, degassed and stored under N_2. Isoprene (99%), 1-hexene (97%), 1,5-hexadiene (97%), 1-decene (94%) and cyclopentene (95%) were degassed and stored under N_2. $Ni(acac)_2$ (Strem, 95%), galvinoxyl, tempo (99%), methylaluminoxane (MAO, 10 wt.% in toluene), hydrogen (GT&S, 99.9%) and 2,2'-azobis(isobutyronitrile) (AIBN, 98%) were used as received.

6.4.2 INSTRUMENTATION

^{1}H-NMR (300MHz) and ^{13}C-NMR (75MHz) spectra were recorded using a Bruker 300-DPX spectrometer. Molecular weights and molecular weight distributions were determined on a Shimadzu gel permeation chromatography (GPC) chromatograph containing a three-column bed (styragel HR 7.8 × 300 mm columns with 5 μm beads size; 100-5000, 500-30,000, and 2,000-4 × 10^6 Da), a Shimadzu RDI-10A differential refractometer, and a Shimadzu SPD-10A tunable absorbance detector (254 nm). GPC samples were run in tetrahydrofuran at a flow rate of 1 ml/min at 35 ^{o}C and calibrated against polystyrene standards. Analysis was done using EZSTART 7.2 software.

6.4.3 POLYMERIZATION OF METHYL METHACRYLATE (MMA) IN THE PRESENCE OF OLEFIN AS CHAIN TRANSFER AGENT

In a typical experiment (entry 2, table 6.1), in a N_2 filled glove box, $Ni(acac)_2$ (0.0376 mmol, 9.7 mg), toluene (20 mL) and methylaluminoxane (1.88 mmol, 1.25 mL) were added

into a reaction vessel equipped with a magnetic stirring bar. Then 1-hexene (0.47 mmol, 40 mg) and MMA (9.4 mmol, 0.94 g) were transferred to this vessel, and the vessel was sealed. The reaction was stirred for 2 hours at 25 ^{o}C. The polymer product was precipitated out in 400 mL methanol/HCl (v/v = 10/1) mixture, collected by filtration and dried under high vacuum overnight. The PMMA tacticity was determined by ^{1}H NMR integration.

6.4.4 POLYMERIZATION OF METHYL METHACRYLATE (MMA) IN THE PRESENCE OF HYDROGEN

In a typical experiment (entry 2, table 6.2), in a N_2-filled glove box, a glass-lined stainless steel autoclave was charged with $Ni(acac)_2$ (0.0376 mmol, 9.7 mg), toluene (20 mL), MMA (9.4 mmol, 0.94 g) and methylaluminoxane (1.88 mmol, 1.25 mL). The autoclave was sealed, removed from glove box, purged with H_2 (50 psi) twice, then it was charged with H_2 (50 psi). The resulting polymer was precipitated out in 400 mL methanol/HCl (v/v = 10/1), collected and dried in vacuum oven overnight. The PMMA tacticity was determined by ^{1}H NMR integration.

6.4.5 FREE RADICAL COPOLYMERIZATION OF METHYL METHACRYLATE (MMA) WITH OLEFIN

In a typical experiment (entry 3, table 6.4), in a N_2 filled glove box, MMA (9.4 mmol, 0.94 g), toluene (20 mL), 1-hexene (37.6 mmol, 3.16 g) and AIBN (0.3 mmol, 50 mg) were added into a reaction vessel equipped with a magnetic stirring bar. Then the reaction vessel was heated with stirring in oil bath at 60 ^{o}C for 5 hours. The polymer product was precipitated out in methanol, collected by filtration and dried under high vacuum overnight. The 1-hexene incorporation was determined by ^{1}H NMR integration.

6.5 REFERENCES

1. Hatada; K., Kitayama, T. *Polym. Int.* **2000**, *49*, 11-47.
2. Endo, K.; Inukai, A. *Polym. Int.* **2000**, *49*, 110-114.
3. Coutinho, F. M. B.; Costa, M. A. S.; Monteiro, L. F.; Santa Maria, L. C. *Polym. Bull.* **1997**, *38*, 303.
4. Coutinho, F. M. B.; Monteiro, L. F.; Costa, M. A. S.; Santa Maria, L. C.; Menezes, S. M. C. *Polym. Bull.* **1998**, *40*, 423-429.
5. Albeniz, A. C.; Espinet, P.; Lopez-Fernandez, R.; Sen, A. *J. Am. Chem. Soc.* **2002**, *124*, 11278-11279.
6. Nagel, M.; Poli, D.; Sen, A. *Macromolecules* **2005**, *38*, 7262-7265.
7. Luo, R.; Sen, A. *Macromolecules* **2006**, *39*, 7798-7800.

VITA

Ying Chen received her BS degree in chemistry from University of Science and Technology of China, Hefei, in 2005. She came to the Pennsylvania State University in 2005 and joined Dr. Ayusman Sen's group. Ying started with her graduate research in Lewis acid catalyzed acrylate/olefin copolymerization. She discovered a simple method to compare the efficacy of different acids, and studied the effect of Lewis acid on monomer reactivity ratios. She also worked on transition metal catalyzed polymerizations, ethylene oligomerizations, synthesis of LCST polymers and etc. She accepted a Sr. Chemist position from Nalco in Shanghai, China.